UNIVERSITY OF LEEDS

# Novel advanced cardiovascular magnetic resonance imaging study in women with gestational diabetes mellitus and preeclampsia

**Sharmaine A Thirunavukarasu**

**MbCHB, MRCP(UK)**

**Supervisors: Associate Prof Eylem Levelt, Prof Sven Plein, Prof John Greenwood**

**''Submitted in accordance with the requirements for the degree'' of Doctor in Medicine (PhD)**

**University of Leeds**

**Leeds Institute of Cardiovascular and Metabolic Medicine**

**April 2023**

# Intellectual Property and Publication Statement

I, Sharmaine A Thirunavukarasu confirm that the work submitted is my own and that appropriate credit has been given where reference has been made to the work of others.

# Acknowledgements

Firstly, I would like to thank my supervisor Dr Eylem Levelt for her unfaltering educational, moral and emotional support throughout this journey. You have not only been the most phenomenal supervisor a student can ever ask for but also a friend and mentor for life. I am ever so grateful to have you as a supervisor and it has been an honour for the supervision. I would also like to thank my co-supervisor Prof John Greenwood who has also been an incredible mentor to me both as a PhD supervisor and a clinical supervisor for my interventional career. You have always guided me and provided advice at every stage of this journey. Lastly, Professor Sven Plein who always willingly gave me your time and expertise.

These 3 years have been the best times of my life and I have shared many ups and downs with my PhD colleagues and peers, Dr Amrit Chowdhary, Dr Nicholas Jex, Dr Sindhoora Kotha and Dr Faiza Ansari. I felt so very supported as a team and their willingness to always help me out and go the extra mile; I am forever appreciative. I could not have completed this project successfully without your assistance.

Thank you to all the radiographers in the CMR department especially Miss Lizette Cash and Mr David Shelley for being so very accommodating and obliging. You have always been eager to help in any situation.

I like to thank Dr David Broadbent for your advice and help at every stage.

I am truly blessed with a wonderful family and want to thank my mum and dad, Shanand, Shastri (my brothers), my grandmothers and all my friends for always being there for me, for your constant words of encouragements, eagerness and interest in my topics of research.

Lastly, I want to thank all the participants for volunteering for my study. I am truly indebted to you and this work would have not been possible without you.

The work in this thesis is my own and original. Chapter 4 has been published. Dr David Broadbent provided physics support for the methods chapter (Chapter 2). Dr Faiza Ansari assisted with the recruitment of the participants in this study and worked on the analysis together. Miss Lizette Cash, Mr David Shelley, Mr Gavin Bainbridge, Mr Julian Tonge, Mrs Margaret Saysell, Mrs Debbie Scarlett, Mrs Lisa Lewis Forbes assisted with the scanning and preparation of the participants. Dr Hunain Shiwani provided the AI analysis for all the participants which is included in Chapter 6.

# Thesis abstract

Pregnant women represent an under-investigated population in clinical research and the mechanisms of long-term cardiovascular complications in women with obstetric complications remain to be elucidated. This is the basis which stemmed our interest in conducting our research in pregnant women with gestational diabetes mellitus (GDM) and preeclampsia(pE).

A third of parous women experience adverse pregnancy outcomes; an increased risk of heart failure, stroke and ischemic heart disease. GDM and pE are the leading obstetric complications of pregnancy. Both are associated with a substantial increase in the risk of long-term cardiovascular disease.

The aims of my longitudinal cohort study were to assess maternal cardiac alterations during the third trimester of pregnancy and their recovery twelve-months post-partum in women with GDM (n=30) or pE (n=22) compared to women with healthy pregnancies (HP)(n=38).

Phosphorus-magnetic resonance spectroscopy (31 P-MRS) and cardiovascular magnetic resonance imaging (CMR) were used to define myocardial phosphocreatine to ATP ratio (PCr/ATP), tissue characteristics, left ventricular (LV) volumes, mass, ejection fraction (EF), global longitudinal shortening (GLS), and diastolic function (mitral in-flow E/A ratio). Participants were monitored to birth, baby birth weights were recorded, placental tissue histology was assessed. Investigations were repeated 12-months postpartum to monitor cardiac changes. With obesity as a major and common risk factor for both GDM and pE, ten overweight and ten normal-weight nulliparous women were recruited as

non-pregnant control groups.

These studies have demonstrated that despite distinct etiologies, women with GDM and pE exhibit a similar myocardial phenotype during and after pregnancy with persistent subtle abnormalities in myocardial PCr/ATP ratio, LV mass and GLS compared to women with HP during pregnancy and twelve months' postpartum assessments. Women with GDM and pE show similar myocardial alterations to nulliparous women with obesity, suggesting that the maternal myocardial changes are predominantly driven by obesity-associated metabolic dysfunction.

In summary, the work in this thesis demonstrates the role of CMR and MRS in elucidating the cardiac structural, functional and energetic abnormalities in pregnancies complicated with gestational diabetes and preeclampsia. Most importantly, this work highlights that the persistent myocardial changes seen in women with GDM and pE at 12 months are mainly driven by obesity-associated metabolic dysfunction. With obesity becoming a huge worldwide health burden, it is very crucial to create societal awareness to support patients for a healthier lifestyle. This can be implemented through evidence based medicine and population based policies. Further research can be conducted to identify patients at risk and implement lifestyle interventions early to avoid long term complications to both the mother and fetus.

# Table of contents

# Abbreviations

| | |
|---|---|
| ACE | Angiotensin converting enzyme inhibitor |
| ACOG | American College of Obstetricians and Gynaecologists |
| ADA | American Diabetes Association |
| ADP | Adenosine diphosphate |
| ATP | Adenosine triphosphate |
| AF | Atrial fibrillation |
| ARB | Angiotensin receptor blocker |
| A wave | Atrial peak filling velocity |
| AMPK | AMP-activated protein kinase |
| APO | Adverse pregnancy outcomes |
| ATP | Adenosine triphosphate |
| AW | Acquisition Weighting |
| BMI | Body mass index |
| BNP | Brain natriuretic peptide |
| BP | Blood pressure |
| bpm | Beats per minute |
| CAD | Coronary artery disease |
| CFR | Coronary flow reserve |
| CMD | Coronary microvascular disease |
| CMR | Cardiovascular magnetic resonance imaging |
| $CO_2$ | Carbon dioxide |
| CoA | Acetyl co-enzyme A |

| | |
|---|---|
| CSI | Chemical shift imaging |
| CV | Cardiovascular |
| CVD | Cardiovascular disease |
| DT | Deceleration time |
| DM | Diabetes Mellitus |
| E wave | Early peak filling velocity |
| EDV | End diastolic volume |
| ESV | End systolic volume |
| ECG | Electrocardiogram |
| ECV | Extracellular volume fraction |
| EF | Ejection fraction |
| eGFR | Estimated glomerular filtration rate |
| FFA | Free fatty acid |
| Gck | Glucokinase |
| GDM | Gestational diabetes |
| GLP-1 | Glucagon like peptide-1 |
| GLS | Global longitudinal shortening |
| GLUT-4 | Glucose transporter 4 |
| HBA1c | Glycated haemoglobin |
| HDL | High-density lipoprotein |
| HF | Heart failure |
| HLA | Horizontal long axis |
| HOMA-IR | Homeostasis model assessment of insulin resistance |
| HP | Healthy pregnancy |

| | |
|---|---|
| hs-cTnT | High-sensitivity cardiac troponin T |
| IHD | Ischaemic heart disease |
| IR | Insulin receptor |
| IRS-1 | Insulin receptor substrate 1 |
| IQR | Interquartile range |
| LA | Left atrial |
| LGE | Late gadolinium enhancement |
| LnRHI | Natural logarithm of reactive hyperemia index |
| LV | Left ventricular |
| LVEDV | Left ventricular end-diastolic volume |
| LVEF | Left ventricular ejection fraction |
| LDL | Low-density lipoprotein |
| MACE | Major adverse cardiovascular events |
| MAPSE | Mitral annular plane systolic excursion |
| MBF | Myocardial blood flow |
| MOLLI | Modified look locker inversion recovery |
| MPRI | Myocardial perfusion reserve index |
| MR | Magnetic Resonance |
| MRI | Magnetic resonance imaging |
| MRS | Magnetic Resonance Spectroscopy |
| NADH | Nicotinamide adenine dinucleotide |
| NTproBNP | N-terminal pro hormone b type natriuretic peptide |
| $^{31}$P-MRS | $^{31}$ Phosphorus magnetic resonance spectroscopy |

| | |
|---|---|
| PAT | Pulse amplitude tonometry |
| PCr | Phosphocreatine |
| pE | Preeclampsia |
| PEDSR | Peak early diastolic strain rate |
| PET | Positron Emission Tomography |
| PI3K | Phosphatidylinositol-3-kinase |
| PIP3 | Phosphatidylinositol-3, 4, 5-phosphate |
| PPAR-γ | Peroxisome proliferator-activated receptor gamma |
| RV | Right ventricle |
| RVEF | Right ventricular ejection fraction |
| SSFP | Steady state free precession |
| SGLT2 | Sodium-glucose co-transporter-2 |
| sEng | Soluble endoglin |
| sFlt-1 | Soluble fms-like tyrosine kinase-1 |
| SSFP | Steady state free precession |
| SV | Stroke volume |
| T | Tesla |
| TE | Echo time |
| TF | Transcription factors |
| TTE | Transthoracic echo |
| TGF | Transforming growth factor |
| VEGF | Vascular endothelial growth factor |
| VLA | Vertical long axis |

# List of Figures

# List of Tables

# Conference Abstracts

**ABSTRACTS AT INTERNATIONAL AND NATIONAL CONFERENCES – ORAL and POSTER PRESENTATIONS**

**International**

**26th annual Society of Cardiovascular Magnetic Resonance Meeting, San Diego, January 2023 (Oral, First Author)**

"Persistent maternal cardiac changes 12 months' post-partum in women with gestational diabetes mellitus"

**43rd European Society of Cardiology Congress, Barcelona, August 2022 (Oral, First Author)**

"Gestational diabetes, pre-eclampsia and the maternal heart"

**53rd Diabetes Pregnancy Study Group Annual Meeting, Madrid September 2022 (Oral, First Author)**

"Gestational diabetes and the maternal heart"

**British Cardiovascular Society Conference, Manchester, June 2022- 'Best of the best' Clinical abstracts (Oral, First Author)**

"Gestational diabetes, preeclampsia and the maternal heart"

**25th annual Society of Cardiovascular Magnetic Resonance Meeting, Virtual January 2022 (Virtual oral, First Author)**

Gestational diabetes and the maternal heart

**The Royal Society of Medicine Cardiology President's prize medal meeting, Virtual March 2022 (Oral, First Author)**

"Empaglifozin reverses the cardiac energy-deficient state, improves cardiac function and reduces myocardial cellular volume in patients with type 2 diabetes"

**European Society of Cardiology Conference 2021- The Digital Experience (Virtual oral, First Author)**

Mechanistic insights from a multi-parametric magnetic resonance imaging study regarding the role of SGLT inhibitors

**American Heart Association, Boston, MA November 2021 (Poster, First Author)**

Comprehensive cardiac magnetic resonance imaging study for characterising remote myocardial remote myocardial zone contractile function, perfusion and fibrosis in type 2 diabetes patients with prior myocardial infarction

**American Heart Association, Boston, MA, November 2021 (Virtual Oral, First Author)**

Myocardial physiological responses to the third trimester of healthy pregnancy

**British Cardiovascular Society Conference 2021- 'Best of the best' Clinical abstracts (Oral, First Author)**

Empaglifozin on cardiac energetics and function

**EURO CMR 2021- Late breaking trials (Oral, First Author)**

Empaglifozin ameliorates the cardiac energy deficient-state, improves cardiac function and reduces myocardial cellular volume in patients with type 2 diabetes

# Publications

1) **Thirunavukarasu S,** Ansari F, Cubbon R, Forbes K, Bucciarelli-Ducci C, Newby DE, Dweck MR, Rider OJ, Valkovič L, Rodgers CT, Tyler DJ, Chowdhary A, Jex N, Kotha S, Morley L, Xue H, Swoboda P, Kellman P, Greenwood JP, Plein S, Everett T, Scott E, Levelt E. Maternal Cardiac Changes in Women With Obesity and Gestational Diabetes Mellitus. ***Diabetes Care***. 2022 Dec 1;45(12):3007-3015. doi: 10.2337/dc22-0401. PMID: 36099225
2) **Thirunavukarasu S**, Jex N, Chowdhary A, Hassan IU, Straw S, Craven TP, Gorecka M, Broadbent D, Swoboda P, Witte KK, Cubbon RM, Xue H, Kellman P, Greenwood JP, Plein S, Levelt E. Empagliflozin Treatment Is Associated With Improvements in Cardiac Energetics and Function and Reductions in Myocardial Cellular Volume in Patients With Type 2 Diabetes. ***Diabetes***. 2021 Dec;70(12):2810-2822. doi: 10.2337/db21-0270
3) **Thirunavukarasu S**, Brown LA, Chowdhary A, Jex N, Swoboda P, Greenwood JP, Plein S, Levelt E. Rationale and design of the randomised controlled cross-over trial: Cardiovascular effects of empaglifozin in diabetes mellitus. ***Diab Vasc Dis Res***. 2021 May-Jun;18(3):14791641211021585. doi: 10.1177/14791641211021585
4) Gorecka M, Jex N, **Thirunavukarasu S**, Chowdhary A, Corrado J, Davison J, Tarrant R, Poenar AM, Sharrack N, Parkin A, Sivan M, Swoboda PP, Xue H, Vassiliou V, Kellman P, Plein S, Halpin SJ, Simms AD, Greenwood JP, Levelt E. Cardiovascular magnetic resonance imaging and spectroscopy in clinical long-COVID-19 syndrome: a prospective case-control study. ***J Cardiovasc Magn Reson***. 2022 Sep 12;24(1):50. doi: 10.1186/s12968-022-00887-9

5) Chowdhary A, Javed W, **Thirunavukarasu S,** Jex N, Kotha S, Kellman P, Swoboda P, Greenwood JP, Plein S, Levelt E. Cardiac Adaptations to Acute Hemodynamic Stress in Function, Perfusion, and Energetics in Type 2 Diabetes With Overweight and Obesity. ***Diabetes Care***. 2022 Dec 1;45(12):e176-e178. doi: 10.2337/dc22-0887

6) Jex N, Chowdhary A, **Thirunavukarasu S**, Procter H, Sengupta A, Natarajan P, Kotha S, Poenar AM, Swoboda P, Xue H, Cubbon RM, Kellman P, Greenwood JP, Plein S, Page S, Levelt E. Coexistent Diabetes Is Associated With the Presence of Adverse Phenotypic Features in Patients With Hypertrophic Cardiomyopathy. ***Diabetes Care***. 2022 Aug 1;45(8):1852-1862. doi: 10.2337/dc22-0083

7) Chowdhary A, **Thirunavukarasu S**, Jex N, Coles L, Bowers C, Sengupta A, Swoboda P, Witte K, Cubbon R, Xue H, Kellman P, Greenwood J, Plein S, Levelt E. Coronary microvascular function and visceral adiposity in patients with normal body weight and type 2 diabetes. ***Obesity*** (Silver Spring). 2022 May;30(5):1079-1090. doi: 10.1002/oby.23413

8) Chowdhary A, Jex N, **Thirunavukarasu S**, MacCannell A, Haywood N, Almutairi A, Athithan L, Jain M, Craven T, Das A, Sharrack N, Saunderson CED, Sengupta A, Roberts L, Swoboda P, Cubbon R, Witte K, Greenwood J, Plein S, Levelt E. Prospective Longitudinal Characterization of the Relationship between Diabetes and Cardiac Structural and Functional Changes. ***Cardiol Res Pract***. 2022 Feb 8;2022:6401180. doi: 10.1155/2022/6401180

9) Gorecka MM, **Thirunavukarasu S**, Levelt E, Greenwood JP. Progressive myocardial dysfunction following COVID-19. ***BMJ Case Rep***. 2021 Nov 11;14(11):e246291. doi: 10.1136/bcr-2021-246291

10) Jex N, Farley J, **Thirunavukarasu S**, Chowdhary A, Sengupta A, Greenwood J, Schlosshan D, Plein S, Levelt E. A 30-Year-Old Man With Primary Cardiac Angiosarcoma. ***JACC Case Rep***. 2021 May 12;3(6):944-949. doi: 10.1016/j.jaccas.2021.03.009

11) Chowdhary A, **Thirunavukarasu** S, Jex N, Levelt E. Global microvascular ischaemia following Takotsubo cardiomyopathy with left ventricular function recovery. ***Eur Heart J Case Rep***. 2021 Mar 10;5(3):ytab093. doi: 10.1093/ehjcr/ytab093

12) Brown LAE, Gulsin GS, Onciul SC, Broadbent DA, Yeo JL, Wood AL, Saunderson CED, Das A, Jex N, Chowdhary A, **Thirunavukarasu S**, Sharrack N, Knott KD, Levelt E, Swoboda PP, Xue H, Greenwood JP, Moon JC, Adlam D, McCann GP, Kellman P, Plein S. Sex-and age-specific normal values for automated quantitative pixel-wise myocardial perfusion cardiovascular magnetic resonance. ***Eur Heart J Cardiovasc Imaging***. 2023 Mar 21;24(4):426-434. doi: 10.1093/ehjci/jeac231.PMID: 36458882

13) Brown LAE, Wahab A, Ikongo E, Saunderson CED, Jex N, **Thirunavukarasu S**, Chowdhary A, Das A, Craven TP, Levelt E, Dall'Armellina E, Knott KD, Greenwood JP, Moon JC, Xue H, Kellman P, Plein S, Swoboda PP. Cardiovascular magnetic resonance phenotyping of heart failure with mildly reduced ejection fraction. ***Eur Heart J Cardiovasc Imaging***. 2022 Dec 19;24(1):38-45. doi: 10.1093/ehjci/jeac204.PMID: 36285884

14) Jex N, Chowdhary A, **Thirunavukarasu S**, Levelt E. A case report of refractory angina in a patient with diabetes and apical hypertrophic cardiomyopathy. ***Eur Heart J Case Rep***. 2022 Aug 16;6(8): ytac347. doi: 10.1093/ehjcr/ytac347

15) Das A, Kelly C, Teh I, Nguyen C, Brown LAE, Chowdhary A, Jex N, **Thirunavukarasu S**, Sharrack N, Gorecka M, Swoboda PP, Greenwood JP, Kellman P, Moon JC, Davies RH, Lopes LR, Joy G, Plein S, Schneider JE, Dall'Armellina E. Phenotyping hypertrophic cardiomyopathy using cardiac diffusion magnetic resonance imaging: the relationship between microvascular dysfunction and microstructural changes. ***Eur Heart J Cardiovasc Imaging***. 2022 Feb 22;23(3):352-362. doi: 10.1093/ehjci/jeab210.PMID: 34694365

# *Chapter 1: Introduction*

## 1.1 Normal pregnancy physiology and heart disease

In England and Wales, there were 624,828 live births in 2021 which was a 1.8% increase from 613,936 in 2020 according to the Office for National Statistics.(1)

Cardiovascular disease is the leading cause of maternal morbidity and mortality with worsened outcomes in pregnancies affected by heart failure, hypertension, arrhythmias and valvular heart disease.(2)Cardiovascular disease accounts for over 33% of pregnancy related maternal deaths (3) and additionally 1-2% of pregnancies are complicated by cardiac disease.(4)The maternal cardiovascular system is adaptive during normal pregnancy to sustain the growth of the fetus, but this can be challenging in women with established cardiovascular disease. These adaptive maternal changes include a hyperdynamic circulation, vasodilatation, increased filling capacity of the vasculature, and consequently volume expansion by approximately 40% by 24 weeks' gestation which then peaks around 30 weeks' gestation.(4) There is a smaller increase in the red blood cell mass in comparison which leads to a fall in serum haemoglobin levels in pregnancy.(5) HbA1c levels are also lower in normal pregnancy due to the increased red blood cell turnover.(6) Furthermore, pregnancy results in a 15-25% increase in heart rate which peaks in the third trimester and normalises 10 days post-partum to the pre-pregnancy state.(4)

Normal pregnancy also requires significant maternal cardio-metabolic adaptation, with a 30–50% increase in cardiac output due to an increase in stroke volume initially, alterations in lipid profile including a circa 50% increase in total cholesterol, and a significant increase in insulin resistance during the second half of gestation to facilitate transfer of glucose to the fetus.(7) The state of insulin resistance encourages breakdown of fat stores and increased endogenous glucose production.(8)

Both mean systolic and diastolic blood pressure drop within the first few weeks of conception due to reduced systemic vascular resistance from peripheral vasodilatation and a low resistance utero-placental circulation but rises from 26-28 weeks' gestation until delivery.(9) Vasodilatation is secondary to the increased prostacyclin and nitric oxide production and a decreased sensitivity to angiotensin. Lastly vasomotor sympathetic activity is increased with activation of the renin-angiotensin aldosterone axis during normal pregnancy (9) and vascular distensibility is increased in the first trimester.(10) All these changes in the normal vasculature prevent any adverse effects on central venous pressure and pulmonary capillary wedge pressure.(11)

In normal pregnancy, perfusion of the placenta occurs through increased uterine blood flow from invasion of the spiral uterine arteries from trophoblasts. Fibrinoid material replaces the vascular smooth muscle cells converting these into large blood vessels for placental perfusion as described above.(12)

Given these remarkable cardio-metabolic changes, pregnancy may act as a "stress test" for future cardiovascular disease (CVD). Women with adverse pregnancy outcomes (APO) have maladaptive responses to pregnancy. Increased mean arterial pressure and systemic vascular resistance, typically accompanied by hyperlipidemia are seen in preeclampsia (pE), whereas more extreme insulin resistance in the absence of overt hypertensive syndrome occurs in gestational diabetes mellitus (GDM) (8). There is an initial increase in insulin sensitivity followed by progressive insulin resistance leading to hyperplasia of the pancreatic beta cells in normal pregnancy. Normal pregnancy constitutes lower fasting blood glucose levels due to fetal and placental uptake. There is also a mild postprandial hyperglycaemia secondary to diabetogenic placental hormones. When insulin resistance outweighs pancreatic function,

this is when gestational diabetes mellitus develops.(11) Whether APO merely unmask a woman's pre-existing CVD risk or are mediators of future CVD pathogenesis is unclear.

From a metabolic standpoint, the main source for maternal energy is derived from fatty acids rather than glucose or amino acids to preserve the latter fuels for fetal metabolism. Maternal consumption of fatty acids increases, with decreased fatty acid storage secondary to decreased lipoprotein lipase activity and increased lipolytic activity towards the end of pregnancy.(13)

Regarding biomarkers during pregnancy, studies have demonstrated that brain natriuretic peptide (BNP) levels are similar throughout pregnancy and at pre-conception levels but there may be a mild physiological rise post-partum. Levels of cardiac troponin I and creatine kinase-MB are similar throughout a normotensive healthy pregnancy. (14)

There have been studies in healthy pregnancy comparing the use of transthoracic echocardiography (TTE) and cardiovascular magnetic resonance imaging (CMR) which demonstrated underestimation of the LV mass, cardiac output and stroke volume in the former compared to the latter modality.(2) CMR remains the reference method of investigation for cardiac volume and ventricular function assessments due to the superior spatial resolution and excellent intra and inter observer reproducibility. (15)

Identifying women at risk is pertinent to allow early diagnosis and treatment to prevent adverse pregnancy related complications and cardiovascular disease later in life.

The table below represents CMR studies which demonstrate the pathophysiological process in pregnancy and the feasibility of performing CMR.

| ***Study*** | ***Imaging modality*** | ***Journal/Year*** | ***Recruited cohort*** | ***Primary objective*** | ***Results*** |
|---|---|---|---|---|---|
| *CHIRP(2)* | ECHO/CMR | 2014 | N=34 | Provide reference values for cardiac indices during normal pregnancy and the postpartum state compare TTE and CMR in the non-invasive assessment of physiologic maternal cardiac remodelling during the peri-partum period | LV mass, stroke volume and cardiac output underestimated by ECHO |
| *Romagano et al.(16)* | CMR | 2018 | N=16 | To assess the role of CMR for the evaluation and management of women with cardiac disorders in pregnancy and postpartum | CMR provides information in pregnant women with complex cardiac disease or suspected aortic pathology |
| *Stewart el al. (17)* | CMR | 2016 | N=23 | To evaluate cardiac remodelling | Substantial cardiac remodelling during pregnancy that is |

| | | | |
|---|---|---|---|
| | | according to maternal habitus throughout pregnancy and post-partum | proportional to maternal size. All changes in cardiac remodelling resolved by 3 months' post-partum |

Table 1.1 : CMR studies demonstrating the pathophysiological process in pregnancy and the feasibility of performing CMR

## 1.2 Gestational diabetes mellitus physiology and heart disease

Gestational diabetes mellitus (GDM) is defined as glucose intolerance with onset or first recognition during pregnancy(18). GDM was first described by Bennewitz in 1824 in Germany(19) from a woman with recurrent glycosuria and polydipsia in 3 pregnancies resulting in one macrosomic baby weighing 5.5 kg. (20)

GDM occurs when there is beta cell dysfunction and chronic insulin resistance(21). Hyperglycemia, impairment of insulin signaling in the heart and systemic insulin resistance are involved in the pathogenesis. (22)

Beta cell dysfunction is a result of the inability to detect blood glucose concentrations and secrete insulin in response but the mechanisms underlying this can be complex and varied. Beta cells can deteriorate from excessive insulin production secondary to the increased in energy consumption which eventually results in exhaustive cells.(21) Defects can occur at any stage of the process: pro-insulin synthesis, post-translational modifications, granule storage, blood glucose sensing concentrations, or the complex machinery underlying exocytosis of granules. (23)

Most susceptibility genes that are associated with GDM are related to beta cell function, including potassium voltage-gated channel KQT-like 1 (Kcnq1) and glucokinase (Gck). (21) Figure 1.1 demonstrates a simplistic version of insulin signaling. Insulin receptor substrate (IRS-1) is activated when insulin binds to the insulin receptor (IR). Via AMP-activated protein kinase (AMPK), adiponectin encourages IRS-1 activation as well as stimulating insulin secretion by upregulating insulin gene expression.(24) IRS-1 then activates phosphatidylinositol-3-kinase (PI3K) and via a cascade of phosphorylation activates phosphatidylinositol-3, 4, 5-phosphate (PIP3). PIP3 activates AKT2, which promotes glucose transporter 4 (GLUT 4) translocation and glucose uptake into the cell. When there is inadequate plasma membrane translocation of GLUT 4 this leads to insulin resistance as there is inadequate amounts of glucose delivery to the cells for energy.

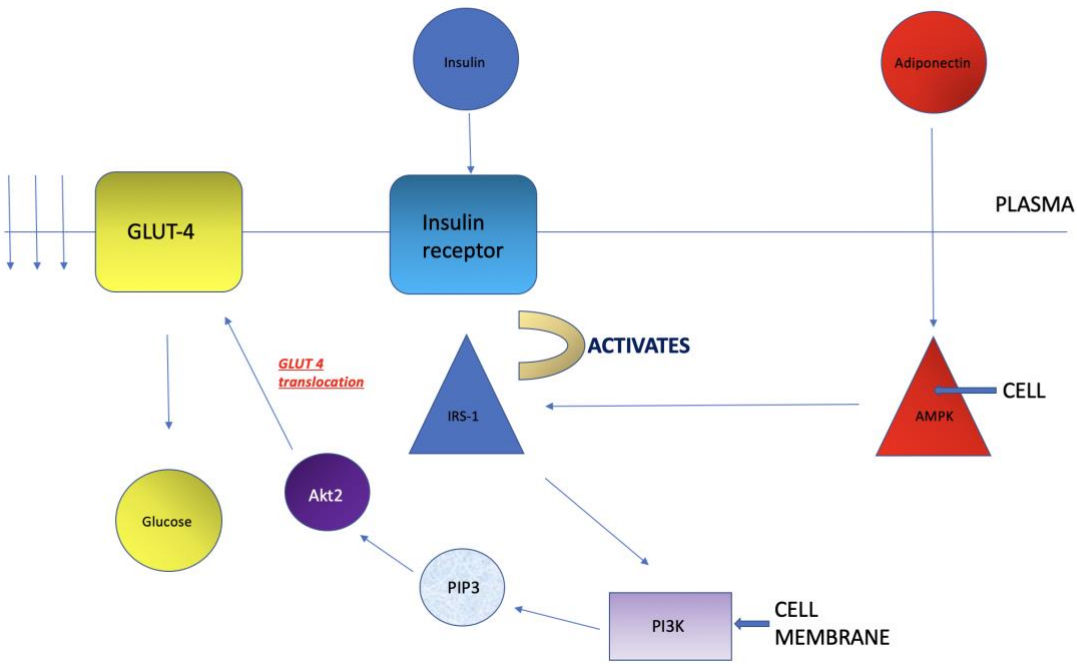

Figure 1.1: demonstrates a simplistic version of insulin signalling. Insulin receptor substrate 1(IRS-1) is activated when insulin binds to the insulin receptor (IR). Via AMP-activated protein kinase (AMPK), adiponectin encourages IRS-1 activation as well as stimulating insulin secretion by upregulating insulin gene expression.(24) IRS-1 then activates phosphatidylinositol-3-kinase (PI3K) and via a cascade of phosphorylation activates phosphatidylinositol-3, 4, 5-phosphate (PIP3). PIP3 activates AKT2, which promotes glucose transporter 4 (GLUT 4) translocation and glucose uptake into the cell. When there is inadequate plasma membrane translocation of GLUT 4 this leads to insulin resistance as there is inadequate amounts of glucose delivery to the cells for energy.

GDM is also associated with a reduction in the number and function of mitochondria within the skeletal muscle which contributes to the reduction in glucose utilization in this cohort of patients. (25)

The overall incidence rate of GDM is 10% and this is further enhanced by the obesity epidemic. (26) Over 60% of the cases are diagnosed after 23 weeks of gestation. GDM is associated with short-term and long-term adverse outcomes for both mothers and their offspring. The diagnosis of GDM identifies women who have a twofold higher CVD risk postpartum, including a greater risk of stroke (HR1.25[1.07 to 1.48]) and ischemic heart disease (IHD) (HR 2.09[1.56 to 2.80]) in later life compared to women without a history of GDM.(26,27) The risk of composite CVD is highest in the first decade after pregnancy in women with GDM(28) and this increased CVD risk is not dependent upon later development of T2D.(28) The risk persists when analysed by subtype of CVD (IHD and stroke).(29) There is growing evidence that coronary

microvascular disease (CMD), with or without obstructive coronary artery disease (CAD), contributes to the pathophysiology of IHD in women.(30) The link between CMD and coronary atherosclerosis is incompletely understood, but microvascular disease partly explains the adverse outcomes in women despite a lower prevalence of obstructive CAD.(30) In this regard, imaging modalities that provide quantification of myocardial blood flow (MBF) and/or coronary flow reserve (CFR), which are surrogate markers of microvascular function, may help identify at-risk patients such as those with APO.

Spontaneous abortion, fetal anomalies, fetal demise, macrosomia, neonatal hypoglycaemia, hyperbilirubinaemia are a few of the specific risks of diabetes in pregnancy.(31) Women with GDM were shown to exhibit a more atherogenic lipid profile by 3 months post-partum with increased low-density lipoprotein (LDL), apoB and increased carotid intima media thickness. (32)

Even without progressing to T2D, women with GDM comprise an at-risk population for CVD and hence a potential opportunity for early risk factor surveillance and risk modification. During pregnancy, fasting glucose targets for women with GDM are <5.3mmol/L or 2-h postprandial glucose <6.7mmol/L for achieving optimal glucose levels.(33) The American College of Obstetricians and Gynaecologists (ACOG) Committee Opinion 762, Pre-pregnancy Counselling highlight the importance of preconception care for all women including aiming for a HbA1c level < 48mmol/mol because ensuring strict glycaemic control during this period is associated with the lowest risk of congenital abnormalities seeing as organogenesis occurs primarily between week 5 to week 8 of gestation as well as lower risk of adverse neonatal outcomes. (6) Glycaemic status is recommended to be assessed at 6 to 12 weeks after delivery and every 3 years thereafter according to the American Diabetes Association (ADA) guidelines.(11)

The management of GDM is focussed on lifestyle behavioural changes and pharmaceutical interventions in addition if necessary with insulin being the preferred treatment option during pregnancy. Metformin or glyburide are not recommended as first line treatment as they cross the placenta. Furthermore, in previous randomised controlled trials metformin and glyburide were shown to be inefficient in provision of adequate glycaemic control in women with GDM.(34,35) However in contrast the Metformin in Women with Type 2 Diabetes in Pregnancy Trial (MiTY) showed the benefits of metformin in maternal glycaemic and neonatal adiposity control.(36) Another anticipated ongoing trial is the Medical Optimization of Management of Type 2 Diabetes Complicating Pregnancy Trial (MOMPOD) where patients are randomised to a regime of insulin/metformin or insulin/placebo for the treatment of type 2 diabetes complicating pregnancy. The results of this trial will shed light on the composite adverse neonatal and perinatal outcomes comparing the two treatment groups to improve outcomes in both the mother and fetus. (37)

## 1.3 Pre-eclampsia physiology and heart disease

Pre-eclampsia(pE), is the leading cause of global maternal mortality and morbidity.(38) pE was first discovered in 1840 by Rayer describing proteinuria in eclampsia and subsequently by Vaquez in 1897 describing gestational hypertension in eclamptic women.(39) pE represents a multisystem disorder attributed by abnormal placentation early in the first trimester, with an excess of antiangiogenic factors in the second and third trimester and increased vascular permeability. (40) It affects 2-8% of pregnancies worldwide (3) and mainly occurs in the third trimester. It is responsible for over 70,000 maternal and 500,000 fetal deaths worldwide every year.(41) pE can eventually result in hypertension and multi-organ dysfunction. There is growing evidence that these effects persist after pregnancy. (42)

The diagnostic criteria of pE consists of hypertension with systolic blood pressure (BP) ≥ 140mmHg or diastolic blood pressure ≥ 90mmHg on 2 occasions at least 4 hours apart after 20 weeks' gestation in a woman with previously normal BP, or systolic BP ≥160mmHg on 1 occasion and ≥300mg proteinuria per 24-hour urine collection or protein/creatinine ratio of ≥ 0.3mg/dl or thrombocytopenia, renal insufficiency, impaired liver function, pulmonary edema, neurological signs and fetal growth restriction in the absence of proteinuria. (42)

Pre-existing cardiovascular disease likely play a role in the development of pE. The women with pE have increased cardiac output and exhibit increased LV wall thickness potentially related to the presence of myocardial oedema causing LV mass increase and pressure loading of the left ventricle with higher BP. Women with pE have a 4-fold increased risk of heart failure with reduced ejection fraction and preserved ejection fraction (risk ratio (RR), 4.19, 95% confidence interval (CI), 2.09-8.38) a 2-fold increased risk in coronary heart disease, stroke respectively (RR, 2.21; 95% CI, 1.83–2.66 and RR, 1.81; 95% CI, 1,29–1.55)(43) and cardiovascular complications that may be related to the hypertensive changes.(44)

The etiology of pE is multifactorial secondary to metabolic, hemostatic, immunological abnormalities and endothelial dysfunction. Clinical and pathological studies suggest that the placenta is central to the pathogenesis of this syndrome.(41) In a normal pregnancy, vascular sinuses at the fetal-maternal junction provide nutrition to the fetus when cytotrophoblasts migrate in to the maternal uterine spiral arteries. pE on the other hand manifests with abnormal trophoblast invasion into the endometrium prior to pregnancy leading to incomplete spiral artery remodeling and a subsequent reduction of blood flow to the placenta.(45) The narrow spiral arteries are susceptible to lipid-laden macrophages within the lumen, necrosis of the arterial wall which also contribute to the compromised arterial flow. The placenta then secretes anti-angiogenic factors such as soluble fms-like tyrosine kinase-1

(sFlt-1) protein product and soluble endoglin (sEng)(46) in the maternal circulation, leading to endothelial damage, vasoconstriction, oxidative stress, placental hypoperfusion and inflammation. The sFLT1 and sENG causes endothelial damage by provoking vascular endothelial growth factor (VEGF) and transforming growth factor (TGF)-β1 signalling. (47) There is rising evidence that VEGF and TGF-β1 are required to maintain endothelial health in several tissues including the kidney and the placenta. During normal pregnancy, vascular homeostasis is maintained by physiological levels of VEGF and TGF-β1 signalling in the vasculature. In pE on the other hand, excess placental secretion of sFLT1 and sENG (both are endogenous circulating antiangiogenic proteins) inhibits VEGF and TGF-β1 signalling respectively in the vasculature.(48) There are also several different other developments on the pathogenesis of preeclampsia which constitute mutations in the atrial natriuretic peptide-converting enzyme and corin which is linked to the development of cardiac hypertrophy during pregnancy and post-partum.(49)


Figure 1.2: demonstrates the pathogenesis of pE

Figure 1.2 demonstrates the pathogenesis of pE. Genetic factors, immunologic factors, other maternal factors cause placental dysfunction which in turn leads to the release of antiangiogenic factors (such as sFLT1 [soluble fms-like tyrosine kinase 1] and sENG [soluble endoglin]) and other inflammatory mediators to induce pE. (41) Immunologic alterations contribute to the pathogenesis of pE with a shift towards the Th1 phenotype from T helper cells resulting in apoptosis.

Atherosclerotic changes in the maternal radial arteries are also evident in pE. Decidual vasculopathy is common to disorders of placental insufficiency combining acute atherotic lesion with medial hypertrophy and perivascular lymphocytes.(50) The decidua in pE demonstrates edematous endothelium, medial vessel hypertrophy and loss of smooth

muscles modifications. (50) Decidual vasculopathy has a link with pE and small for gestational age babies with abnormalities on Doppler imaging. Poor uterine decidualization and stromal transformation may also affect progression of pE. Hypoxia plays a significant role in the development of pE with upregulation of hypoxia-inducible transcription factors (TFs) and hypoxia-related gene signatures.(51) Intermittent hypoxia and re-oxygenation caused by poor spiral artery invasion eventually leads to oxidative stress.

Risk factors for pE include obesity,(52) insulin resistance, hypertension, history of pE, metabolic abnormalities, hypercoagulable states including antiphospholipid syndrome, pro-inflammatory, endothelial dysfunction and dyslipidemia.(53) Biochemical risk factors for cardiovascular disease (CVD) including raised concentrations of total cholesterol and triglycerides, have been shown to persist many years after a hypertensive disorder of pregnancy.(54)

In terms of maternal cardiovascular findings on imaging assessments of the heart, during a hypertensive pregnancy, the relative wall thickness increases, indicating that the ventricular wall thickens disproportionately to the increase in ventricular volume, and this does not fully resolve to a pre-pregnancy state postpartum.(55) Cardiac remodeling of the left ventricle due to an increase in peripheral vascular resistance leads to microcirculatory problems associated with structural and functional vascular changes.(56) Cardiac adaptations persist between 25-72% of patients in the postpartum period increasing the susceptibility to developing CVD in later life. After pE, elevation of myocardial mass, reduction in circumferential and longitudinal strain and diastolic impairment has been reported. While the cure for pE is delivery of the placenta, supporting the crucial etiological role of the placenta in the development of pE , maternal effects of pE do not cease with the birth of the infant and delivery of the

placenta.(26) In some cases, persistent postpartum changes exist and emerged as one of the most important risk factors for peri-partum morbidity.

A study by Chen et al using transthoracic echocardiography(TTE) demonstrated that cardiac output of healthy pregnant women and women with pE did not significantly differ, nor did left ventricular (LV) end-diastolic volume or ejection fraction. Similar right ventricular end-diastolic volume and ejection fraction was found between the groups. LV mass or mass index on CMR did not significantly differ between women with healthy pregnancy and women with pre-eclampsia, although both groups met diagnostic criteria for increased LV mass by the standard definitions on CMR.(57) A study by Birukov et al investigated cardiac alterations in post-pre-eclamptic women ( 2.00 ± 1.00 years) and control subjects (4 ± 5.25 years) using CMR which demonstrated a 13% increase in left atrial (LA) diastolic volume, 19% increase in LA stroke volume and a slight increase in LV hypertrophy in the post-pre-eclamptic group ( 2.00 ± 1.00 years). A history of pE and changes in LA dimensions associations increased when adjusted for BMI, age, parity, diastolic BP, smoking status and post-partum. (58) In a Danish study on the long-term effects of post-partum cardiomyopathy on cardiac structure and function, patients were symptom free with a mean LV ejection fraction (EF) of 62% but with evidence of diastolic dysfunction and lower exercise capacity in women with pE compared to control group.(59)

Non-invasive cardiac imaging could assist in the early detection of myocardial abnormalities, especially in the preclinical stage, when these changes are likely to be reversible. Moreover, imaging studies can improve our insights into the relationship between preeclampsia and heart failure and can be used for monitoring. (43) Interventional studies would be important to conduct especially during the asymptomatic phase to delay the onset of CVD in women and subsequently undertaking mediations to mitigate risk of cardiovascular disease after

adverse pregnancy outcomes. Transitional clinics, lifestyle interventions, targeted pharmacotherapy, and clinician and patient education represent promising strategies for improving postpartum maternal cardio-metabolic health in women with adverse pregnancy outcomes. Aspirin has been shown to be beneficial in preventing pE from the Perinatal Antiplatelet Review of International study with a relative risk reduction of 0.90 (CI 0.84-0.97). (60) Based on this study 75-150 mg daily aspirin is now recommended for women who are at high-risk of developing pE from 12 weeks of pregnancy untill the delivery.

The table below represents CMR studies which demonstrate the pathophysiological process in women with pE.

| *Study* | *Imaging modality* | *Journal/Year* | *Recruited cohort* | *Primary objective* | *Results* |
|---|---|---|---|---|---|
| *Birukov A et al.(58)* | CMR 0.5-20 years after delivery | JACC CVI 2020 | 22 control subjects and 22 people with preeclampsia | Structural or functional change in the heart-combined outcome | -Increased LA EDV 13%<br>-Increased LA stroke volume 19%<br>-Increased LV hypertrophy |
| *Ersbøll et al.(61)* | CMR | J Card Fail 2021 | 28 | Assessment of the relation between biomarkers and cardiac function after pE or peri-partum cardiomyopathy | -No significant remaining alterations in ventricular structure and function |
| *Ersbøll et al.(59)* | CMR | Journal of American Heart Association 2018 | 28 | Assessment of the long-term effect of peri-partum cardiomyopathy and pE on cardiac function | -No significant remaining alterations in ventricular structure and function |
| *Kalapathorakos et al.(62)* | CMR | Pregnancy Hypertension 2020 | 8 | Assessment of ventricular structure and function in formerly pre-eclamptic women | -Left ventricular mass was increased immediately postpartum (48 (44–57) g/m2vs. 57 (53–68) g/m2, p= 0.01), but returned to baseline levels after later examinations |
| *Levine et al.,*(63) | CMR | Pregnancy Hypertension 2019 | 80 people withT2D and HFrEF | Assessment of ventricular structure and function in formerly pre-eclamptic women in the early postpartum period | -Global longitudinal strain(GLS) was diminished in the pE group (−15.15 (−17.63–−12.62) % vs.−13.11(−15.54–−10.76) %, p= 0.04<br>-E/A ratio was diminished in the pE group (1.80 (1.29–2.31) vs. 1.45 (1.13–1.77), p= 0.006) |

| | | | | | |
|---|---|---|---|---|---|
| *Melchiorre et al.*(64) | Cardiac MRI before and 36 weeks after | Hypertension 2011 | 105 patients with NYHA functional class II to IV with a left ventricular (LV) ejection fraction ≤40% and type 2 diabetes or prediabetes | Changes from baseline to 36 weeks in left ventricular end systolic volume index (LVESVi) and LV GLS measured using cMRI | -Reduction in LV volumes in patients with heart failure with reduced ejection fraction(HFrEF) and type 2 diabetes or prediabetes |

Table 1.1: represents CMR studies which demonstrate the pathophysiological process in women with pE.

## 1.4 Cardiovascular magnetic resonance in pregnancy

Cardiovascular magnetic resonance (CMR) is the reference technique for comprehensive evaluation of myocardial structure, function and perfusion with excellent reproducibility. It is not limited by variations in interventricular geometry, body habitus, or exposure to ionizing radiation.(65) CMR has also excellent spatial and temporal resolution. Women whom are pregnant with or without cardiovascular conditions often require cardiovascular imaging during pregnancy to confirm diagnosis, risk stratify, risk prognosticate and for guidance regarding appropriate management options.(66)

CMR imaging exploits the magnetic properties of hydrogen nuclei protons, longitudinal relaxation time (T1) and transverse relaxation time (T2)(67). CMR parametric mapping methods (such as T1- and T2-mapping) are quantitative techniques that provide a pixel-by-pixel representation of numerical T1 or T2 properties. These techniques provide information on myocardial tissue type and composition without the need for contrast agents(68); they

allow direct comparison of quantitative maps within individuals longitudinally over time, and between individuals.(69) Native T1 reflects myocardial tissue changes involving the intracellular and extracellular compartments and detects conditions associated with increased myocardial water content such as myocardial infarction, fibrosis, and inflammation.(69) T2 values are sensitive to free water content in tissue, and T2-mapping is considered particularly useful for detecting myocardial oedema.(69)

While there is scarcity of prospective data on the use of CMR for assessment of CVD in pregnancy, most available data from registries and retrospective cohorts suggest that magnetic resonance imaging (MRI) performed at any stage of pregnancy does not harm the baby.(70) In over 30 years of evaluating fetal outcomes in pregnant women, there has been no evidence of harm from the use of CMR and other forms of MRI up to 3T in pregnancy.(71)In a population-based cohort study involving more than 1.4 million pregnancies, first-trimester MRI was not associated with stillbirth or neonatal death, congenital anomaly, neoplasm, or hearing loss, and in a separate study safety of MRI was also demonstrated in the third trimester.(72,73) Less data are available on the use of contrast, but increased risk of neonatal death or stillbirth with gadolinium exposure is reported by Ray et al.(72) In accordance to current guidance, if the benefits of giving contrast outweigh the risks to the fetus and a diagnosis is pertinent to the mother, administration of gadolinium-based contrast agents is permissible.(74) CMR nonetheless can provide insight into pathophysiological mechanisms underlying CVD and can be safely performed during pregnancy *without* gadolinium-based contrast agents.(72) However, there is scarcity of CMR data on pregnancy-associated CV physiological adaptive changes in pregnancy and it is currently unknown whether pregnancies complicated by GDM or pE are associated with abnormalities of myocardial structure, function or tissue characteristics on CMR which this study aims to demonstrate.

## 1.5 Maternal cardiac metabolism in pregnancy

Metabolic shifts occur during pregnancy to ensure adequate support to the fetus and to maximize maternal efficiency from anabolic metabolism during early gestation to catabolic, diverting nutrients to the growing fetus. (75) Adenosine triphosphate (ATP), a cardiac high-energy phosphate metabolite which is formed within the mitochondria by ATP synthase is derived mainly from mitochondrial oxidative phosphorylation.(76)The heart is highly dependent on a continuous energy supply and ATP turnover occurs every 10 seconds with minimal reserves. (7) ATP is the energy source for contraction, and phosphocreatine (PCr) is the major energy storage compound hence vital for normal heart function and both needed in adequate amounts. The heart has a very high metabolic demand and consumes more ATP in comparison to any other organ per gram of tissue.(77). Efficient matching of energy supply to demand in the heart is essential for cardiac function. In pregnancy, cardiomyocytes increase utilization of fatty acids and decrease glucose utilization. This increased reliance on fatty acid metabolism might be an adaptive mechanism to prevent any deterioration in cardiac function. (7) Impairments in cardiac energetics, requiring a quick reaction from the mitochondria can lead to progression of cardiac disease, although the causal relationship between energy starvation and contractile dysfunction has yet to be established. Cardiac 31 phosphorus magnetic resonance spectroscopy ( $^{31}$P-MRS) is able to provide us with non-invasive measurements of in vivo biochemical information.(78) Using $^{31}$P-MRS, multiple studies have shown compromised myocardial energetics in the metabolic phenotype of diabetic heart, non-ischaemic heart failure(79) (80) (81), ischaemic heart disease and hypertensive heart disease.(82,83)

There have been no studies to date using $^{31}$P-MRS to quantify myocardial energetics in the normal pregnancy or assess abnormalities or physiological adaptation to pregnancy in GDM and pE. The metabolic changes that occur in the heart during pregnancy have not been studied in detail and very little is known about it.

There are four major factors necessary for effective cardiac metabolism.(84)

1. Adequate perfusion: To deliver substrate and oxygen under both resting and exercise, a healthy myocardial blood supply with an appropriate hyperemic response during exercise is vital.
2. Substrate utilisation: This involves uptake of mainly free fatty acids and glucose and their subsequent breakdown via beta oxidation and glycolysis. These processes result in the formation of acetyl coenzyme A (CoA), which is fed into the Krebs cycle producing NADH and carbon dioxide ($CO_2$).(85)
3. Energy production: ATP which is a form of high energy phosphate bonds are made via a series of electron transfers in the mitochondria. Respiratory-chain complexes I through IV transfer electrons from NADH to oxygen, this creates a proton electrochemical gradient across the inner mitochondrial membrane as well as NAD and water.(86) This gradient drives ATP synthase, which produces ATP by phosphorylating ADP (adenosine diphosphate). Uncoupling proteins cause mitochondria to produce heat rather than ATP.
4. Energy transfer and utilisation: Creatine kinase energy shuttle is essentially the heart's energy transfer mechanism. Mitochondrial creatine kinase catalyzes the transfer of the high-energy phosphate bond in ATP to creatine to form PCr. This molecule is smaller and less polar and hence diffuses out of the mitochondria into the cytoplasm. At the site of energy usage, mainly at the sarcomere and for ion pump function, ATP

is reformed in the reverse reaction. Creatine, which is not produced in the heart, is taken up by the creatine transporter. (87)

The relative concentration of phosphocreatine to ATP (PCr/ATP) is a marker of the myocardium's ability to convert substrate into ATP for active processes, and a sensitive index of the energetic state of the myocardium.(77) $^{31}$P-MRS allows non-invasive measurement of the concentration of phosphocreatine (PCr) to ATP and this technique can be performed supine for patient comfort and tolerability which we aim to demonstrate in this study.

## 1.6 Aims of this research

Pregnancy requires significant cardio-metabolic adaptation and is considered a "stress test" for future cardiovascular disease (CVD). Pregnant women represent an under-investigated population and there is limited information on myocardial adaptive changes to pregnancy. Pregnancy complications of GDM and pE have long-term implications for maternal CV health. The magnitude and reversibility of maternal changes in myocardial structure, function and tissue characteristics or energetics with the onset of these obstetric complications have not been characterized before. This thesis intended to fill the gaps in knowledge in the current understanding of the pathogenesis of cardiovascular disease in women with these obstetric complications. The overall aim of the work in this thesis was to provide insight into pathophysiological mechanisms underlying CVD excess risk in these women using advanced imaging techniques.

Myocardial energetic compromise, indicated by decreased PCr/ATP, is a predictor of mortality(88) and linked to contractile dysfunction.(88,89) The effects of gestational metabolic and hemodynamic alterations on the myocardial energetic state can be assessed non-invasively by $^{31}$P-MRS without the need for ionizing radiation or contrast exposure.

Moreover, CMR allows comprehensive evaluation of myocardial structure, function, strain and tissue characteristics with excellent reproducibility. CMR therefore provides insight into cardiovascular physiology and non-contrast CMR studies can be safely performed during pregnancy.(70-73) As a result, utilising CMR and $^{31}$P-MRS in the third trimester, I sought to investigate the effect of pregnancy-associated cardio metabolic stresses in women with pregnancies complicated by GDM or pE on maternal myocardial energetics, structure, function or tissue characteristics.

The overall objectives of my study were:

1. To assess the physiological effects of pregnancy in women in the third trimester of a healthy singleton pregnancy on myocardial energetics, function and tissue characteristics.
2. To demonstrate if pregnancies complicated by GDM or pE are associated with maternal cardiac alterations during the third trimester of pregnancy and their recovery twelve-months post-partum in women with GDM or pE compared to women with healthy pregnancies.

# *Chapter 2: General methods*

## 2.1 General Methods

This single-center longitudinal prospective cohort study complied with the Declaration of Helsinki and was approved by the National Research Ethics Committee (REC20/NE/0117 for pregnancy scans and REC18/YH/0168 for non-pregnancy studies), and informed written consent was obtained from each participant. The pregnant participants were recruited via the Leeds Teaching Hospitals NHS Trust antenatal clinics attendance register and GDM clinics. The pE participants were identified from the database once diagnosed and upon admission to hospital for assessment in the third trimester. Healthy nulliparous volunteers with similar age and were recruited to serve as a healthy control cohort via word of mouth and study posters advertised on the information boards in the antenatal department.

## 2.2 Eligibility Criteria

Subjects were eligible for inclusion in the study if:

- Aged between 18 and above.
- 26-38 weeks' gestation
- Singleton pregnancy
- Willing to participate in a research study on a voluntary basis

**Gestational diabetes mellitus group:**

- Fasting glucose ≥5.6 mmol/L (≥100.8 mg/dL) and/or 2-hour glucose ≥7.8 mmol/L (≥140.4 mg/dL) after 75g oral glucose at ~26 weeks' gestation(90)

**Preeclampsia group:**

- BP> 140/90 mmHg and protein: creatinine ratio >0.3mg/dL

**Healthy nulliparous volunteers:**

- Willing and able to give informed consent for participation in the study

- Female, aged 18 and above
- Age-matched healthy volunteers with no known history of cardiac disease, hypertension or diabetes
- Able (in the investigator's opinion) and willing to comply with all study requirements

Subjects were **excluded** if any of the following were present:

- Contra-indications to magnetic resonance imaging (pacemaker, cranial aneurysm clips, metallic ocular foreign bodies, severe claustrophobia)
- Diagnosis or history of type 1 diabetes mellitus
- Atrial fibrillation
- Severe anaemia
- Presence of severe asthma (contraindication to adenosine)
- Known hypersensitivity to adenosine or gadolinium
- Participants with a diagnosis of significant (>moderate, diagnosed by their GP or a Cardiologist) valve disease
- Patients who are on insulin therapy
- Any other significant disease or disorder which may either put the participant at risk because of participation in the study, or may influence the result of the study, or the participant's ability to participate

- Patients who were diagnosed with hypertension previously, or blood pressure measurement at screening revealing systolic levels >140 mmHg and diastolic levels of >90mmHg (apart from preeclampsia group)
- All research participants with estimated glomerular filtration rate (eGFR) <30ml/min (stage 3-5 renal disease) were excluded from the study. Participants had a blood test to assess kidney function at the first screening visit
- Previous renal transplant
- Involvement in other studies thought to compromise resulting study data or the health of the participant
- Current smoker
- Women with pre-existing diagnosis of pE
- Antenatally small for gestational age babies on transabdominal ultrasound (<10$^{th}$ centile for estimated fetal weight)
- Congenital heart disease

## 2.3 Clinical assessments

On the **Visit 1** all subjects underwent a clinical assessment. This included history for:

- The presence of exclusion criteria as documented above
- Medical history and drug history including allergies
- Cardiovascular examination was also performed to assess for the presence of ventricular hypertrophy and valvular heart disease

Blood tests were performed which included:

- Serum cholesterol (total cholesterol levels, low density lipoprotein (LDL) and high density lipoprotein (HDL)), estimated glomerular filtration rate, glucose, HBA1c, insulin, free fatty acids, triglyceride, NT-proBNP, full blood count and aminotransferase (ALT), bilirubin and albumin

The following investigations were carried out:

- Blood pressure measurements using a manual sphygmomanometer (an average of three supine measures taken over 10 minutes (DINAMAP-1846-SX, Critikon Inc., Tampa, Florida)
- Hip circumference (cm) and waist circumference (cm) measurements
- Height (cm) and weight (kg) using calibrated scales.
- 12 lead electrocardiogram (ECG)
- Urine samples for albumin: creatinine ratio
- Multi-parametric CMR and $^{31}$P-MRS scans

**Visit 2** included obtaining information on fetal growth velocities for the pregnancy cohorts.

**Visit 3** included also included CMR and $^{31}$P-MRS scans 12 months after delivery. On the day of arrival all participants had:

- Blood pressure measurements using a manual sphygmomanometer (an average of three supine measures taken over 10 minutes (DINAMAP-1846-SX, Critikon Inc., Tampa, Florida)
- 12 lead electrocardiogram, (ECG)
- Hip circumference (cm) and waist circumference (cm) measurements
- Height (cm) and weight (kg) using calibrated scales.

- Blood tests after an 8 hour fast for serum cholesterol (total cholesterol, low density lipoprotein (LDL) and high density lipoprotein(HDL)), creatinine check to measure glomerular filtration rate, glucose, HBA1c, insulin, free fatty acids, triglyceride, NT-proBNP, full blood count and aminotransferase (ALT), bilirubin and albumin.

**Delivery and placental tissue assessments**

- Placental tissue and umbilical cord will be obtained following delivery
- Morphological features of placental dysfunction (terminal villi volume and terminal villi surface area)(91) and angiogenic gene expression will be assessed from cultured endothelial cells obtained from the placental specimens to determine the role of feto placental endothelial cells in angiogenesis in HP and in pregnancies complicated by preeclampsia or gestational diabetes mellitus(92)

## 2.4 Scan Protocols

Participants underwent a comprehensive CMR protocol which measured the following in the first visit

(i) $^{31}$P-MRS at rest

(ii) SSFP cine imaging for assessments of volumes, cardiac mass and function

(iii) T1 mapping of the 3 short axis slices of the heart (base, mid and apex)

(iv) T2 weighted imaging of the mid short axis slice of the heart

The second visit protocol comprised of the following sequences

(i) $^{31}$P-MRS at rest

(ii) SSFP cine imaging for assessments of volumes, cardiac mass and function

(iii) T1 mapping of the 3 short axis slices of the heart (base, mid and apex)

(iv) T2 weighted imaging of the mid short axis slice of the heart

(v) Rest and stress adenosine perfusion

(vi) Late gadolinium enhancement, (LGE) to assess patchy fibrosis

(vii) 3D whole heart coronary imaging

(viii) Post contrast T1 mapping (15 minutes from the injection of the gadolinium)

All scanning was conducted on a Siemens 3T Trio MR system (Erlangen, Germany). Average scan time is ~150 minutes for the Visit 2 while it was 30 minutes for the Visit 1; figure 2.1 shows the scan timeline for Visit 1 and Visit 2


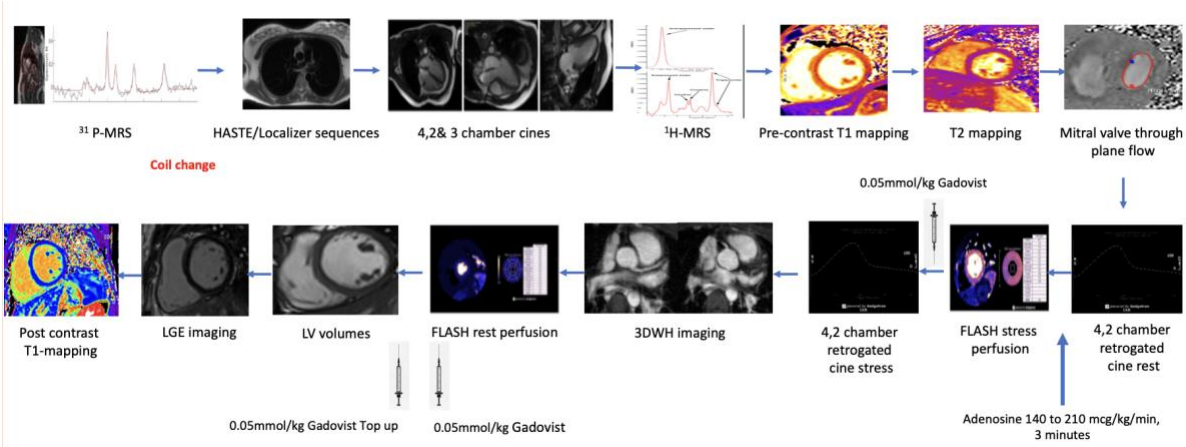

Figure 2.1: Timeline for the scan protocols for visits 1 and 2. Average scan time was ~150 minutes for the Visit 2 while it was 30 minutes for the Visit 1.

## 2.5 Cardiac Volumes, Function and Mass

CMR is precise, reproducible and well validated for measuring left ventricular volumes and mass.(93) We acquired cardiac volumes using Steady State Free Precession (SSFP) cine imaging. Pilot, horizontal long axis, vertical long axis, left ventricular outflow tract (LVOT) views, left and right ventricular short axis stack of contiguous images were acquired with the patient in the supine position. Each slice was 8mm thick with no inter slice gap and was retrospectively gated with echo time (TE), 1.4 ms; repetition time (TR), 3.9 ms; flip angle, 52°. To minimize the effects of respiratory motion, the slices were obtained during a breath-hold at the end of normal expiration.

Left ventricular (LV) and right ventricular (RV) short axis epicardial and endocardial borders were contoured manually from base to apex at end diastole and the endocardial border was again traced at end systole, (figure 2.2) for determining end diastolic volume (EDV); end systolic volumes (ESV); stroke volume (SV) using CVI42© (Circle Cardiovascular Imaging Inc., Calgary, Canada). The basal slice was selected for the LV when at least 50% of the blood volume was surrounded by myocardium in both end-diastole and end-systole. The apical slice was defined as the final slice displaying intracavity blood pool at both end-diastole and end-systole. For the right ventricle, volumes below the pulmonary valve were included (figure 2.2). From the inflow tract, RV volumes were excluded if the surrounding muscle was thin and not trabeculated, suggestive of the right atrium.

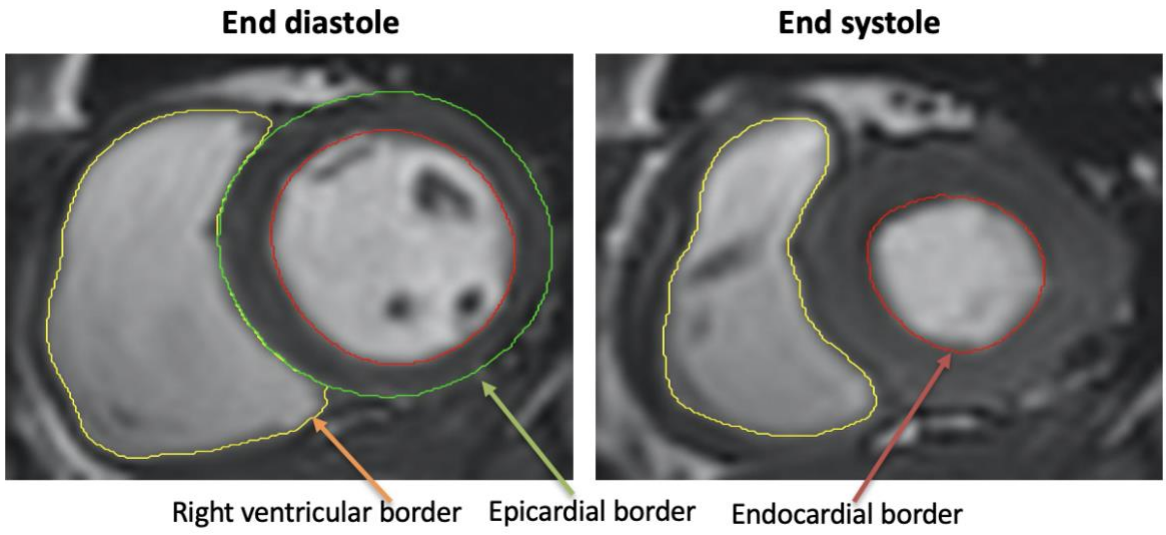


Figure 2.2: Left and right ventricular contours in end-diastole and end-systole

Ejection fraction (EF) and cardiac output (CO) were calculated with the formula: EF = SV/EDV, CO=SV x heart rate. Myocardial mass was calculated by subtracting the endocardial volume from the epicardial volume. Based on our prior knowledge of myocardial specific gravity (1.05 g/cm$^3$), left ventricular mass was calculated.

The left atrial (LA) volume and LA EF were calculated using the biplane area-length method in the horizontal and vertical long axes. The LA endocardial border was manually contoured in both the horizontal and vertical long axes views with the mitral annulus serving as the division between the LA and LV. The maximum LA area was contoured in the frame immediately prior to mitral valve opening. The minimum LA area was contoured in the frame immediately after mitral valve closure. LA volumes (LAV) were calculated using the area-length method, where: volume = (0.85 × area$^2$)/length. LAEF was derived as follows: LAEF = (LAVmax − LAVmin) /LAVmax.

## 2.6 Phosphorus Magnetic Resonance Spectroscopy

All scans were performed on a 3.0 Tesla MR system (Prisma, Siemens, Erlangen, Germany). 31P-MRS was performed to obtain the PCr/ATP from a voxel placed in the mid-ventricular septum, with the subjects lying supine with the 31P transmitter/receiver cardiac coil (Rapid Biomedical GmbH, Rimpar, Germany) placed over their heart, in the iso-centre of the magnet. Coil position was standardised to be placed above the mid ventricular septum (figure 2.3). A series of inversion-recovery free induction decay signals were acquired, in order to allow for correction of transmit efficiency differences between subjects (due to variable coil loading) during analysis.(94) Four fiducial markers were positioned on the anterior coil surface to allow spatial localisation of the coil relative to the patient anatomy and spectroscopy acquisition. These data allowed determination of study-specific flip angle maps to allow correction for the differential radiofrequency saturation of metabolites. 31P-MRS data were acquired with a non-gated 3-D acquisition-weighted chemical shift imaging (CSI) sequence.(95) The acquisition matrix was 16 x 8 x 8 for the protocol. Field of view was 240 x 240 x 200 mm. The acquisition was run with a fixed TR of 720ms. Two 25mm saturation bands were placed over the chest wall muscle and an additional 25 mm saturation band was placed over the liver.

$^{31}$P-MRS spectra was processed with a custom Matlab (The Mathworks Inc., Nattick, MA) implementation of the Advanced Method of Accurate, Robust, and Efficient Spectroscopic (AMARES) fitting algorithm(96), using prior knowledge(97) specifying 11 Lorentzian peaks (α,β,γ-ATP multiplet components, PCr, PDE, and 2×2,3-DPG),fixed amplitude ratios and scalar couplings for the multiplets, and a fixed begin time.(98).Peak areas were corrected for Nuclear Overhauser Effects (NOE) using the following empirical correction factors(94): PCr 0.80, β-ATP 0.88, α-ATP 0.88, γ-ATP 0.79, 2,3-DPG 0.70. Partial saturation corrected the

excitation flip angle at the centre of the chosen voxel and literature $T_1$ values(99): PCr 3.8 s, γ-ATP 2.4 s, α-ATP 2.5 s, β-ATP 2.7 s, 2,3-DPG 1.39 s, and PDE 1.1 s. The resulting ATP amplitudes were averaged and corrected for blood contamination by subtracting 11% of the total 2,3-DPG amplitude.(100)

Acquisition time was 9 minutes. $^{31}$P-MRS post processing analysis was performed as previously described.(101,102)

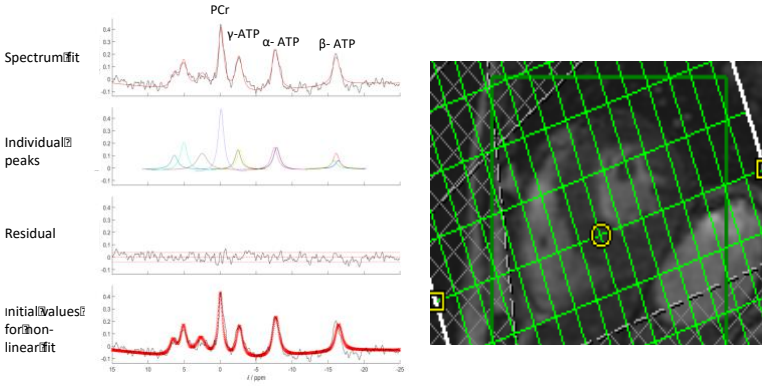


Figure 2.3: Magnetic resonance spectroscopy (MRS) voxel position and phosphocreatinine/adenosine triphosphate( PCr/ATP) spectra obtained at rest. PCr/ATP was reported as the blood and

saturation-corrected values of PCr to the average of γ-ATP, α-ATP and β-ATP.

## 2.7 Strain Imaging

### Strain and mitral annular plane systolic excursion (MAPSE):

A convolutional neural network (CNN) model (103) was used for the automated measurement of Global Longitudinal Shortening (GL-Shortening) and mitral annular plane systolic excursion (MAPSE) in the 2-chamber and 4-chamber cine images implemented directly on the CMR scanners. The inferoseptal and anterolateral mitral annular hinge points were detected from the 4-chamber view. The anterior and inferior points were detected from the 2-chamber view. The apex was marked for all views. The detection was performed for every cine phase covering the entire cardiac cycle (figure 2.4).

For strain analysis, semi-automated feature tracking analysis in Circle cvi[42] software (Circle Cardiovascular Imaging Inc., Calgary, Alberta, Canada) was used. Left ventricular epicardial and endocardial borders were manually traced in the 2-, 3-, and 4-chamber views at end-diastole, which were then propagated throughout the cardiac cycle. Automatic feature tracking yielded GLS measures. All contour tracings were inspected to ensure fidelity with manual adjustments as necessary. GLS measures included at least 2 long-axis images for strain assessment and were expressed as a percentage in which higher (less negative) values indicated worse contractile function.

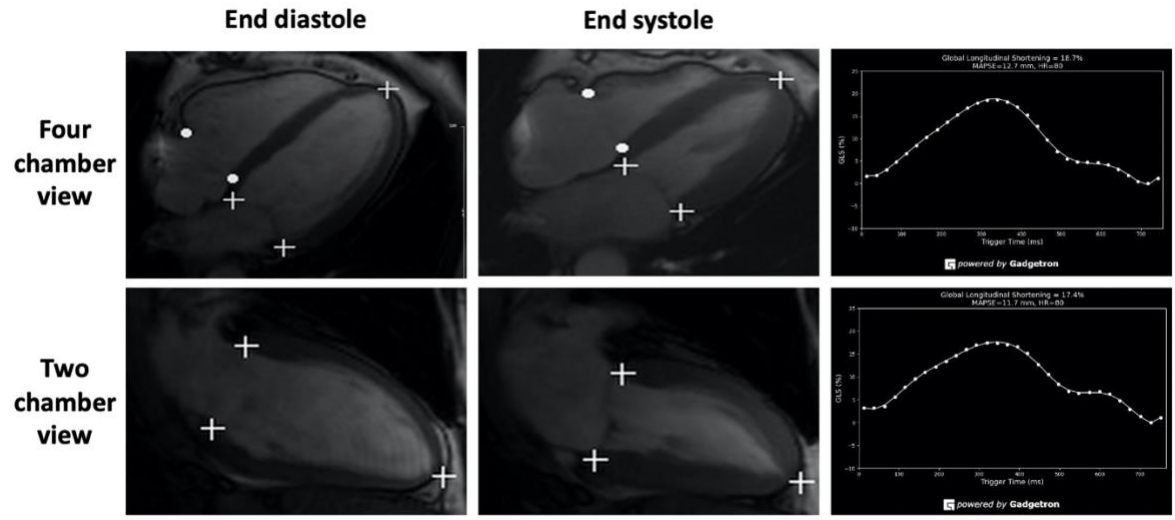


Figure 2.4: Global longitudinal shortening (GLS) and mitral annular plane systolic excursion (MAPSE) in two chamber and four chamber views

## 2.8 Diastolic function assessment

To perform assessments of the diastolic function, phase contrast imaging of the mitral valve was performed (figure 2.5). The phase contrast slice was positioned at the tip of the mitral valve leaflets as seen in systole to avoid the left ventricular outflow tract and this was then assessed in the horizontal long axis, vertical long axis and left ventricular outflow tract views. A free breathing, time-resolved acquisition with velocity-encoding perpendicular to this plane was acquired. Post processing was done using CVI42© by contouring round the mitral valve (MV) leaflets in end systole and propagating the contour to all acquired phases followed by manual correction of the contours as required. Using this method peak E and A waves were obtained.

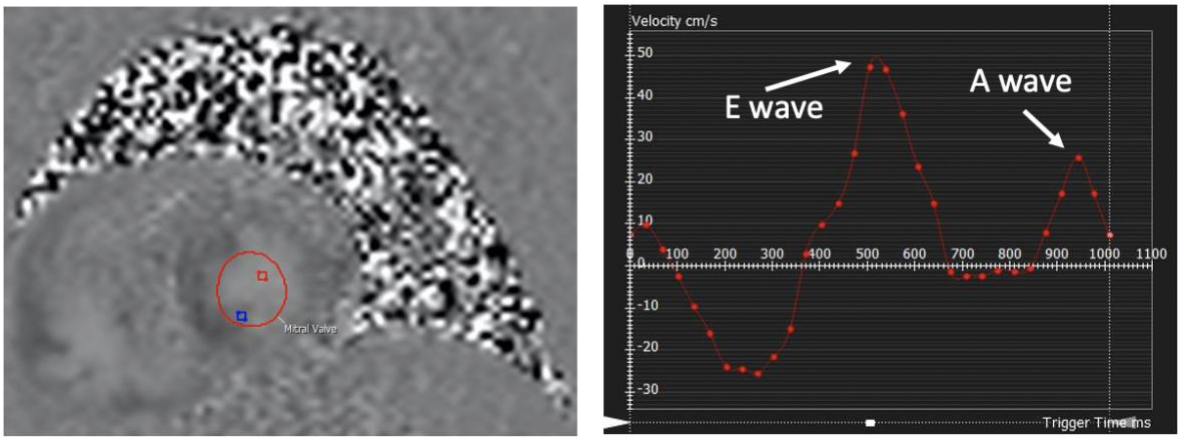


Figure 2.5: Phase contrast imaging of the mitral valve inflow and the E and A waves obtained

## 2.9 Native T1, post contrast T1 measurements and T2 mapping

Native T1 mapping was acquired in three slices using a breath-held modified Look-Locker inversion recovery acquisition, as previously described (104) (pre-contrast 5 seconds [3 seconds] 3 seconds and post-contrast 4 seconds [1 second] 3 seconds [1 second] 2 seconds schemes) and were planned using the 3 of 5 method (105). Post-contrast T1 mapping acquisition was performed exactly 15 minutes after the last contrast injection using identical planning as the native T1 map in the same three slices (figure 2.6). Post-contrast T1 was used in chapter 6.

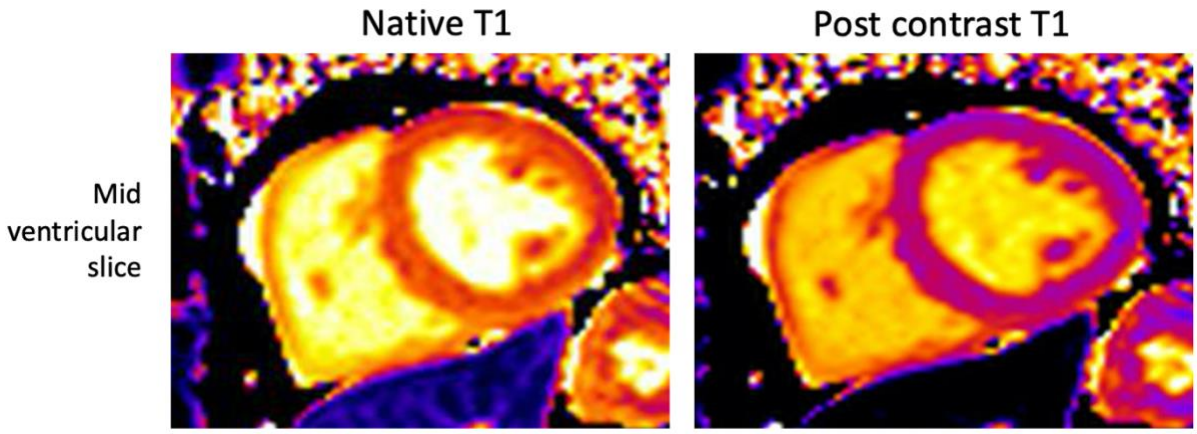

Figure 2.6: Native T1 and post-contrast T1 images at the mid-ventricular level

T2 maps were acquired from the matching 3 short-axis positions to native T1 mapping using a T2 prepared true fast imaging with steady-state precession (TrueFISP) pulse sequence to produce single-shot T2 prepared images, each with different T2 preparation times as previously described(106). The T2 prepared TrueFISP images were acquired were acquired with 3 recovery heartbeats to allow for sufficient magnetization recovery in between acquisitions. Motion correction was enabled to prevent mis registration between images(107). T2 was estimated by pixel-wise fitting assuming mono exponential signal decay, and a color, scaled, motion-corrected myocardial T2 map was then generated(107). T2 mapping parameters were as follows: acquisition window duration, 193.27ms; echo spacing, 2.5ms; echo time, 1.32ms; field-of-view (FOV) read, 360 mm; FOV phase, 80.2%; phase resolution, 75%; slice thickness, 8mm.

## 2.10 Quantitative Perfusion

In chapter 6, perfusion imaging used a free-breathing, fast low-angle shot (FLASH) MR protocol with motion-corrected (MOCO) automated in-line perfusion mapping using the Gadgetron streaming software image reconstruction framework, as previously described (108). Stress perfusion imaging was performed with adenosine which was infused at a rate of 140 µg/kg/min and increased up to a maximum of 210 µg/kg/min according to hemodynamic and symptomatic response (a significant hemodynamic response to adenosine stress was defined as a >10-beats/min increase in heart rate or a BP drop < 10 mm Hg and >1 adenosine-related symptom, e.g., chest tightness, breathlessness). The participants had continuous ECG

and HR monitoring with BP monitoring at 90 second intervals. A minimum 10-minute interval was kept between perfusion acquisitions to ensure equilibration of gadolinium kinetics and resolution of all hemodynamic effects of adenosine. For each perfusion acquisition, an intravenous bolus of 0.05 mmol/kg of gadobutrol (Gadovist, Leverkusen, Germany) was administered at 5 mL/s followed by a 20-mL saline flush using an automated injection pump (Medrad MRXperion Injection System, Bayer, Leverkusen, Germany). (Figure 2.7)

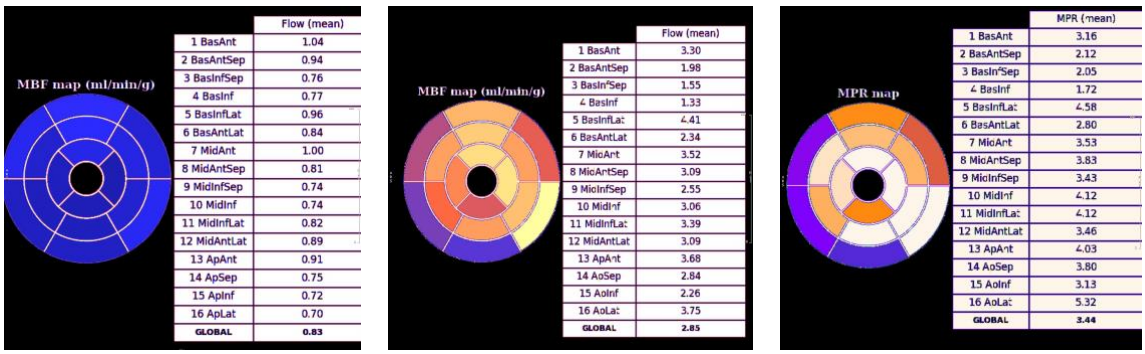


Figure 2.7: Representative quantitative perfusion maps of myocardial blood flow (MBF) at rest, MBF at stress and myocardial perfusion reserve (MPR)

## 2.11 Late Gadolinium Enhancement

For LGE assessment, a top-up bolus of 0.05 mmol/kg of body weight of a gadolinium-based contrast agent- gadobutrol (Gadovist®, Bayer Pharma, Berlin, Germany) followed by a 20-mL saline flush were administered through an intravenous cannula inserted into the antecubital fossa. Electrocardiographically gated images were acquired at least 5mins after contrast

administration in matching short axis plane slices as T1 images a to exclude the presence of previous silent myocardial infarction or regional fibrosis. Areas of LGE were visually scored as absent or present.

## 2.12 Three-dimensional whole heart coronary magnetic resonance angiography

This protocol was conducted by performing 4 chamber cine free breathing using 40-50 phases to generate more trigger times for assessment. Following this the 3D navigator whole heart imaging sequence was performed using position acquisition volumes to cover the heart and liver dome navigators positioned accordingly.(109) The data window duration was set to less than 150ms using the number of segments. The data window start, which should be the same time as the lowest value trigger time, was controlled by the trigger delay value. Once scout mode was applied, scanning took place for approximately 8 minutes' duration.

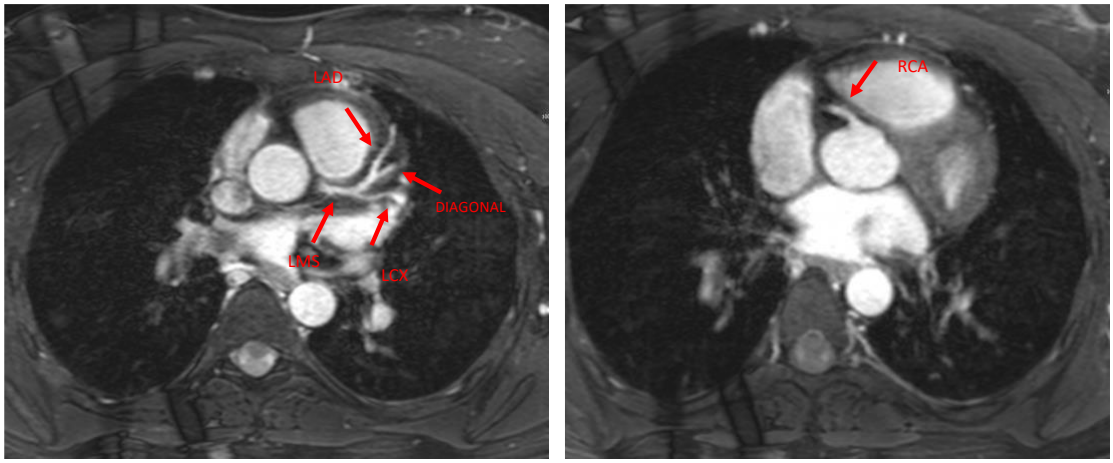


Figure 2.8 : Representative images of the coronary arteries; left main stem (LMS), left anterior descending (LAD), left circumflex (LCx), right coronary artery (RCA) using 3D whole heart imaging

## 2.13 Statistical Analysis

Statistical analyses were performed using SPSS (IBM SPSS statistics, version 26.0). All data were checked for normality using Shapiro-Wilk test and presented as mean ± standard deviations, and median (interquartile range) as appropriate. Normally distributed data sets were analysed with the independent Student *t* test. Categorical data were compared with Pearson's chi-square test. Comparisons between more than two groups were performed by 1-way analysis of variance with post hoc Bonferroni corrections. Bivariate correlations were performed using the Pearson correlation coefficient. For these tests a p-value of ≤0.05 was considered statistically significant.

The primary endpoint was myocardial PCr/ATP ratio to confirm alterations in myocardial energetics in GDM and pE cohorts. Our pilot data showed the mean rest PCr/ATP ratio in GDM to be 1.75 (SD:0.2), in pE 1.7 (SD 0.5) compared to 2.50 (SD:0.5) for HP controls. With 20 participants providing data in myocardial energetics in each group, there would be 90% power to detect a difference of at least 0.30 between GDM or pE cohorts compared to those HP based on our pilot data based on a one-way analysis of variance at 5% significance level.

# *Chapter 3: Myocardial physiological responses to the third trimester of healthy pregnancy*

## 3.1 Abstract

**Background-** Pregnancy requires significant cardio-metabolic adaptation and is therefore considered a "stress test" for future cardiovascular disease (CVD). Despite recognized hemodynamic and metabolic changes during pregnancy, there is limited information on myocardial adaptive changes to pregnancy.

**Objectives-** We aimed to investigate the physiological effects of pregnancy in women in the third trimester of a healthy singleton pregnancy on myocardial energetics, function and tissue characteristics compared to age matched nulliparous controls.

**Methods-** Thirty-nine healthy pregnant women (first pregnancies for all) and fifteen age-matching nulliparous healthy female controls were recruited. Participants underwent $^{31}$phosphorus magnetic resonance spectroscopy and cardiovascular magnetic resonance (cine imaging, velocity-encoded mitral in-flow imaging, T1 mapping) at 3T. Blood samples were taken for biochemistry and N-terminal pro brain natriuretic peptide (NTproBNP) measurements.

**Results-** Plasma total cholesterol (Pregnancy:6.8±1.7mmol/L, Controls:4.8±1.1mmol/L; p=0.0001), triglyceride (Pregnancy:2.4±1.0mmol/L, Controls:0.9±0.4mmol/L; p=0.0001) and insulin levels (Pregnancy: 222±163pmol/L vs Controls: 73±66pmol/L, p=0.0012) were higher and hemoglobin was lower in pregnancy (Pregnancy:122±9g/L, Controls:134±7g/L; p=0.0001). There were no significant differences in blood pressure measurements, NTproBNP, HbA1c, or glucose levels. The mean resting heart rate was 40% higher and consistent with this the mean cardiac output was 20% increased in the pregnant group. However, there were no significant differences in left-ventricular volumes, mass or ejection fraction, diastolic function (mitral in-flow E/A and deceleration time) or global longitudinal strain between the groups. Despite the differences in plasma metabolic profile and the resting

heart rates between the two groups, there were no significant differences in myocardial PCr/ATP ratio (Pregnancy:2.5±0.5, Controls:2.7±0.5; p=0.08). Myocardial native T1 was higher in pregnant women (Pregnancy:1326±34ms, Controls:1298±47ms; p=0.02).

**Conclusions-** Healthy pregnancy is associated with no significant changes in cardiac size, mass, function or myocardial energetics. Consistent with the increased heart rate in pregnancy, the cardiac output is higher in pregnant women. Pregnancy is also associated with mildly increased myocardial native T1 values which may reflect increased myocardial interstitial water retention and/or increased myocardial blood volume during pregnancy. CMR is well-tolerated in pregnancy and may play a significant role in assessing myocardial involvement in women at risk of perinatal complications.

## 3.2 Introduction

Cardiovascular disease (CVD) is the leading cause of maternal morbidity and mortality(110). Unlike the recent trends for men, the mortality from CVD is increasing in younger women(111,112). However, the mechanisms that contribute to worsening risk factor profiles in young women are not fully elucidated. Normal pregnancy requires significant maternal cardio metabolic adaptations including hyperdynamic circulation, systemic vasodilatation, increased filling capacity of the vasculature, volume expansion and alterations in lipid profile and insulin resistance.(8) Maternal inability to adapt to these physiological changes can expose underlying, previously silent, cardiac pathology, leading to appreciation of pregnancy as "nature's stress test"(113). Moreover, insufficient hemodynamic changes can result in adverse pregnancy outcomes (APO) with maternal and fetal morbidity(113). A better understanding of maternal myocardial adaptations to pregnancy is paramount for early detection of adverse myocardial alterations. The early detection of adverse myocardial alterations might offer the opportunity of early initiation of risk-modifying treatment prior to the onset of overt CVD, and prevention of adverse maternal cardiovascular outcomes and associated adverse fetal events(113).

Cardiovascular magnetic resonance (CMR) allows comprehensive evaluation of myocardial structure, function, strain and tissue characteristics with excellent reproducibility(114). CMR non-contrast parametric mapping methods are quantitative techniques that provide information on myocardial tissue type and composition in view of the surrounding environment without the need for contrast agents(68). CMR therefore provides insight into cardiovascular physiology and can be safely performed during pregnancy *without* gadolinium-based contrast agents(72). Data from registries and retrospective cohorts consistently indicate that non-contrast magnetic resonance imaging (MRI) performed at any stage of

pregnancy does not harm the baby(70-73). Despite this, there is only limited information on maternal adaptive changes to pregnancy in myocardial structure, function or tissue characteristics from prospective CMR studies(115) .

The relative concentration of phosphocreatine to ATP (PCr/ATP) is a sensitive index of the energetic state of the myocardium(77). $^{31}$P-MRS allows non-invasive assessment of the myocardial PCr/ATP ratio. Despite the recognized hemodynamic and metabolic changes during pregnancy the magnitude of adaptive changes to pregnancy in myocardial energetics has not been characterized previously.

Endothelial dysfunction has been shown to be prevalent in women with adverse pregnancy outcomes, and could remain complications beyond pregnancy, predisposing these women to further vascular complications and serving as a prognostic marker for future CVD(116,117). The peripheral endothelial vasodilator function can be measured non-invasively by the Endo-PAT 2000 device(118,119).

Combining CMR, $^{31}$P-MRS and Endo-PAT in an observational prospective case-control study we sought to assess the physiological effects of pregnancy in women in the third trimester of a healthy singleton pregnancy on myocardial energetics, function, tissue characteristics and peripheral vascular function.

## 3.3 Research design and methods

This single-center, cross-sectional, case-control study complied with the Declaration of Helsinki, it was approved by the National Research Ethics Committee (REC20/NE/0117 for pregnancy scans and REC18/YH/0168 for non-pregnancy studies), and informed written consent was obtained from each participant.

## Participants

A total of 54 participants including 39 pregnant women with an uncomplicated singleton pregnancy and 15 age-matching nulliparous healthy female controls were recruited in the study. The pregnant participants were recruited via the Leeds Teaching Hospitals NHS Trust maternity services and the antenatal clinics attendance register. Recruitment of the pregnant group was restricted to first pregnancies. Fetal growth assessments were performed at gestational week 33 with a transabdominal ultrasound as part of the routine clinical care, confirming uncomplicated progress of the pregnancy for each pregnant participant. All pregnancies were monitored to birth, all were deemed low risk antenatally with routine clinical maternal assessments and the week 33 transabdominal fetal ultrasound findings within the expected normal range. Non-pregnant women (nulliparous controls) were matched for age and ethnicity and were recruited from among the University of Leeds researchers.

## Inclusion and exclusion criteria

Participants with healthy on-going pregnancy, >18 years of age, 26-38 weeks' gestation and healthy nulliparous women were recruited. Women with a diagnosis of pE, GDM, antenatally small for gestational age babies on week 33 transabdominal ultrasound or any other adverse pregnancy outcomes, known cardiovascular problems (congenital or acquired heart disease), contra-indications to CMR (pacemaker, cranial aneurysm clips, metallic ocular foreign bodies, severe claustrophobia), subjects with medical conditions that could affect cardiac function including women with severe anemia, maternal diabetes (type I or type II), chronic renal

disease, renal transplantation, chronic hypertension, chronic liver disease were excluded. Controls were excluded if they had a history of cardiovascular or any other significant medical condition, tobacco smoking, contraindications to CMR or abnormal findings on 12-lead ECG.

### Anthropometric measurements

Height and weight were recorded and body mass index (BMI) was calculated. Brachial artery blood pressure (BP) was recorded as an average of 3 supine measures taken over 10 minutes (DINAMAP-1846-SX, Critikon Corp) and a 12-lead ECG was performed. A venous blood sample was taken from each participant for assessments of full blood count, estimated glomerular filtration rate (eGFR), lipid profile, liver function, glycated hemoglobin (HbA1c), insulin, triglycerides, high density lipoprotein (HDL), low density lipoprotein (LDL), total cholesterol levels and N-terminal pro hormone B-type natriuretic peptide (NT-proBNP) levels.

### $^{31}$Phosphorus magnetic resonance spectroscopy

$^{31}$P-MRS was performed to obtain the PCr/ATP ratio from a voxel placed in the mid-ventricular septum, with the subjects lying supine and a $^{31}$P transmitter/receiver cardiac coil (Rapid Biomedical GmbH, Rimpar, Germany) placed over the heart, in the iso-center of the magnet on a 3.0 Tesla MR system (Prisma, Siemens, Erlangen, Germany). A series of inversion-recovery free induction decay signals were acquired, to allow for correction of transmit efficiency differences between subjects during analysis[120]. Four fiducial markers were positioned on the anterior coil surface to allow spatial localization of the coil relative to the patient anatomy and spectroscopy acquisition. These data allowed determination of study-specific flip angle maps to allow correction for the differential radiofrequency saturation of metabolites. $^{31}$P-MRS data were acquired with a non-gated 3-D acquisition-weighted

chemical shift imaging (CSI) sequence[121]. The acquisition matrix was 16x8x8 for the protocol. Field of view was 240x240x200mm. The acquisition was run with a fixed TR of 720ms. Two 50mm saturation bands were placed over the chest wall muscle and an additional 25mm saturation band was placed over the liver.

## Cardiovascular magnetic resonance imaging

All scans were performed on a 3.0 Tesla MR system (Prisma, Siemens, Erlangen, Germany) and all participants underwent cardiac magnetic resonance imaging (MRI) scans. The CMR protocol (Figure 3.1) consisted of cine imaging using a steady-state free precession (SSFP) sequence, velocity-encoded mitral in-flow imaging, native T1 mapping and T2 mapping.

To capture cross-sectional mitral valve flow, velocity-encoded mitral in-flow imaging was planned from an acquisition plane placed at the position of the mitral valve at the moment of end-systole. Velocity sensitivity was set at 200 cm/s. The phase-contrast images were acquired using retrospective ECG gating under free breathing conditions, with the following average parameters: slice thickness 6mm, field of view 42 $cm^2$, matrix 256 × 192, repetition time 37.12ms, echo time 2.47ms, flip angle 20° and 2 averages. Complete coverage of the cardiac cycle was accomplished using view-sharing to acquire 60 cardiac phases per cycle.

Native T1 maps were acquired in 3 short-axis slices using a breath-held modified look-locker inversion recovery (MOLLI) acquisition (ECG triggered, native 5s(3s)3s; post-contrast 4s(1s)3s(1s)2s schemes; single shot, parallel imaging factor 2; trigger delay set for end diastole; flip angle 20°; slice thickness 8mm).

T2 maps were acquired from the matching 3 short-axis positions to native T1 mapping using a T2 prepared true fast imaging with steady-state precession (TrueFISP) pulse sequence to produce single-shot T2 prepared images, each with different T2 preparation times as

previously described(106). The T2 prepared TrueFISP images were acquired were acquired with 3 recovery heartbeats to allow for sufficient magnetization recovery in between acquisitions. Motion correction was enabled to prevent mis registration between images(107). T2 was estimated by pixel-wise fitting assuming mono exponential signal decay, and a color, scaled, motion-corrected myocardial T2 map was then generated(107). T2 mapping parameters were as follows: acquisition window duration, 193.27ms; echo spacing, 2.5ms; echo time, 1.32ms; field-of-view (FOV) read, 360 mm; FOV phase, 80.2%; phase resolution, 75%; slice thickness, 8mm.

Identical T1 and T2 mapping acquisition protocols were used for all participants in the study. A quality assurance standardization T1 and T2 phantom assessment was undertaken using the T1 Mapping and ECV Standardization (T1MES) phantom and analysis pipeline(122). These phantom tests were performed to assess the impact of heart rate variation on the T1 and the T2 mapping assessments set at different heart rates, starting from a minimal heart rate of 50bpm with an incremental rise of 10 beats per minute reaching up to maximal tested heart rate of 140bpm. A total of 10 phantom acquisitions were thus obtained.

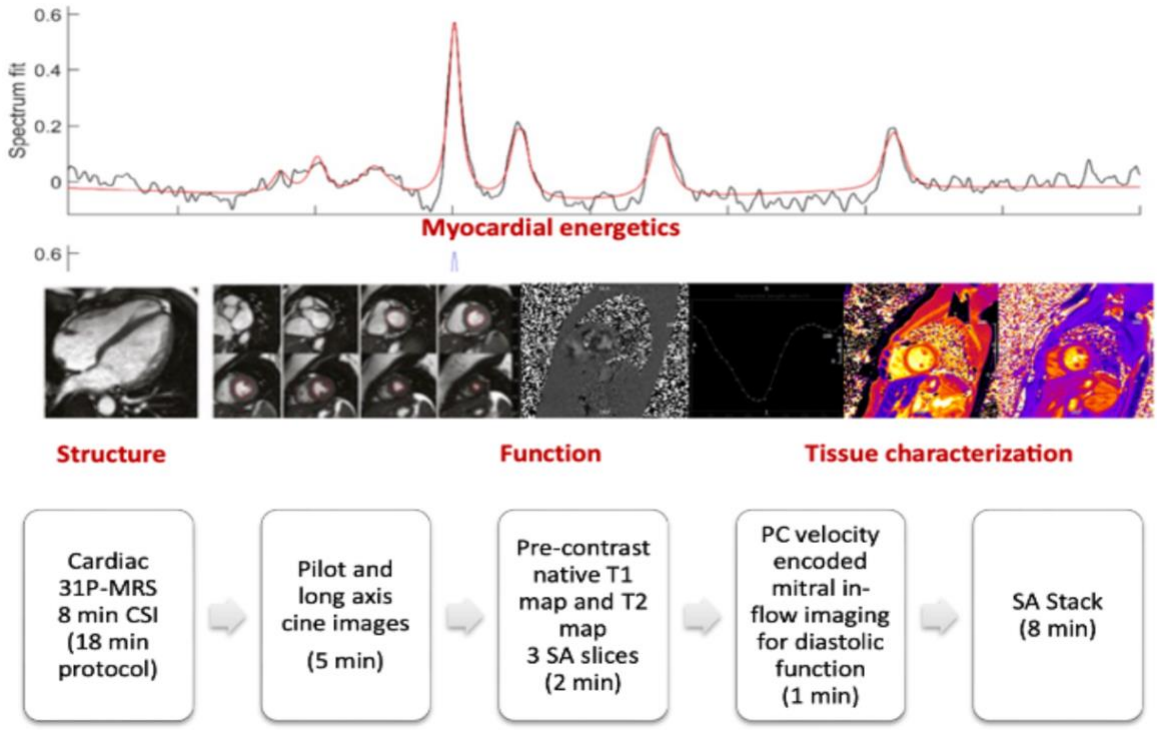


Figure 3.1: $^{31}$P Magnetic Resonance Spectroscopy( $^{31}$P-MRS) and cardiac magnetic resonance (CMR) Protocol (cine imaging, velocity-encoded mitral in-flow imaging, T1 and T2 mapping)

## Quantitative analysis

All $^{31}$P-MRS analysis was performed off-line by ST (with 2 years of $^{31}$P-MRS and CMR experience) using software within Matlab version R2012a (Mathworks, Natick, Massachusetts) as previously described(123). CMR post processing analysis using cvi42 software (Circle Cardiovascular Imaging, Calgary, Canada) was performed off-line blinded to all participant details by ST after completion of the study and all scan contours were subsequently reviewed by EL (with 8 years of CMR experience; level 3 EACVI accreditation) who was also blinded to participant details.

Global longitudinal shortening (GLS) data were derived from horizontal long-axis (HLA) and vertical long-axis (VLA) images, and image reconstruction and processing was implemented using the Gadgetron software framework with the previously developed convolutional neural

network for labelling landmarks on CMR images. The performance of this network was shown to be comparable to manual labeling(124).

Diastolic function was measured from mitral in-flow velocity-encoded images(125). Regions of interest were manually drawn on one frame to encircle the entire cross section of MV leaflets on the short-axis images and propagated using a semi-automated contouring mode on Circle cvi42 software (Circle Cardiovascular Imaging Inc., Calgary, Alberta, Canada) with manual override, yielding velocity vs time graphs characterizing diastolic E and A waves. The mean of maximum velocity obtained for MV was recorded. The deceleration time (DT) was calculated as previously described from the same images(125). On the CMR flow curve, a vertical line was drawn from the peak of the E wave to intersect the baseline which displayed the time delay at which the E wave peak occurred. A second line was drawn from the peak of the E wave following the downslope intersecting the baseline which gave the time delay of the E wave downslope. The time delay of the peak E wave was subtracted from the time delay of the E wave downslope intersecting the baseline to calculate the DT.

Native T1 and T2 maps were analyzed using cvi42 software (Circle Cardiovascular Imaging, Calgary, Canada) which were measured for each of the 16 segments using the AHA classification as previously described(107,126). Care was taken when placing the endo- and epicardial contours to avoid contamination by blood-pool and extra-myocardial structures to minimize the partial volume effect on myocardial T1 and T2 values. Non-contrast T1 and T2 mapping phantom scan tests were analysed by DB (with >6 years CMR physics expertise).

## Statistical analysis

Statistical analysis was performed using SPSS (IBM SPSS statistics, version 26.0). Categorical data were compared with Pearson's chi-square test. Continuous variables are presented as mean ±SD and were checked for normality using the Shapiro-Wilk tests. Comparisons of all CMR and biochemistry data were performed with two-tailed paired t-test or Mann Whitney U Test as appropriate. P≤0.05 was considered statistically significant. Bivariate correlations were performed using the Pearson or Spearman method as appropriate.

## 3.4 Results

### Participant demographics and biochemical characteristics:

Demographic, clinical, and biochemical data of the two study groups are shown in Table 3.1. Participants in both groups were of similar age (Pregnancy: 29±10y vs Controls 28±3y, p=0.7) and there were no significant differences in blood pressure between the two groups. Total cholesterol (Pregnancy: 6.8± 1.7mmol/L vs Controls 4.8±1.1, p=0.0001mmol/L) and triglyceride levels (Pregnancy: 2.3 ± 1.0mmol/L vs Controls 0.9±0.4mmol/L, p=0.0001) were higher, hemoglobin (Pregnancy: 122±9 g/L vs Controls 134±7 g/L, p= 0.0001) and hematocrit (Pregnancy: 0.37±0.03L/L vs Controls: 0.42± 0.02L/L, p= 0.0001) were lower in pregnancy. There were no significant differences in NT-proBNP between the two groups. While the glucose and HbA1c levels were comparable between the two groups, insulin levels were higher in the pregnant group (Pregnancy: 222±163pmol/L vs Controls: 73±66pmol/L, p=0.0012). Resting heart rates (Pregnancy: 86±23bpm vs Controls 61±9bpm, p=0.0002) were higher in the pregnant group.

| Variable | Non-pregnant participants (n=15) | Pregnant participants (n=39) | P value |
|---|---|---|---|
| **Age, y** | 28±3 | 29±10 | 0.7 |
| **Ethnicity, white, %** | 67 | 87 | 0.2 |
| **Gestational date at CMR** | - | 29±2 | - |
| **BMI, kg/m$^2$** | 23±4 | 27±4 | **0.003** |
| **Heart rate, bpm** | 61±9 | 86±23 | **0.0002** |
| **Systolic blood pressure, mmg** | 112±7 | 116±12 | 0.2 |
| **Diastolic blood pressure, mmHg** | 73±6 | 72±7 | 0.6 |
| **Hemoglobin, g/L** | 134±7 | 122±9 | **0.0001** |
| **Hematocrit, L/L** | 0.42±0.02 | 0.37±0.03 | **0.0001** |
| **Total cholesterol, mmol/L** | 4.8±1.1 | 6.8± 1.7 | **0.0001** |
| **HDL, mmol/L** | 1.9±0.4 | 2.2±0.5 | **0.04** |
| **LDL, mmol/L** | 2.4±0.5 | 3.6±1.2 | **0.0005** |
| **TG, mmol/L** | 0.9±0.4 | 2.4±1.0 | **0.0001** |
| **Creatinine, umol/L** | 55±6 | 46±11 | **0.005** |
| **eGFR, ml/min/1.73m$^2$** | 90 ± 0 | 90± 0 | 1 |
| **Urine Alb/creatinine ratio** | - | 1.6±2 | - |
| **HBA1c, mmol/mol** | 32± 3 | 31±6 | - |
| **Glucose, mmol/L** | 5.1±0.5 | 5.1±1.4 | 1.0 |
| **C-peptide, pmol/L** | 1468±892 | 1592±966 | 0.7 |
| **Insulin, pmol/L** | 73±66 | 222±163 | **0.02** |
| **NT- proBNP, ng/L** | 55±15 | 72±47 | 0.2 |
| **Free fatty Acids (FFA), mmol/L** | - | 0.3±0.1 | - |
| **D-3-Hydroxybutyrate, mmol/L** | - | 0.1±0.04 | - |

Values are means (SD) or median (IQR) for continuous variables and number (%) for categorical variables. BMI indicates body mass index; kg, kilograms; n, number; bpm, beats per minute; mmHg, millimeters of mercury; g/l, gram per Liter; HDL, high density lipoprotein; mmol/L, millimoles per litre; LDL, low density lipoprotein; TG, triglyceride; eGFR, estimated glomerular filtration rate; ml/min/1.73m2, millilitre per minute per (1.73 square meters);

pmol/L, picomoles per litre; NT-pro BNP, N-terminal pro hormone B-type natriuretic peptide; HBA1c, glycated haemoglobin; FFA, free fatty acids

Table 3.1: Clinical characteristics of study cohort

### Myocardial structure and function global comparisons:

CMR results for biventricular volumes, systolic function, LV mass, diastolic function and strain parameters are summarized in Table 3.2.

The two groups were comparable in terms of LV volumes, mass and EF. However, in parallel with the higher resting heart rates, cardiac output was higher in pregnancy (Pregnancy: 6.6±1l/min vs Controls: 5.8±1.1l/min; p=0.01). There were no significant differences in diastolic function (mitral in-flow E over A ratio or DT measurements), or in GLS between the two groups. (Figure 3.2) Right ventricular volumes and function were also comparable between the groups.

| Variable | Non-pregnant participants (n=15) | Pregnant participants (n=37) | P value |
|---|---|---|---|
| **LV end diastolic volume (ml)** | 134±20 | 142±23 | 0.2 |
| **LV end diastolic volume index (ml/m$^2$)** | 79±10 | 75±13 | 0.3 |
| **LV end systolic volume (ml)** | 52±10 | 59±12 | 0.05 |
| **LV end systolic volume index (ml/m$^2$)** | 31±5 | 31±6 | 1 |
| **LV stroke volume (ml)** | 82±11 | 83±15 | 0.8 |
| **LV ejection fraction (%)** | 62±4 | 60±5 | 0.1 |
| **LV mass (g)** | 82±11 | 88±16 | 0.2 |
| **LV mass index (g/m$^2$)** | 49±7 | 47±8 | 0.4 |

| | | | |
|---|---|---|---|
| **Cardiac output (l/min)** | 5.8±1.1 | 6.6±1 | **0.01** |
| **Cardiac index (l/min/m²)** | 3.4±0.6 | 3.5±0.5 | 0.5 |
| **Wall thickness (mm)** | 5.5±1.2 | 5.6 ± 1.2 | 0.8 |
| **RV end diastolic volume (ml)** | 148±21 | 155±27 | 0.4 |
| **RV end diastolic volume index (ml/m²)** | 87±12 | 83±14 | 0.3 |
| **RV end systolic volume (ml)** | 67±15 | 71±16 | 0.4 |
| **RV end systolic volume index (ml/m²)** | 40±8 | 38±8 | 0.4 |
| **RV stroke volume (ml)** | 79±11 | 83±14 | 0.3 |
| **RV ejection fraction (%)** | 55±5 | 55±6 | 1 |
| **Global longitudinal strain (%)** | 21±2 | 20±3 | 0.3 |
| **Mean native T1 relaxation time (ms)** | 1298±47 | 1326±34 | **0.02** |
| **T2 relaxation time, (ms)** | 42±2 | 40±3 | **0.02** |
| **E/A ratio** | 1.5±0.5 | 1.7±0.4 | 0.1 |
| **PCr/ATP** | 2.7±0.5 | 2.5±0.5 | 0.08 |
| **Deceleration time DT (ms)** | 164±40 | 151±37 | 0.2 |

Values are means (SD) or median (IQR) for continuous variables and number (%) for categorical variables. LV indicates left ventricular; ml, milliliter; ml/$m^2$, milliliters per square meter of body surface area; g, gram; g/$m^2$, gram per square meter of body surface area; LVEF, left ventricular ejection fraction; RV, right ventricular; LA, left atrium; MAPSE, mitral annular plane systolic excursion; DT, deceleration time

Table 3.2: CMR findings of the study cohort

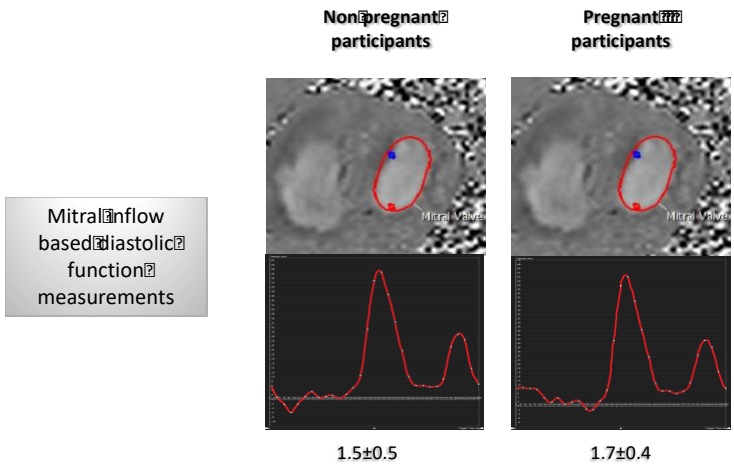


Figure 3.2: Representative examples of diastolic function (mitral in-flow E over A ratio or deceleration time (DT) measurements between the pregnant participants and non-pregnant participants (nulliparous controls)

## Myocardial tissue characteristics

Compared to non-pregnant controls, myocardial native T1 was 2% higher in pregnant women (Pregnancy 1326±34ms vs Controls: 1298±47ms, p=0.02), whilst T2 was 5% lower (Pregnancy:40 ±3ms vs controls 42±2ms, p=0.02), (Figures 3.3 and 3.4).

However, due to the presence of significant heart rate differences between the pregnant participants and the nulliparous controls, the impact of heart rate variation on the T1 and the T2 mapping assessments were tested by phantom scans set at different heart rates. These phantom scans revealed that whilst the T1 measurements remain stable across the different heart rates (Figure 3.5), the T2 measurements showed significant heart rate dependency with a trend to lower T2 values at higher heart rates.

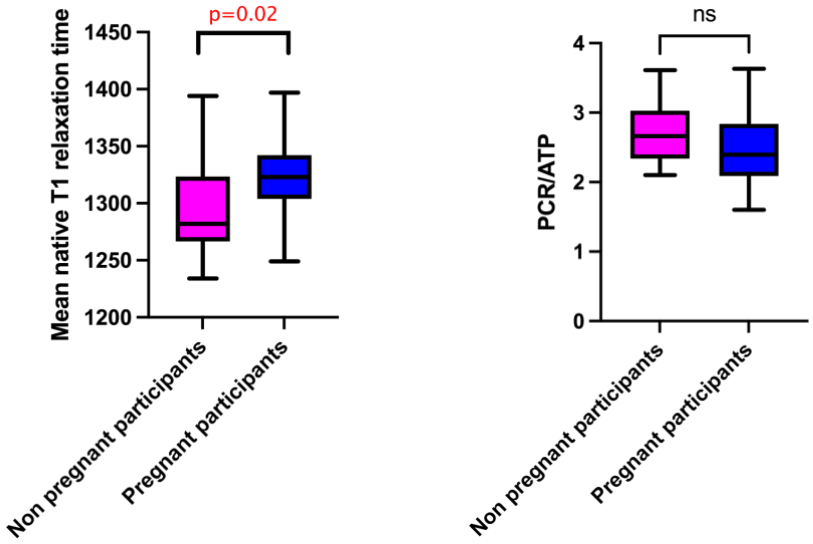


Figure3.3: Box plots demonstrating mean native T1 relaxation time and phosphocreatinine/adenosine triphosphate (PCR/ATP) ratio between the pregnant participants and non-pregnant participants (nulliparous controls).

Error bars indicate standard deviations. NS=Non-significant

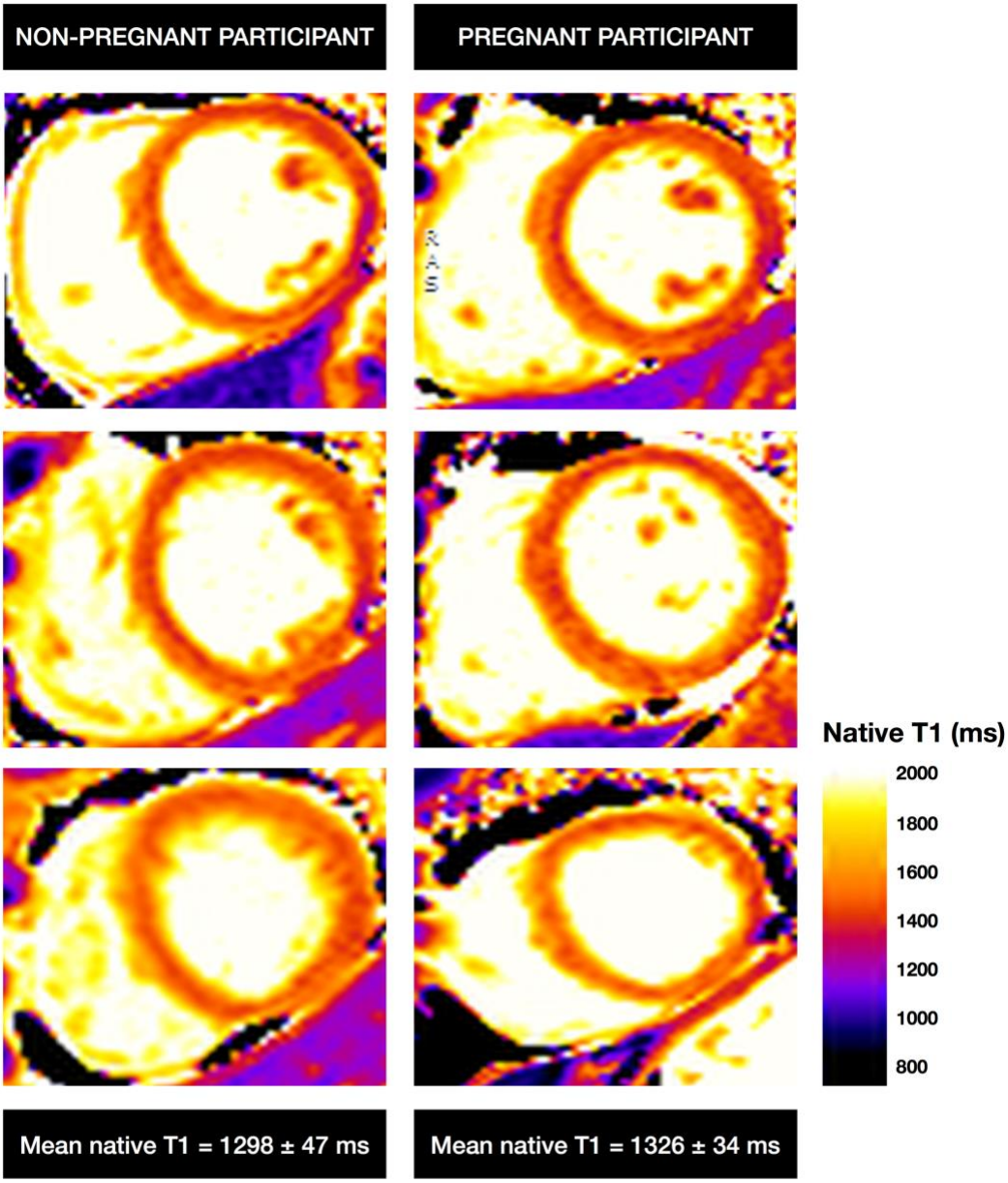


Figure 3.4 : Representative examples of mid-left ventricular myocardial native T1 maps from a pregnant participant and a non-pregnant participant (nulliparous control) with group mean values and standard deviations provided

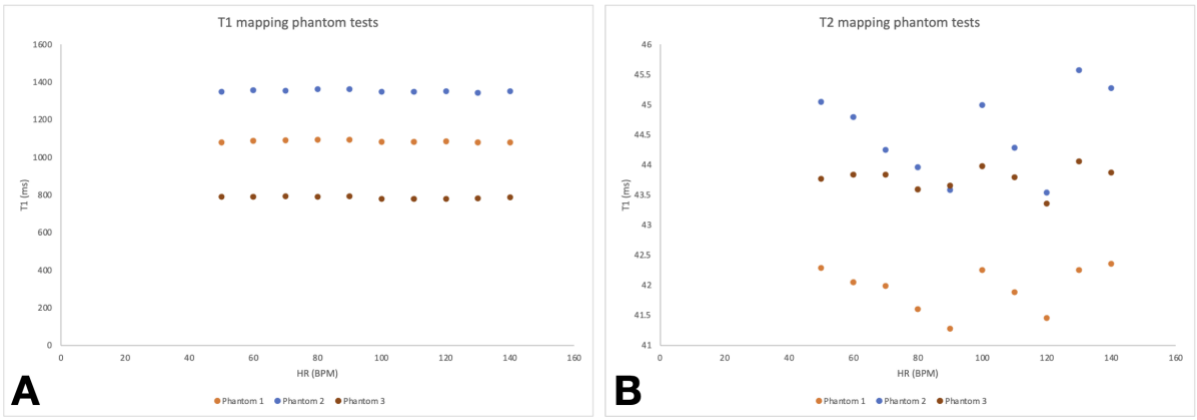


Figure 3.5 : T1 and the T2 mapping assessments were tested by phantom scans set at different heart rates

## Myocardial energetics

There were no significant differences in myocardial energetics between the two groups (Pregnancy: 2.5±0.5 vs Controls 2.7±0.5bpm, p=0.08).

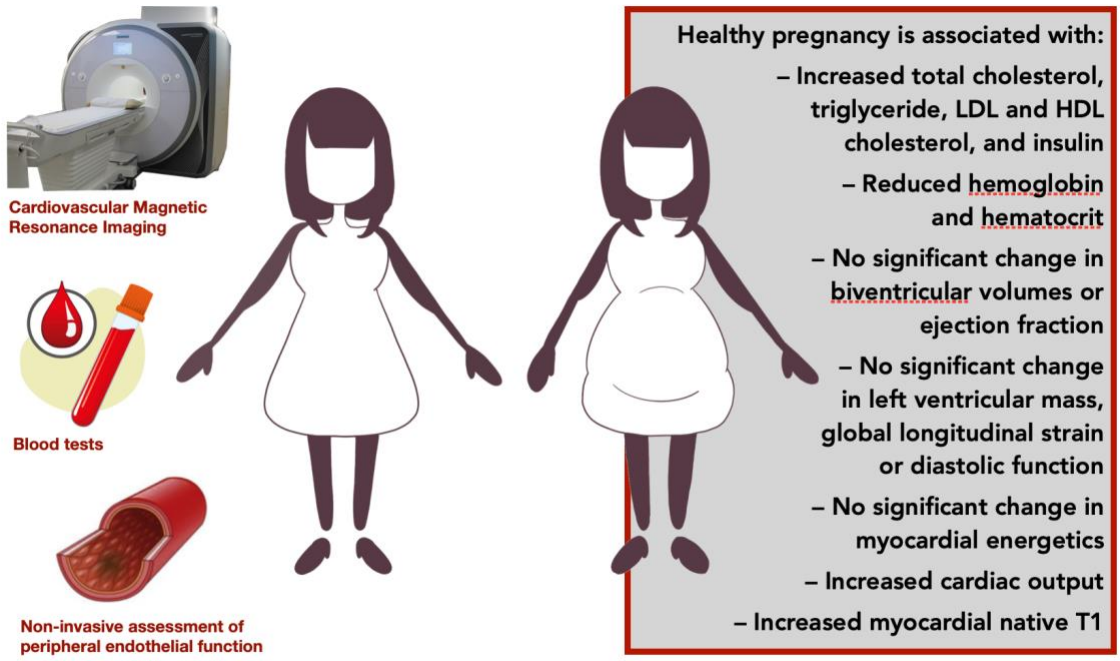


Figure 3.6 : Illustration demonstrating the physiological changes in pregnancy

## 3.5 Discussion

During pregnancy, the maternal cardiovascular system is modified to meet the increasing demands of the developing fetus(127). Pregnant women represent an under-investigated population in clinical research because of their assumed vulnerability even in observational studies using safe imaging tools such as CMR(128). Up to a third of parous women experience one or more APO which are associated with an increased risk of CV mortality and morbidity in later life(129). Although the importance of research into the mechanisms contributing to the development of APO and APO-associated CVD risk is clear, improved understanding of maternal myocardial physiological adaptations to pregnancy is the paramount initial step for detection of adverse myocardial alterations.

Utilizing $^{31}$P-MRS and CMR, the current study provides important insights into the physiological effects of pregnancy on myocardial energetics, function and tissue characteristics. We compared cardiovascular findings of the women in the third trimester of a healthy singleton pregnancy to age- and ethnicity-matching healthy nulliparous women. Consistent with the previous studies, the mean resting heart rate and in parallel with this, the mean cardiac output was higher in the pregnant group(130). Plasma glucose and HbA1c levels were comparable between the two groups, but there were striking increases in plasma lipid, triglyceride and insulin levels in pregnancy. Despite the increased cardiac workload in the pregnant group, with a 40% higher mean resting heart rate, worsened plasma metabolic profile and physiological reductions in hemoglobin levels, we show for the first time that the myocardial energetics were maintained at normal levels in healthy pregnancy suggesting normal function of the myocardial metabolic machinery(77). Moreover, contrary to the common assertion that pregnancy leads to cardiac remodeling, there were no significant

differences in cardiac size, mass, systolic or diastolic function or strain between the pregnant and non-pregnant women during supine acquisitions in this study. However, compared to non-pregnant controls, the third trimester of a normal pregnancy was associated with alterations in myocardial tissue characteristics, with increased myocardial native T1 values. Whilst the T2 measurements also showed statistically significant differences between the two groups, with decreased T2 values in the pregnant group, due to the presence of the resting heart rate differences between the two groups we have further explored the impact of heart rate variation on T1 and T2 mapping data. We showed that the native T1 values were stable across the different heart rates confirming heart rate independence of the technique, whilst the T2 values showed variability of a similar scale to the differences seen between groups and therefore heart rate dependence. As we couldn't rule out heart rate related measurement errors being the cause of the observed difference, the detected changes in T2 values were not deemed to represent a true difference between the pregnant participants and the nulliparous controls in this study

### Hemodynamic changes in healthy pregnancy

Pregnancy is a dynamic process associated with significant physiological changes in the cardiovascular system. Our results indicate that the cardiac output increase in the third trimester of healthy pregnancy is mainly attributable to heart rate changes as we have not detected any significant differences in stroke volumes between the two groups. In our study the mean resting heart rate was 40% higher in the pregnant group and there was no difference in either systolic or diastolic blood pressure between nulliparous and pregnant women. Higher resting heart rate in pregnancy is a consistent finding and it is mechanistically linked to the changes in sympathetic nervous system activity(130,131). Normal pregnancy is

associated with a significant increase in sympathetic nervous system activity, 50% to 150% above non pregnant levels before returning to baseline levels by 6 weeks post-partum(131). While traditionally it has been suggested that the blood pressure drops by 10-15mmHg during the middle of pregnancy, in support of our findings these commonly suggested substantial decreases in blood pressure during pregnancy were also not evident in a recent meta-analysis study(132).

While our finding of higher cardiac outputs in pregnancy compared to non-pregnant participants is consistent with other studies(130), our results diverge from the previous literature where higher end-diastolic cardiac volumes have been reported in pregnant women compared to non-pregnant nulliparous controls with a similar cohort size to our study(2). These differences are likely related to the positional differences during scan acquisitions between our study and the previous studies where image acquisitions were performed with women in left lateral decubitus position while we have scanned our participants in supine position. Supporting this theory, the LV end-diastolic and end-systolic dimensions have previously been shown to be increased only in the lateral position while no significant changes in end-diastolic dimensions were noted in the supine position in the same participants with echocardiography(133). Moreover, this early landmark study also showed no significant changes in LV wall thickness in keeping with our findings of no significant difference in LV mass or wall thickness between the pregnant group and nulliparous controls(133) and contrary to the findings of a smaller recent CMR study(115).

### Myocardial tissue characteristics in healthy pregnancy

CMR has the unique ability to provide detailed tissue characterization. Given the safety concerns of using gadolinium-based contrast agents during pregnancy scans(72), techniques

which can perform tissue characterization without the need for contrast agents are of significant value during pregnancy. Native T1 mapping is acquired without the administration of exogenous agents to provide a quantitative map of T1 relaxation times of the tissues imaged on a pixel-by-pixel basis(68). Native T1 values reflect signals originating from the intracellular and extracellular (including interstitial and intravascular) compartments and reflect intrinsic differences in tissue properties(134). A deviation from the normal range of native T1 values may indicate a pathology such as myocardial oedema, inflammation, fibrosis, iron loading, fat accumulation or a change in physiology(135). Native T1 values are prolonged by increased free water content(134). Pregnancy is associated with significant increases in total blood volume, plasma volume, and red blood cell mass(136). Plasma volume increases proportionally more than the red blood cell mass, resulting in a “physiological anemia” from hemodilution(136). The higher native T1 measurements in the pregnancy group may thus be linked to either increased myocardial interstitial fluid retention or increased myocardial blood volume(137). Sex differences in native myocardial T1 values have been demonstrated previously with higher native myocardial T1 in non-pregnant women compared to men(138). Moreover, women were also shown to have higher myocardial blood volume compared to men(137). These changes are expected to be even more accentuated in pregnant women given the alterations in hormonal milieu during healthy pregnancy.

### Sex differences in cardiovascular disease and complications of pregnancy as novel sex-specific risk factors

There are substantial sex differences in the prevalence and burden of CVD, with cardiovascular mortality increasing in younger women(111). The mechanisms that contribute to worsening risk factor profiles in young women are not fully elucidated, and diagnostic

pathways and effective and specific therapeutic strategies for addressing this excess CVD risk are lacking. Pregnancies complicated by APO can capture women at increased risk of subsequent development of CVD.

In women with APO, pregnancy-associated cardio metabolic stresses may play an important role in the developmental programming of CVD in later life. There is a substantial body of evidence showing that APO, including hypertensive disorders of pregnancy, gestational diabetes, preterm delivery, delivery of a small-for-gestational-age infant, miscarriage, and placental abruption-associated CVD risk persists into later life, far beyond the affected pregnancy period(139,140). Biochemical risk factors for CVD, including raised concentrations of cholesterol and triglycerides, have been shown to persist many years after APO(54). A history of APO should therefore prompt vigorous modification of CVD risk factors to reduce future CVD morbidity and mortality. The American Heart Association guidelines for the prevention of CVD in women now include pregnancy complications as a major risk factor(141). Pregnancy is therefore a window of opportunity for identifying those women with perinatal complications who may benefit from early risk detection and early CVD prevention. However, there is little consensus on the most effective screening methods. In this study, we showed that CMR is well-tolerated in pregnancy. CMR may play a significant role in assessing myocardial involvement in women at risk of perinatal complications, as a tool for early detection of adverse myocardial alterations. Thus, it may aid prevention of adverse maternal CV outcomes, and associated adverse fetal events, through early initiation of risk-modifying treatment prior to the onset of overt CVD. While transthoracic echocardiography is an indispensable tool for cardiac assessments, CMR is the gold standard technique for assessing cardiac volumes and function based on its superior accuracy and

reproducibility(68,142)and CMR overcomes the limitations of echocardiography in individuals with poor acoustic windows which is a common challenge in pregnant women.

## 3.6 Limitations

Whilst the studies confirm that non-contrast magnetic resonance imaging (MRI) does not harm the baby when performed at any stage of the pregnancy(70), an increased risk of neonatal death or stillbirth with gadolinium based contrast exposure has been reported(72). As a result, only non-contrast scans were performed in our study.

## 3.7 Conclusions

Healthy pregnancy is associated with no significant changes in cardiac size, mass, function or myocardial energetics. Consistent with the increased heart rate in pregnancy, the cardiac output is higher in pregnant women. Pregnancy is also associated with increased myocardial native T1 values which may reflect increased myocardial interstitial water retention and/or increased myocardial blood volume during pregnancy. CMR is well-tolerated in pregnancy and may play a significant role in assessing myocardial involvement in women at risk of perinatal complications.

# *Chapter 4: Maternal cardiac changes in women with obesity and gestational diabetes mellitus*

## 4.1 Abstract

**Background-** Gestational diabetes mellitus (GDM) is the most prevalent metabolic disorder during pregnancy and is associated with increased risks of cardiovascular morbidity and mortality in later life. Compromised cardiac energy production is an important contributor to most forms of heart disease. The changes in myocardial energetics in GDM have not been characterized previously.

**Objective-** We investigated if women with GDM in the third trimester of pregnancy exhibit adverse cardiac alterations in myocardial energetics, function or tissue characteristics.

**Methods-** Thirty-eight healthy pregnant (HP) women and thirty women with GDM were recruited. Participants underwent phosphorus magnetic resonance spectroscopy and cardiovascular magnetic resonance for assessment of myocardial energetics (phosphocreatine to ATP ratio (PCr/ATP)), tissue characteristics, biventricular volumes and ejection fractions, left ventricular (LV) mass, global longitudinal shortening (GLS) and mitral in-flow E/A ratio.

**Results-** Participants were matched for age, gestational age and ethnicity. The women with GDM had higher body-mass index (27±4 versus 33±5kg/$m^2$; p=0.0001), systolic (115±11 versus 121±13mmHg; p=0.04) and diastolic (72±7 versus 76±9mmHg; p=0.04) blood pressure. There was no difference in NT proBNP concentrations between the groups.

The women with GDM had lower myocardial PCr/ATP ratio (2.2±0.3 versus 1.9±0.4; p<0.0001), accompanied by lower LV end-diastolic volumes (76±12 versus 67±11mL/$m^2$; p=0.002) and higher LV mass (90±13 versus 103±18g; p=0.001). While ventricular ejection fractions were similar, the GLS was reduced in women with GDM (-20±3 versus -18±3%; p=0.008).

**Conclusions-** Despite no prior diagnosis of diabetes, women with obesity and GDM manifest impaired myocardial contractility and higher LV mass, associated with reductions in myocardial energetics in late pregnancy compared to lean women with healthy pregnancy. These findings may aid our understanding of the long-term cardiovascular risks associated with GDM.

## 4.2 Introduction

Defined as hyperglycemia with onset or first recognition during pregnancy that is below diagnostic thresholds for type 2 diabetes (T2D), gestational diabetes mellitus (GDM)(143) is increasing in prevalence affecting 5 to 18% of all pregnancies worldwide, driven by the increasing burden of obesity among women of reproductive age(144,145). The diagnosis of GDM has long-term implications for maternal cardiovascular health, with up to a two-fold higher cardiovascular disease (CVD) risk postpartum, including a greater risk of heart failure [Hazard Ratio (HR) 2.8, 95% confidence interval (CI) 2.25-3.48], stroke [HR1.77, 95% CI 1.53-2.04] and ischemic heart disease [HR 2.61, 95% CI 2.25-3.48] in later life compared to women without a history of GDM(26,27,29,146). Moreover, women with a history of GDM have an up to 7-fold increased risk of developing T2D later in life(147). A recent meta-analysis suggests that women with a history of GDM have double the risk of major cardiovascular events compared to women with uncomplicated pregnancies, irrespective of a T2D diagnosis later in life(27). In a population-based study of parous women the estimated proportion of CVD risk attributable to subsequent T2D in women with GDM was 23%(146).

The metabolic abnormalities underlying GDM include insulin resistance and pancreatic beta-cell defects(148). Normal pregnancy requires maternal hemodynamic and metabolic adaptations to meet the increasing demands of the developing fetus(8). The hemodynamic changes include hyperdynamic circulation, systemic vasodilatation, increased filling capacity of the vasculature, and volume expansion(8). However, a recent study has shown maternal hemodynamic maladaptation to pregnancy in women with GDM including lower cardiac output and stroke volume, and higher total vascular resistance(149).

To meet the energy needs of pregnancy, hepatic glucose production increases by 30% in healthy pregnant women by the end of gestation, and peripheral insulin sensitivity decreases

by approximately 50%(150). While in women with normal glucose tolerance, there is a 2–3-fold increase in insulin secretion in response to the decreased insulin sensitivity, in women who were normoglycemic before pregnancy but go on to develop GDM in late gestation, the beta cell insulin secretion is unable to compensate for pregnancy-induced insulin resistance, resulting in hyperglycaemia(150).

Maternal inability to adapt to these metabolic and hemodynamic changes can expose underlying, previously silent pathology, leading to appreciation of pregnancy as "nature's stress test"(113). Despite being the most prevalent metabolic disorder during pregnancy the impact of GDM on maternal myocardial energetics has not been assessed previously. Myocardial energy depletion is a common feature of metabolic disorders and compromised cardiac energy production is an important contributor to most forms of heart disease(151). Phosphorus magnetic resonance spectroscopy ($^{31}$P-MRS) reveals the biochemistry of ATP, ADP, and phosphocreatine (PCr), which are critical to the supply of energy for contractile work in the myocardium(77). The relative concentration of phosphocreatine to ATP (PCr/ATP) is a marker of the myocardium's ability to convert substrate into ATP for active processes, and a sensitive index of the energetic state of the myocardium (Figure 4.1).

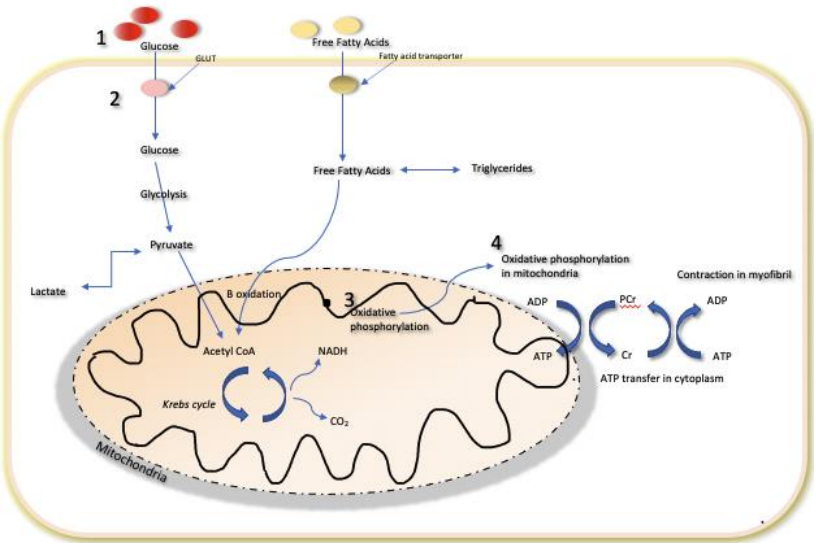

Figure 4.1: Cardiac Energy Metabolism. Energy metabolism in the heart has four components: 1. Adequate blood supply; 2. Substrate utilisation; 3. Oxidative phosphorylation; 4. Energy transfer and utilisation. GLUT denotes glucose transporter, PCr phosphocreatine, Cr free creatine

Myocardial energetic compromise, indicated by decreased PCr/ATP, is a predictor of mortality(88) and linked to contractile dysfunction(88,89). The effects of gestational metabolic and hemodynamic alterations on the myocardial energetic state can be assessed non-invasively by $^{31}$P-MRS without the need for ionizing radiation or contrast exposure.

Moreover, cardiovascular magnetic resonance (CMR) allows comprehensive evaluation of myocardial structure, function, strain and tissue characteristics with excellent reproducibility. CMR parametric mapping methods (such as T1- and T2-mapping) are quantitative techniques that provide a pixel-by-pixel representation of numerical T1 or T2 properties. These techniques provide information on myocardial tissue type and composition without the need for contrast agents(68).

CMR therefore provides insight into cardiovascular physiology and non-contrast CMR studies can be safely performed during pregnancy(70-73). Utilising CMR and $^{31}$P-MRS in the third trimester, we sought to investigate the effect of pregnancy-associated cardio metabolic stresses in women with pregnancies complicated by GDM on maternal myocardial energetics, structure, function or tissue characteristics.

## 4.3 Research design and methods

This single-center, observational, case-control study complied with the Declaration of Helsinki, it was approved by the National Research Ethics Committee (REC20/NE/0117), and

informed written consent was obtained from each participant.

### Participants

A total of 68 participants including 38 pregnant women with an uncomplicated pregnancy and 30 pregnant women with a diagnosis of gestational diabetes were recruited in the study (Figure-4.2). The pregnant participants were recruited via the Leeds Teaching Hospitals NHS Trust antenatal clinics attendance register and GDM clinics.

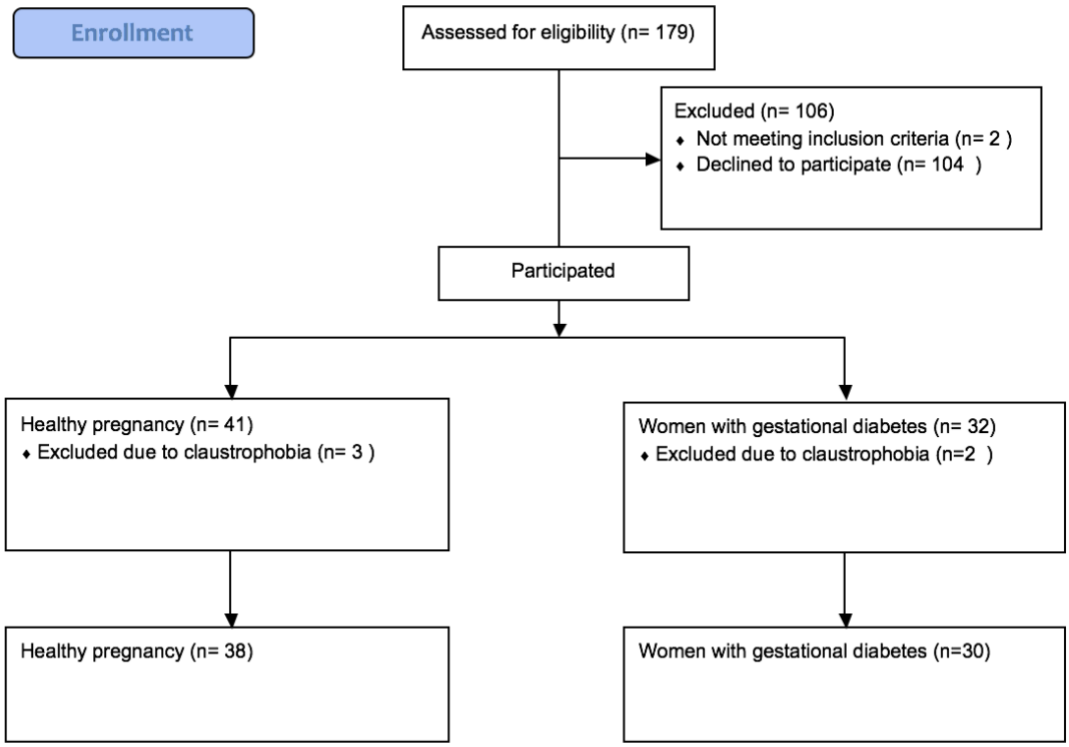


Figure 4.2: Consort flow diagram demonstrating the recruitment pathway for study participants with healthy pregnancy and gestational diabetes mellitus

### Inclusion and exclusion criteria

Participants with on-going pregnancy, >18 years of age, 26-38 weeks' gestation were recruited. Recruitment for both groups was restricted to singleton first pregnancies. Women with a diagnosis of pre-eclampsia, antenatally small for gestational age babies on week 33 transabdominal ultrasound (<10$^{th}$ percentile for estimated fetal weight) or any other adverse pregnancy outcomes, known cardiovascular problems (congenital or acquired heart disease), contra-indications to CMR (pacemaker, cranial aneurysm clips, metallic ocular foreign bodies, severe claustrophobia), subjects with medical conditions that could affect cardiac function including women with severe anemia, maternal diabetes (type I or type II), chronic renal disease, chronic hypertension, liver disease, former or current smokers were excluded. Ethnicity group was self-reported by participants.

The presence of pre-existing diabetes was checked on electronic health care records at pre-screening stage. The absence of pre-existing diabetes was then confirmed with the participants during the research visit.

### Oral glucose tolerance test

Diagnosis of GDM was confirmed on a 75g oral glucose tolerance test (OGTT) in all participants in the GDM group at the antenatal clinics using the U.K. National Institute for Health and Care Excellence (NICE) guideline criteria for GDM of fasting glucose ≥5.6 mmol/L (≥100.8 mg/dL) and/or 2-hour glucose ≥7.8 mmol/L (≥140.4 mg/dL) after 75g oral glucose at ~26 weeks' gestation(90).

### Anthropometric measurements

All women had height and weight recorded, and body-mass index (BMI) calculated at the

booking visit performed at approximately the 8th gestational week in antenatal clinics. Brachial artery blood pressure (BP) was recorded as an average of 3 sitting measures taken over 10 min (DINAMAP-1846-SX, Critikon Corp) after an initial 5-minute rest using the appropriate cuff size based on the mid arm circumference. These assessments were then repeated during the research CMR scan visit performed at third trimester. A standard 12-lead ECG was performed in all participants on the same day as the CMR. A venous blood sample was taken for assessments of full blood count, estimated glomerular filtration rate (eGFR), liver function, glycated hemoglobin (HbA1c), lipid profile (triglycerides and high-density lipoprotein (HDL), low-density lipoprotein (LDL) and total cholesterol concentrations) and N-terminal pro hormone B-type natriuretic peptide (NT-proBNP) also on the same day as the CMR. Given the pregnant status of the participants a flexible approach to blood tests were used and participants were requested to fast for 4 hours prior to research visits as per the recommendations of the local patient and public involvement group at the stage of study design.

### $^{31}$Phosphorus magnetic resonance spectroscopy

$^{31}$P-MRS was performed to obtain the PCr/ATP ratio from a voxel placed in the mid-ventricular septum, with the participants lying supine and a $^{31}$P transmitter/receiver cardiac coil (Rapid Biomedical GmbH, Rimpar, Germany) placed over the heart, in the iso-center of the magnet on a 3.0 Tesla MR system (Prisma, Siemens, Erlangen, Germany). $^{31}$P-MRS data were acquired with a non-gated 3-D acquisition-weighted chemical shift imaging (CSI) sequence as previously described(152).

### Cardiovascular magnetic resonance imaging

All scans were performed on a 3.0 Tesla MR system (Prisma, Siemens, Erlangen, Germany) and all participants underwent cardiac magnetic resonance imaging (MRI) scans. The CMR protocol (Figure-4.3) consisted of cine imaging, velocity-encoded mitral in-flow imaging, native T1 mapping and T2 mapping.

To capture cross-sectional mitral valve (MV) flow, velocity-encoded mitral in-flow imaging was planned from an acquisition plane placed at the position of the mitral valve at end-systole. Velocity sensitivity was set at 200 cm/s. The phase-contrast images were acquired using retrospective ECG gating, using established methods(125).

Native T1 maps were acquired in 3 short-axis slices using a breath-held modified look-locker inversion recovery (MOLLI) acquisition as previously described(153). T2 maps were acquired from the matching 3 short-axis positions to native T1 mapping using a T2 prepared true fast imaging with steady-state precession pulse sequence to produce single-shot T2 prepared images, each with different T2 preparation times as previously described(106).

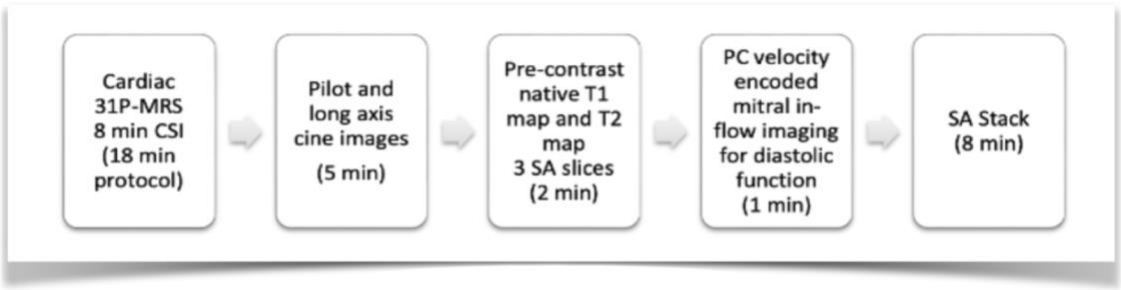


Figure 4.3: $^{31}$P Magnetic Resonance Spectroscopy ($^{31}$P-MRS) and cardiac magnetic resonance (CMR) protocol employed (3 T) (cine imaging, velocity-encoded mitral in-flow imaging, T1 and T2 mapping)

### Quantitative imaging data analysis

All $^{31}$P-MRS analysis was performed off-line by ST using the OXSA toolbox as previously described(123). CMR post processing analysis using cvi42 software (Circle Cardiovascular Imaging, Calgary, Canada) was performed off-line blinded to all participant details by ST after completion of the study and scan contours were subsequently reviewed by EL who was also blinded to participant details.

Global longitudinal shortening data were derived from horizontal long-axis and vertical long-axis images, and image reconstruction and processing were implemented using the Gadgetron software framework with the previously developed convolutional neural network for labelling landmarks on CMR images(124).

Diastolic function was measured from mitral in-flow velocity-encoded images(125). Regions of interest were manually drawn on one frame to encircle the entire cross section of MV leaflets and propagated using a semi-automated contouring mode on Circle cvi42 software (Circle Cardiovascular Imaging Inc., Calgary, Alberta, Canada), yielding velocity versus time graphs characterizing diastolic E and A waves. The mean of maximum velocity obtained for MV was recorded. The deceleration time (DT) was calculated as previously described from the same images(125).

Native T1 and T2 maps were analyzed using cvi42 software (Circle Cardiovascular Imaging, Calgary, Canada) which were measured for each of the 16 segments using the AHA classification.

## 4.4 Statistical analysis

Statistical analysis was performed using SPSS (IBM SPSS statistics, version 26.0). Categorical data were compared with Pearson's chi-square test. Continuous variables are presented as

mean ±SD and were checked for normality using the Shapiro-Wilk tests. Comparisons of all CMR and biochemistry data were performed with two-tailed paired t-test or Mann Whitney U test as appropriate. P≤0.05 was considered statistically significant. Bivariate correlations were performed using the Pearson or Spearman method as appropriate.

A priori sample size calculations were performed before the study showing that to detect a 20% difference in the mean myocardial PCr/ATP ratio between the two groups a minimum of twenty-six participants per group would be needed (with 80% power at $\alpha$=0.05). These recruitment goals were exceeded in the study.

In this study pre-specified hypotheses were tested on three variables: myocardial PCr/ATP ratio, left ventricular (LV) mass and GLS. Linear regression models were used to test for associations between these three variables and systolic and diastolic blood pressure, body-mass index, plasma triglyceride concentrations and HbA1c.

## 4.5 Results

### Study population

Demographic, clinical, and biochemical data of the two study groups are shown in Table-4.1.

A total of 38 HP and 30 GDM participants were prospectively recruited. Maternal age, gestational age and ethnicity distribution were similar between the groups. Ethnicity distribution (33/38 participants in the HP arm were Caucasian, 3 Pakistani, 1 Chinese and 1 Black-African; in the GDM group, 26/30 participants Caucasian, 1 Indian, 2 Chinese and 1 Black-African) was broadly in line with the local population demographics. Both groups included similar numbers of participants classified as advanced maternal age (>35 years of age) (HP: 6 versus GDM: 4, p=0.8). None of the participants in either group had a family history of T2D.

Diagnosis of GDM was confirmed by OGTT in all participants with GDM as per clinical guidelines(154)**.** On the day of OGTT, the mean fasting glucose in the GDM group was 5.1±0.7 mmol/L and the mean 2-hour plasma glucose was 9.0±1.4 mmol/L. Of the participants with GDM, 12 (40%) were receiving metformin treatment and 4 (13%) were receiving additional insulin treatment for glycemic control. The remaining 18 women with GDM received dietary advice alone.

The women with GDM had higher BMI than those in the HP arm, both at the booking antenatal clinic visit and at the third trimester CMR scan visit. However, both groups had a similar gestational weight gain (Table-4.1).

There was no significant difference in resting heart rate between the two groups, but the GDM group had higher resting systolic and diastolic BP measurements both at the booking antenatal clinic visit and at the third trimester CMR scan visit (Table-4.1).

The plasma triglyceride, free fatty acid, ketone (beta-hydroxybutyrate) and HbA1c levels were all significantly higher in the GDM group. There was no significant difference in NTproBNP levels between the two groups.

| **Variable** | **Healthy pregnancy (n=38)** | **Gestational diabetes mellitus (n=30)** | **P value** |
|---|---|---|---|
| **Age, y** | 31±4 | 31±5 | 1 |
| **Ethnicity, white, %** | 87 | 87 | 1 |
| **Gestational date at CMR, wks** | 30±2 | 31±2 | 0.2 |
| **Booking BMI, kg/m$^2$** | 25±5 | 31±5 | **0.0001** |

| | | | |
|---|---|---|---|
| **BMI at scan visit, kg/m²** | 27±4 | 33±5 | **0.0001** |
| **Heart rate, bpm** | 88±12 | 91±14 | 0.3 |
| **Hip circumference, cm** | 104±13 | 117±16 | **0.004** |
| **Waist circumference, cm** | 100±11 | 110±14 | **0.002** |
| **Booking systolic BP, mmHg** | 113±10 | 120±9 | **0.004** |
| **Systolic BP, mmHg** | 115±11 | 121±13 | **0.04** |
| **Booking diastolic BP, mmHg** | 69±8 | 74±8 | **0.01** |
| **Diastolic BP, mmHg** | 72±7 | 76±9 | **0.04** |
| **Biochemistry** | | | |
| **Hemoglobin, g/L** | 121±9 | 122±9 | 0.7 |
| **HDL, mmol/L** | 2.2±0.4 | 1.9±0.4 | **0.003** |
| **LDL, mmol/L** | 3.6±1.3 | 3.3±1.2 | 0.3 |
| **TG, mmol/L** | 2.5±1.0 | 3.1±0.8 | **0.009** |
| **Creatinine, umol/L** | 47±7 | 46±10 | 0.6 |
| **eGFR, ml/min/1.73m²** | 90± 0 | 89±3 | **0.04** |
| **Urine Alb/creatinine ratio** | 1.3±1.3 | 1.9±3.2 | 0.3 |
| **HbA1c, mmol/mol** | 31±3 | 33±3 | **0.008** |
| **Glucose, mmol/L** | 5.2±1.1 | 6.6±7.1 | 0.2 |
| **NT-proBNP, ng/L** | 55±32 | 46±17 | 0.2 |
| **FFA, mmol/L** | 0.3±0.1 | 0.4±0.2 | **0.009** |
| **Beta-hydroxybutyrate, mmol/L** | 0.1±0.07 | 0.2±0.2 | **0.006** |
| **Pregnancy specific parameters** | | | |

| | | | |
|---|---|---|---|
| **Gestational weight gain, kg** | 8.9±4.9 | 7.9±4.4 | 0.38 |
| **Birthweight, grams** | 3429±1166 | 3196±667 | **0.04** |
| **Birthweight for gestational age centile (%)** | 42±25 | 41±26 | 0.8 |
| **Gender, F (%)** | 29 | 47 | **0.1** |

Values are means (SD) or median (IQR) for continuous variables and number (%) for categorical variables. BMI indicates body mass index; kg, kilograms; n, number; bpm, beats per minute; mmHg, millimeters of mercury; g/l, gram per Liter; HDL, high density lipoprotein; mmol/L, millimoles per litre; LDL, low density lipoprotein; TG, triglyceride; eGFR, estimated glomerular filtration rate; ml/min/1.73m2, millilitre per minute per (1.73 square meters); pmol/L, picomoles per litre; NT-pro BNP, N-terminal pro hormone B-type natriuretic peptide; HBA1c, glycated haemoglobin; FFA, free fatty acids.

Table 4.1: Clinical characteristics and the biochemistry

### Myocardial energetics, structure and function comparisons

$^{31}$P-MRS results for myocardial energetics and CMR results for biventricular volumes, systolic function, left ventricular (LV) mass, diastolic function and GLS are summarized in Table 4.2.

| Variable | HP (n=38) | GDM (n=30) | P value | Adj p value for BMI | Adj p value for GWG |
|---|---|---|---|---|---|
| **Left ventricular structural parameters** | | | | | |
| **LV end diastolic volume (ml)** | 143±23 | 136±24 | 0.2 | 0.2 | 0.2 |
| **LV end diastolic volume index (ml/m²)** | 76±12 | 67±11 | **0.002** | **0.003** | **0.03** |
| **LV end systolic volume (ml)** | 59±12 | 59±14 | 1 | 1 | 1 |
| **LV end systolic volume index (ml/m²)** | 31±6 | 29±7 | 0.2 | 0.2 | 0.2 |
| **LV stroke volume (ml)** | 84±15 | 77±13 | **0.04** | **0.02** | 0.1 |
| **LV stroke volume index (ml/m²)** | 49±12 | 46±8 | 0.2 | 0.2 | 0.2 |
| **LV ejection fraction (%)** | 59±4 | 57±6 | 0.05 | 0.05 | 0.05 |
| **LV mass (g)** | 90±13 | 103±18 | **0.001** | **0.009** | **<0.001** |
| **LV mass index (g/m²)** | 46±8 | 50±7 | 0.3 | 0.3 | **0.03** |
| **LV mass/LV EDV (g/ml)** | 0.6±0.1 | 0.8±0.2 | **0.0007** | **<0.001** | **0.004** |
| **Wall thickness (mm)** | 7.6±1.2 | 9.5±1.2 | **0.0001** | **<0.001** | **<0.001** |
| **Myocardial energetics** | | | | | |
| **PCr/ATP** | 2.2±0.3 | 1.9±0.4 | **<0.0001** | **0.001** | **0.003** |
| **Functional parameters** | | | | | |
| **LV ejection fraction (%)** | 59±4 | 57±6 | 0.05 | 0.05 | 0.05 |
| **RV ejection fraction (%)** | 55±6 | 54±7 | 0.5 | 0.5 | 0.5 |
| **Global longitudinal shortening (%)** | -20±3 | -18±3 | **0.008** | **<0.001** | **0.002** |
| **MAPSE (mm)** | 14±3 | 14±2 | 1 | 1 | 1 |
| **E/A ratio** | 1.7±0.4 | 1.7±0.4 | 1 | 1 | 1 |
| **Deceleration time DT (ms)** | 152±38 | 179±75 | 0.06 | 0.06 | 0.06 |

Values are means (SD) or median (IQR) for continuous variables and number (%) for categorical variables. LV indicates left ventricular; ml, milliliter; ml/m$^2$, milliliters per square meter of body surface area; g, gram; g/m$^2$, gram per square meter of body surface area; LV, left ventricular; RV, right ventricular; LA, left atrium; MAPSE, mitral annular plane systolic excursion; DT, deceleration time; PCr/ATP phosphocreatine to adenosine triphosphate ratio

Table 4.2: CMR and $^{31}$P-MRS findings

The women with GDM showed significant reductions in myocardial PCr to ATP ratio (HP: 2.2 [95% Confidence intervals: 2.1-2.4] versus GDM: 1.9 [1.7-2.0]; p=<0.0001) (Figure-4.4).

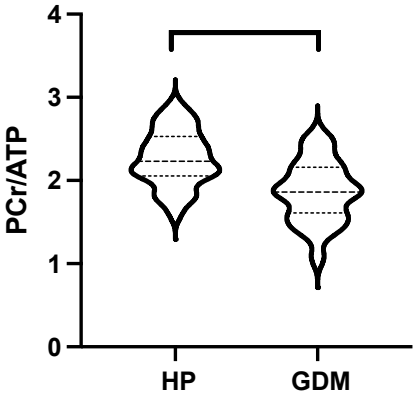


Figure 4.4: Violin plots demonstrating the differences in phosphocreatinine/adenosine triphosphate (PCr/ATP) between the participants with gestational diabetes mellitus and participants with healthy pregnancies

This was accompanied by important structural and functional differences. The women with GDM had lower LV end-diastolic volumes (EDV) indexed for body surface area (HP:76[72-80] versus GDM:67[63-71]ml/m$^2$; p=0.002), but higher LV mass (HP: 90 [85-94] versus GDM: 103 [96-112] g; p=0.001) and higher LV mass over LV EDV ratio suggestive of increased concentricity of the LV (HP: 0.6 [0.6-0.7], GDM: 0.8 [0.7-0.8] g/ml; p= 0.0001) (Figure-4.5). LV end-diastolic wall thickness was also higher in women with GDM (HP: 7.6 [7.2-8.0] versus GDM: 9.5 [9.3-10.0] mm; p=0.0001). When adjusted for booking BMI and for gestational weight gain the comparisons of myocardial energetics, GLS and cardiac concentricity between the two groups remained statistically significant.

While the LV ejection fraction was similar between the two groups, the LV GLS was

significantly lower in the GDM group (HP: -20 [18-21%], versus GDM: -18 [17-19] %; p=0.008) (Figure-4.6).

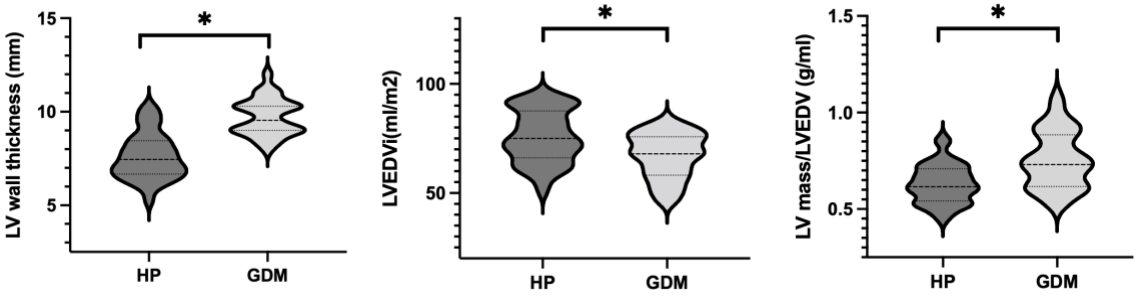


Figure 4.5: Violin plots demonstrating the differences in left ventricular end-diastolic wall thickness, left ventricular end-diastolic volumes indexed for the body surface area, and left ventricular mass over left ventricular end diastolic volume ratio as a measure of concentricity index between the participants with gestational diabetes mellitus and participants with healthy pregnancies

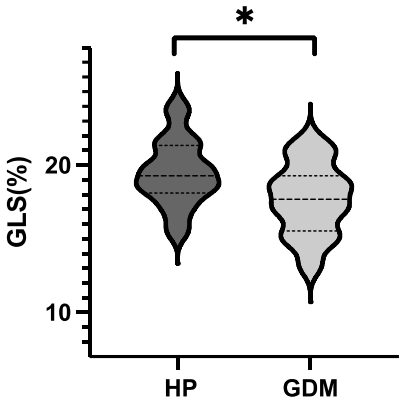


Figure 4.6: Violin plots demonstrating the differences in left ventricular global longitudinal shortening between participants with gestational diabetes mellitus and participants with healthy pregnancies

Both pregnancy groups exhibited similar mitral inflow E/A ratio and deceleration time measured from mitral in-flow velocity-encoded images.

Similar to LV EDV differences, the right ventricular (RV) EDV was smaller in the GDM group

(HP:85[79-88] versus GDM:77[67-80] ml; p=0.04). There were no significant differences in RV ejection fraction between the two groups.

There were no significant differences in left atrial volumes or function between the groups.

### Myocardial tissue characteristics

While numerically the HP group had higher myocardial native T1 measurements this difference has not reached statistical significance (HP: 1325±34 versus GDM:1308±38 ms; p=0.05). There was no significant difference between the groups on T2 mapping measurements (HP: 40±3 versus GDM: 39±3 ms, p=0.2).

### Birth weight, birthweight for gestational age, and sex comparisons

A subtle difference in birthweight was detected between the HP and the GDM group babies, with a higher birthweight in the HP group. Birthweight for gestational age was slightly lower in the GDM group (HP: 42±25 versus GDM: 41±26, p=0.8). There were no differences in sex distribution of the babies.

## 4.6 Correlations

There was significant correlation between the PCr/ATP and LV mass (r=-0.37, p=0.005). Multilinear regression showed that LV mass was independently associated with systolic BP and BMI (Table-4.3). There were no other significant bivariate correlations.

| ***PCr/ATP*** | Beta | SE | 95% CI lower bound | 95% CI upper bound | P value |
|---|---|---|---|---|---|
| *Constant* | 4.85 | 1.99 | 0.75 | 8.94 | 0.02 |
| Systolic BP | -0.021 | 0.018 | -0.060 | 0.016 | 0.25 |

| | | | | | |
|---|---|---|---|---|---|
| Diastolic BP | 0.021 | 0.028 | -0.037 | 0.08 | 0.46 |
| HbA1c | -0.004 | 0.046 | -0.1 | 0.09 | 0.92 |
| Triglyceride | -0.162 | 0.165 | -0.5 | 0.18 | 0.33 |
| BMI | -0.368 | 0.026 | -0.09 | 0.02 | 0.17 |
| ***LV mass*** | | | | | |
| *Constant* | 37.60 | 54.36 | -72.65 | 147.8 | 0.49 |
| Systolic BP | -0.89 | 0.41 | -1.72 | -0.07 | **0.03** |
| Diastolic BP | 1.33 | 0.67 | -0.04 | 2.70 | 0.05 |
| HbA1c | 0.75 | 1.33 | -1.95 | 3.46 | 0.57 |
| Triglyceride | -2.7 | 4.68 | -12.19 | 6.78 | 0.56 |
| BMI | 1.61 | 0.75 | -0.09 | 3.12 | **0.04** |
| ***GLS*** | | | | | |
| *Constant* | 32.81 | 7.24 | 18.10 | 47.53 | <0.0001 |
| Systolic BP | -0.014 | 0.053 | -0.124 | 0.095 | 0.7 |
| Diastolic BP | -0.10 | 0.09 | -0.29 | 0.088 | 0.28 |
| HbA1c | -0.25 | 0.18 | -0.61 | 0.12 | 0.17 |
| Triglyceride | 1.08 | 0.64 | -0.23 | 2.39 | 0.1 |
| BMI | -0.02 | 0.1 | -0.22 | 0.18 | 0.82 |

PCr/ATP phosphocreatine to adenosine triphosphate ratio, BMI indicates body mass index; BP, blood pressure; HBA1c, glycated haemoglobin; LV, left ventricular; GLS, global longitudinal shortening.

Table 4.3: Linear regression model for dependent variables PCr/ATP, LV mass and GLS

## 4.7 Discussion

In this prospective study, diagnosis of GDM was associated with subclinical alterations in cardiac energetics, structure and function. Compared to age, gestational age and ethnicity matched women with a healthy uncomplicated pregnancy, young women with GDM

displayed enhanced LV concentricity with higher LV wall thickness and mass, and smaller LV chamber size. These structural alterations were accompanied by significant reductions in myocardial energetics and in LV GLS in the GDM group. These findings may aid our understanding of the long-term cardiovascular risks posed by GDM.

### Reductions in myocardial energetics in gestational diabetes mellitus

During healthy pregnancy, the maternal physiology adapts to compensate for many changes in energy demands. In our study, using $^{31}$P-MRS we show for the first time that despite their young age women with obesity and GDM display significant reductions in myocardial energetics, while these were maintained at normal levels in HP. This suggests insufficient adaptation of the maternal myocardial metabolic machinery to cope with the challenging metabolic and hemodynamic demands of the pregnancy in the GDM group.

The heart has a very high energy demand, while having minimal energy storing capacity(155). Efficient matching of energy supply to demand in the heart is therefore essential for maintaining cardiac function. Compromised cardiac energy production is an important contributor to most forms of heart disease(151,156-158) and myocardial metabolic insult of a pregnancy with GDM may be a potential driver of the enhanced CVD risk. Manipulating myocardial energy metabolism may therefore be a promising strategy to improve cardiovascular outcomes in women with GDM.

The metabolic and hemodynamic challenges of pregnancy were augmented in the GDM group with higher plasma HbA1c, triglyceride, ketone body and free fatty acid levels, lower HDL levels, and higher resting blood pressure measurements in the GDM group compared to the

HP cohort. Given the multitude of metabolic and hemodynamic alterations in the GDM group, the driving factor for this energetic impairment is likely to be multifactorial.

Consistent with the previous reports(159), in our study women with GDM had higher booking BMI which is a close estimate of pre-pregnancy weight, but the gestational weight gain was similar between the groups in this study. Being overweight or obese before pregnancy is considered the most significant GDM risk factor(159). Our results add further evidence for increased body weight as an integrating determinant of maternal myocardial alterations in women with GDM. In our study, BMI was associated with myocardial PCr/ATP ratio, while diabetes-specific parameters such as HbA1c and plasma glucose concentrations did not correlate with cardiac parameters. In a similar pattern to this study in previous studies of established T2D cohorts we have not detected correlations of HbA1c or plasma glucose with the cardiac parameters including energetics, cardiac structural changes or cardiac contractile function measured by GLS(160,161). These findings are in keeping with the long standing existing evidence that despite the strict glycemic control in T2D patients the excess risk of heart failure persists(162).

Reductions in myocardial PCr/ATP ratio have been demonstrated in chronic obesity(163) and in overt T2D(158). Numerous previous studies have reported an increased risk of GDM among women who are overweight or obese compared to women with normal body weight(159). Therefore, it is clear the GDM risk is in a big part driven by the obesity epidemic and maintaining a healthy body weight throughout the reproductive life would likely confer great benefits in reducing the risk of GDM. In this study, while the comparisons of principal findings between the two groups remained statistically significant even when adjusted for booking BMI and for gestational weight gain, the potential impact of prior overweight status on the findings cannot be ruled out by our study design.

However, it is not possible to draw conclusions from comparison with existing literature on cardiac studies in overweight cohorts due to their significant methodological differences from this study(164,165). The existing reports of cardiac assessments in overweight cohorts included older adults, with a significant proportion of male participants and significantly higher BMI in the obesity cohort and a lower BMI in the control group than our study; all of which are likely to have a significant impact on the cardiac findings. Despite the significantly younger age and lower BMI of our participants we have detected significant reductions in energetics and cardiac contractile function in the GDM cohort which likely suggests at least an additive impact of GDM and overweight status on the cardiac findings.

With regards to the long term cardiovascular outcomes, a higher incidence of CVD was found in women with both a history of GDM and obesity (HR 1.76, 95% CI 1.59–1.95) compared with women with a history of GDM alone (HR 1.43, 95% CI 1.38–1.49), with a multiplicative interaction between GDM and obesity (146).

### Cardiac structural and functional changes in gestational diabetes mellitus

The enhanced cardiac concentricity revealed in our study may be an important component of the worsened cardiovascular outcomes in women with GDM in the longer term. While initially an adaptive response for maintaining cardiac output, sustained hypertrophic growth of the myocardium induced by pathological stimuli is a leading predictor for the development of heart failure and for cardiovascular death(166).

To the best of our knowledge our study is the only CMR and $^{31}$P-MRS study in women with GDM. Consistent with our findings, using echocardiography, two prospective studies have reported increased LV mass and abnormalities in GLS in women with GDM(167,168). Moreover, in a multi center longitudinal observational CARDIA (Coronary Artery Risk

Development in Young Adults) study, 609 women (64 with GDM) were followed with echocardiograms over a 20-year period(169). After adjusting for potential confounders including BMI, blood pressure, lipid levels and incident T2D, women with prior GDM were shown to have higher LV mass index and systolic dysfunction at the end of the study.

While these observational clinical studies, including our own study, cannot prove causality, using a GDM model of female rats (HIP rats), Verma and colleagues have reported supportive evidence of a causal relationship between pathological cardiac hypertrophy and GDM(170). Their results implicated altered calcium handling as the central mechanism that underlies the maternal myocardial hypertrophic response in GDM, leading to activation of calcineurin-dependent transcriptional pathway for cardiac hypertrophy (nuclear factor of activated T-cells signaling), as well as calcium/calmodulin-dependent kinase II /Class IIa histone deacetylase signaling (CaMKII/HDAC pathway), leading to expression of pro-hypertrophic genes(170,171).

### Birthweight for gestational age

Contrary to expectation the birthweight for gestational age was slightly lower in the GDM group, which is likely due to careful monitoring and controlled GDM status of our participants. Larger population studies suggest an opposite finding with higher birthweight in GDM(172).

## 4.8 Limitations

This study is limited by a relatively small sample size, in line with its proof-of-principle nature. While there are no prior studies evaluating nulliparous overweight/obese women of similar age to our study population, as the scans were performed during pregnancy once a diagnosis of GDM was established, we cannot reliably rule out that these cardiac alterations were not

present pre-pregnancy reflecting underlying pre-existing cardio metabolic risk factors in women with GDM. Moreover, longitudinal assessments are needed for the evaluation of reversibility of the maternal cardiac changes detected in this study following pregnancy.

Without an additional control group of women with obesity but without GDM, we cannot reliably exclude that the changes demonstrated in this study are driven by the GDM only or obesity only, or a combination of both conditions. Future studies are needed to address this.

Whilst studies confirm that non-contrast magnetic resonance imaging (MRI) does not harm the fetus when performed at any stage of the pregnancy(70), an increased risk of neonatal death or stillbirth with gadolinium based contrast exposure has been reported(72). As a result, only non-contrast scans were performed in our study.

## 4.9 Conclusions

This study demonstrates for the first time that young primiparous women with obesity and gestational diabetes mellitus manifest impaired myocardial contractility and significantly higher LV mass, associated with impaired myocardial energetics in late pregnancy compared to lean women with healthy pregnancy. These findings may aid our understanding of the long-term cardiovascular risks posed by gestational diabetes mellitus.

# *Chapter 5: Preeclampsia and the maternal heart*

## 5.1 Abstract

**Background-** Preeclampsia (pE) is associated with an increased risk of cardiovascular mortality (CV) and morbidity in later life affecting 3–5% of pregnancies worldwide. Compromised cardiac energy production is an important contributor to most forms of heart disease. The changes in myocardial energetics in pE have not been characterized previously.

**Purpose-** We investigated if women with pE in the third trimester of pregnancy exhibit adverse cardiac alterations in myocardial energetics, function or tissue characteristics.

**Methods-** Thirty-eight healthy pregnant (HP) women and twenty-two women with pE were recruited. Participants underwent phosphorus magnetic resonance spectroscopy and cardiovascular magnetic resonance for assessment of myocardial energetics (phosphocreatine to ATP ratio (PCr/ATP)), tissue characteristics, biventricular volumes and ejection fractions, left ventricular (LV) mass, global longitudinal shortening (GLS) and mitral in-flow E/A ratio.

**Results-** Participants were matched for age and ethnicity. The women with pE had higher body-mass index 27(26,29) versus 33(30,36) kg/m$^2$; p=0.0001), systolic 115(111,119) versus 136(131,140) mmHg; p=0.001) and diastolic 72(70,74) versus 88(84,91) mmHg; p=0.001) blood pressure. There was no difference in NTpro-BNP concentrations between the groups. The women with pE had lower myocardial PCr/ATP ratio 2.2(2.1,2.4) versus 1.9(1.8,2.1), p<0.0001), accompanied by lower LV end-diastolic volumes 76(72,80) versus 64(57,71) mL/m$^2$; p=0.006) and higher LV mass 90(85,94) versus 118(111,125) g; p=0.001). While ventricular ejection fractions were similar, the GLS was reduced in women with pE -20(18,21) % versus -16(14,17) % p=0.01). Multilinear regression showed that gestational age was independently associated with LV mass (r=0.2, p= 0.0008) but there were no other significant bivariate correlations between gestational age and PCr/ATP or GLS.

**Conclusions-** To the best of our knowledge, this is the only CMR and $^{31}$P-MRS study in women pE. Despite no prior diagnosis of hypertension, women with pE manifest impaired myocardial contractility and higher LV mass, associated with reductions in myocardial energetics. These findings may aid our understanding of the long-term cardiovascular risks associated with these conditions.

## 5.2 Introduction

Preeclampsia (pE) is a multisystem disorder defined by new-onset hypertension (BP >140/90mmHg) and proteinuria after gestational week 20, or new onset pE-associated signs in the absence of proteinuria. It is the leading cause of maternal and perinatal mortality.(26) pE complicates 3-5% of all pregnancies and is estimated to cause at least 42,000 maternal deaths annually.(173)

The potential cardiac changes in women with pE are speculated to be secondary to diastolic dysfunction due to an increase in afterload from endothelial dysfunction, vasoconstriction, interstitial oedema and capillary leak.(174) This condition results in placental mal-perfusion from the release of soluble factors into the circulation.(174)

While the cure for pE is delivery of the placenta despite the placenta providing an important role the development of pE, maternal effects of pE do not cease with the birth of the infant and delivery of the placenta.(26) Biochemical risk factors for cardiovascular disease (CVD), including raised concentrations of total cholesterol and triglycerides, have been shown to persist many years after a hypertensive disorder of pregnancy.(54) Several large-population–based studies demonstrate that women with pregnancy complicated by pE have an up to 8-fold increased lifetime risk of hypertension, CVD and premature death compared with women with healthy pregnancies.(175,176) For subtypes of CVD, a history of pE is associated with higher odds of experiencing heart failure(42), fatal ischemic heart disease (42), and non-fatal stroke.(177)

During healthy pregnancy, the maternal physiology adapts to compensate for many changes in energy demands. In pE pregnancies, normal hemodynamic adaptions fail. It is well established that patients with chronic hypertension show myocardial energetic deficit as assessed by phosphorus magnetic resonance spectroscopy($^{31}$P-MRS). (113) It is therefore

highly likely that women with pregnancies complicated by pE may also show alterations in myocardial energetics.

This study therefore aims to explore the magnitude of maternal changes in myocardial structure, function, tissue characteristics or energetics in women with preeclampsia.

## 5.3 Methods

### Study design and Oversight

The details of the study methodology are provided earlier in sections of Chapter 2, 3 and 4.

### Participants

A total of 60 participants including 38 pregnant women with an uncomplicated pregnancy and 22 pregnant women with a diagnosis of preeclampsia were recruited in the study. The pregnant participants were recruited via the Leeds Teaching Hospitals NHS Trust antenatal clinics attendance register and hypertension clinics. 28 healthy pregnant women and 12 women with preeclampsia returned for the 2$^{nd}$ study visit.

### Inclusion and exclusion criteria

Participants with on-going singleton pregnancy, >18 years of age, 26-38 weeks' gestation were recruited. Recruitment for both groups was restricted to singleton first pregnancies. Women with a diagnosis of gestational diabetes mellitus, antenatally small for gestational age babies on week 33 transabdominal ultrasound (<10$^{th}$ percentile for estimated fetal weight) or any other adverse pregnancy outcomes, known cardiovascular problems (congenital or acquired heart disease), contra-indications to CMR (pacemaker, cranial aneurysm clips, metallic ocular foreign bodies, severe claustrophobia), subjects with medical conditions that

could affect cardiac function including women with severe anemia, maternal diabetes (type 1 or type 2), chronic renal disease, chronic hypertension, liver disease, former or current smokers were excluded. Ethnicity group was self-reported by participants.

The presence of pre-existing hypertension was checked on electronic health care records at pre-screening stage. The absence of pre-existing hypertension was then confirmed with the participants during the research visit.

### Diagnosis of preeclampsia

The diagnosis of pE was confirmed with a blood pressure of > 140/90mmHg measured on 2 occasions at least 4 hours apart and protein: creatinine ratio > 0.3mg/dL on urinalysis. The cases of pE were identified from the attendance register in the antenatal day units. Cases of pE were also identified directly by members of the clinical team during their clinic appointments.

### Study investigations

The study investigations including the CMR and 31P-MRS protocols, blood tests, statistical analyses methods were all identical to the assessments described in Chapters 3 and 4.

## 5.3 Methods

We enrolled 22 women with pE. Any pregnant women with congenital or acquired cardiac lesions or those with cardiac arrhythmias were excluded. Baseline data recorded at the first visit included age, gestational age, New York Heart Association (NYHA) functional class, parity status, medications, use of cigarettes and/or alcohol, 12-lead ECG.

## 5.4 Results

### Participant demographics and clinical characteristics:

Between February 2021 and August 2022, 61 participants (38 healthy pregnancy, 22 pre-eclampsia) with similar age were recruited. Maternal age, gestational age and ethnicity distribution were similar between the groups. Ethnicity distribution (33/38 participants in the HP arm were Caucasian, 3 Pakistani, 1 Chinese and 1 Black-African; in the pE group, (20/22 participants Caucasian, 1 Chinese and 1 Black-African) and this was broadly in line with the local population demographics.

Table 5.1 demonstrates clinical characteristics and biochemical comparisons between the women with pE and healthy pregnancies (HP). The women in the pE group had higher average BMI than the HP group (33[30,36] vs 27[26,29] kg/$m^2$, p=0.001). The systolic BP (136(131,140) vs 115(111, 119) mmHg, p=0.0001) and diastolic BP (88[84,91] vs 72[70,74] mmHg, p=0.0001) were also higher in the pE group compared to the HP group as expected. The women with pE also had a higher gestational weight gain and plasma triglyceride concentrations than the HP group (3.0(2.5,3.5) vs 2.5(2.1,2.8) mmol/L, p=0.0001). There was no significant difference in NT-proBNP levels between the groups.

| | Healthy pregnancy baseline (n=38) | Pre-eclampsia baseline (n=22) | P value |
|---|---|---|---|
| ***Age, y*** | 31(30,33) | 31(29,33) | 0.8 |
| ***Ethnicity, white, %*** | 87 | 87 | 1 |
| ***Gestational date at CMR, wks*** | 30(29,31) | 34(32,36) | **0.0001** |
| ***Booking BMI, kg/m²*** | 25(23,26) | 30(25,35) | **0.0001** |
| ***BMI at scan visit, kg/m²*** | 27(26,29) | 33(30,36) | **0.0001** |
| ***Heart rate, bpm*** | 88(76,89) | 88(82,95) | 0.4 |
| ***Booking systolic BP, mmHg*** | 113(110,115) | 125(114,136) | **0.004** |
| ***Systolic BP, mmHg*** | 115(111,119) | 136(131,140) | **0.001** |
| ***Booking diastolic BP, mmHg*** | 69(65-74) | 80(75,85) | **0.01** |
| ***Diastolic BP, mmHg*** | 72(70,74) | 88(84,91) | **0.001** |
| ***Hemoglobin, g/L*** | 121(118,124) | 123(117,128) | 0.4 |
| ***HDL, mmol/L*** | 2.2(2.0-2.3) | 1.9(1.8,2.1) | **0.03** |
| ***TG, mmol/L*** | 2.5(2.1,2.8) | 3.0(2.5,3.5) | **0.001** |
| ***Creatinine, umol/L*** | 47(44,48) | 50(43,57) | 0.6 |
| ***eGFR, ml/min/1.73m²*** | 90(89,90) | 89(89,90) | **0.04** |
| ***Urine Alb/creatinine ratio*** | 1.3(0.8-1.5) | 5.6(1.4,9.7) | **0.001** |
| ***HbA1c, mmol/mol*** | 31(30,32) | 34(33,36) | 0.08 |
| ***Glucose, mmol/L*** | 5.2(4.8,5.5) | 4.7(4.3,5.1) | 0.2 |
| ***NT-proBNP, ng/L*** | 55(42,66) | 50(36-64) | 0.2 |

| | | | |
|---|---|---|---|
| ***FFA, mmol/L*** | 0.3(0.2,0.3) | 0.3(0.2,0.5) | 0.3 |
| ***Beta-hydroxybutyrate, mmol/L*** | 0.1(0.1,0.2) | 0.2(0.03,0.3) | **0.09** |

Values are means (SD) or median (IQR) for continuous variables and number (%) for categorical variables. [LL of 95% confidence interval – UL of 95% confidence interval].BMI indicates body mass index; kg, kilograms; n, number; bpm, beats per minute; mmHg, millimeters of mercury; g/l, gram per Liter; HDL, high density lipoprotein; mmol/L, millimoles per litre; LDL, low density lipoprotein; TG, triglyceride; eGFR, estimated glomerular filtration rate; ml/min/1.73m2, millilitre per minute per (1.73 square meters); pmol/L, picomoles per litre; NT-pro BNP, N-terminal pro hormone B-type natriuretic peptide; HBA1c, glycated haemoglobin; FFA, free fatty acids.

Table 5.1: Clinical Characteristics and Biochemistry

The antenatal medication lists were recorded, most patients were receiving labetolol (73% of the total group) at dose varying from 100 mg bd to 400 mg qds and 6 patients were on 150mg OD aspirin. Table 5.2 demonstrates the details of the labetalol treatment per patient.

| Total doses of labetalol per day (mg) | Number of patients receiving labetalol |
|---|---|
| **200** | 2 |
| **300** | 1 |
| **400** | 2 |
| **600** | 4 |
| **800** | 3 |
| **1200** | 1 |
| **1600** | 3 |

Table 5.2: demonstrates the number of patients on the respective doses of labetalol ranging from 200mg to 1600 mg per day.

### Myocardial energetics, structure and function comparisons:

Baseline CMR/$^{31}$P-MRS results are shown in Table-5.3.

The women with pE showed significant reductions in myocardial PCr to ATP ratio (1.9 [1.7-2.1] vs 2.2 [1.9-2.4], p=0.0004).

The women with pE exhibited lower LV end-diastolic volumes (EDV) indexed for body surface area (76[72,80] vs 65[58,73] ml/m$^2$; p=0.0001), but higher LV mass (117[110, 124] versus 90[85,94] g, p=<0.0001) and higher LV mass over LV EDV ratio suggestive of increased concentricity of the LV (0.92[0.82,1.03)]vs 0.64 [0.61-0.67] g/ml; p <0.0001). LV end-diastolic wall thickness was also higher in women with pE (9.5[8.6,10.2] vs 7.6[7.2,8.0] mm; p<0.0001), Whilst the LV ejection fraction was similar between the two groups, the LV global longitudinal shortening (GLS) was significantly reduced in the pE group ( -16[15,17] versus -20[18,21] %;

p=0.01). The native myocardial T1 values were significantly lower in the pE cohort when compared to the HP cohort (1296 [1281,1311] ms versus 1326 [1314,1337], p=0.01. T2 values were not measured due to the differences in heart rate variability with phantom testing (this was expanded in Chapter 3). The pE group also exhibited a lower but non-significant reduction in mitral inflow E/A ratio measured from mitral in-flow velocity-encoded images (1.7 [1.5,1.8] versus 1.5[1.3,1.9], p=0.09. The mitral annular plan systolic excursion (MAPSE) was also reduced in the pE cohort.

As with the differences in LV EDV between the two groups, the right ventricular (RV) EDV was smaller in the pE group (65[57,73] vs 83[79,88]; p<0.001). There were no significant differences in RV ejection fraction, left atrial volumes or function between the two groups.

| | **Healthy pregnancy baseline (n=38)** | **Pre-eclampsia baseline (n=22)** | **P value** |
|---|---|---|---|
| ***LV end diastolic volume index (ml/m²)*** | 76(72,80) | 64(57,71) | **0.006** |
| ***LV end systolic volume index (ml/m²)*** | 31(29,33) | 29(25,32) | 0.4 |
| ***LV stroke volume (ml)*** | 84(78,88) | 77(69,85) | 0.2 |
| ***LV ejection fraction (%)*** | 59(57,60) | 58(56,60) | **0.02** |
| ***LV mass (g)*** | 90(85,94) | 118(111,125) | **0.0001** |
| ***LV mass index (g/m²)*** | 46(45,50) | 57(54,59) | **0.03** |
| ***LV mass/LV EDV (g/ml)*** | 0.62(0.58,0.65) | 0.9(0.8,1) | **0.0001** |
| ***Cardiac output (l/min)*** | 6.6(6.3-7) | 6.1(5.4-6.9) | **0.01** |
| ***Cardiac index (l/min/m²)*** | 3.5(3.3-3.7) | 3.0(2.6-3.4) | 0.2 |
| ***Wall thickness (mm)*** | 7.6(7.2,8.0) | 9.5(8.6,10.2) | **<0.0001** |
| ***RV end diastolic volume index (ml/m2)*** | 83(79,88) | 65(57,73) | **0.001** |

| | | | |
|---|---|---|---|
| ***RV end systolic volume index (ml/m²)*** | 38(35,40) | 28(24,32) | 0.1 |
| ***RV stroke volume (ml)*** | 86(80,91) | 76(67,86) | 0.1 |
| ***PCr/ATP*** | 2.2(2.1,2.4) | 1.9(1.8,.2.1) | **<0.0001** |
| ***Native T1 relaxation time (ms)*** | 1326 (1314,1337) | 1296 (1281,1311) | **0.01** |
| ***RV ejection fraction (%)*** | 55(53,57) | 57(54,60) | 0.6 |
| ***Global longitudinal shortening (%)*** | -20(18,21) | -16(14,17) | **0.01** |
| ***MAPSE, (mm)*** | 14(14,15) | 12(11,14) | **0.02** |

Values are means (SD) or median (IQR) for continuous variables and number (%) for categorical variables. [LL of 95% confidence interval – UL of 95% confidence interval].LV indicates left ventricular; ml, milliliter; ml/$m^2$, milliliters per square meter of body surface area; g, gram; g/$m^2$, gram per square meter of body surface area; LV, left ventricular; RV, right ventricular; LA, left atrium; MAPSE, mitral annular plane systolic excursion; PCr/ATP phosphocreatine to adenosine triphosphate ratio

Table 5.3: Baseline CMR findings

### Birthweight for gestational age

In line with the literature, the birthweight for gestational age was slightly lower in the preeclampsia group (2736 ± 997g) when compared to healthy pregnancy (3390±492g), p=0.01. (178)

## 5.5 Discussion

In this prospective study, diagnosis of pE was associated with subclinical alterations in cardiac energetics, structure and function. Compared to age, gestational age and ethnicity matched women with a healthy uncomplicated pregnancy, young women with preeclampsia displayed increased LV concentricity with higher LV wall thickness and mass, and smaller LV chamber size. These structural alterations were accompanied by significant reductions in myocardial energetics and in LV GLS in the preeclampsia group. These findings may aid our understanding of the long-term cardiovascular risks posed by pE.

Reductions in myocardial PCr/ATP ratio have been demonstrated in patients with chronic hypertension. (179) Chronic hypertension results in remodelling of the heart muscle, leading to changes in the metabolic processes involved in energy production. (180)In hypertensive heart disease, the heart's demand for energy may increase due to the increased workload required to pump blood against elevated BP. (181)In a similar way, here we show for the first time that women with hypertensive pregnancy complications also show evidence of an early cardiac remodelling phenotype accompanied by reduction in myocardial energetics compared to women with healthy pregnancies.

In chronic hypertensive disorders, several therapies aimed at improving myocardial energetics have been studied, including beta-blockers and angiotensin converting enzyme inhibitors.(182) In an earlier study we have detected significant improvements in systolic BP and improvements in myocardial PCr/ATP ratio and reduction in LV mass in patients with T2D after 3 months of empagliflozin treatment(152). Lifestyle changes such as regular exercise and healthy diet can also improve myocardial PCr/ATP ratio. (183)While the changes in PCr/ATP or cardiac structural remodelling (LV wall thickness increase or LV mass increase) were not dramatic but significantly different between the two groups of women in this study

despite a short exposure to hypertensive disorder in these young women. However, neither ACE inhibitors nor empagliflozin are safe during pregnancy, leaving only option of beta blockers for BP modification for this cohort.(184)

The significantly lower myocardial native T1 values in the pE group is hypothesised secondary to an insufficient hyperaemic response to increased cardiac workload.

Over and above the BP changes in the pE group in this study there were additional metabolic and hemodynamic challenges present, including higher BMI, higher triglyceride and LDL concentrations, lower HDL levels and an increase in urine albumin/creatinine ratio in these women. The association of obesity and reduction in myocardial PCr/ATP is well established further contributing to the cardiac findings in the pE cohort this study. In line with our findings, in a prospective study of 15,000 women, those with a history of preeclampsia or gestational hypertension also had a higher BMI, blood pressure and cholesterol levels.(11)

Given the multitude of metabolic and hemodynamic alterations in the pE group, the driving factor for this energetic impairment is likely to be multifactorial rather than solely attributed to hypertension.

### Cardiac structural and functional changes in preeclampsia

The enhanced cardiac concentricity revealed in our study may be an important component of the worsened cardiovascular outcomes in women with preeclampsia in the longer term. Increased cardiac concentricity is well known to be associated with poorer long term cardiovascular outcomes.(185) (186) Diastolic dysfunction is also present in our cohort of patients with preeclampsia with a reduced MAPSE and mitral inflow E/A ratio with preserved systolic function. Diastolic dysfunction, which prevails changes in systolic dysfunction is an

energy-dependent process resulting in a quick decrease in LV pressure after the end of contraction and during early diastole. Myocardial relaxation is more vulnerable than contraction and is compromised in preeclampsia which is also evident in our study. (187)

These changes are an adaptive response to reduce the wall stress associated with increased afterload(64) to maintain a balance between myocardial oxygen demand and supply. Consistent with our findings, using echocardiography, two studies have reported a reduction in diastolic function in cohorts with preeclampsia when compared to healthy controls. (188) (189)

Oxidative stress and endothelial dysfunction could perhaps be other reasons to explain the structural changes in patients with preeclampsia as this condition is associated with vascular stiffness and vasoconstriction. (64) Increased levels of reactive oxygen species could lead to ischaemic reperfusion injury. These aspects such as peripheral endothelial function was not assessed in this study.

Prior studies have looked at the association between maternal cardiac outcomes and prior heart failure, stroke, myocardial dysfunction.(190) A study demonstrated that women with pE complicated by pulmonary oedema had increased left ventricular mass but normal systolic function compared with normotensive controls.(191)

Previous studies have demonstrated a link between vitamin D deficiency as a risk factor for pE given its benefits of improving vascular inflammation, endothelial dysfunction and vascular stiffness. This could be a target for future interventional studies however at present, there is insufficient evidence to support a recommendation for screening all pregnant women for vitamin D deficiency.(11)

## 5.6 Limitations

This study is limited by a relatively small sample size, in line with its proof-of-principle nature. While there are no prior studies evaluating nulliparous women with pE of similar age to our study population, as the scans were performed during pregnancy once a diagnosis of pE was established, we cannot reliably rule out that these cardiac alterations were not present pre-pregnancy reflecting underlying pre-existing cardio metabolic risk factors in women with pE. We have recruited a cohort of obese and lean nulliparous controls in the longitudinal follow up in Chapter 6 to overcome the limitation of BMI matching in this study.

## 5.7 Conclusions

We show here for the first time that despite no prior diagnosis of hypertension, women with pE manifest impaired myocardial contractility and higher LV mass, associated with reductions in myocardial energetics. These findings may aid our understanding of the long-term cardiovascular risks associated with these conditions.

# *Chapter 6: Maternal cardiac changes twelve-month post-partum in women with gestational diabetes mellitus or preeclampsia compared to healthy pregnancies*

## 6.1 Abstract

**Background:** Gestational diabetes mellitus (GDM) and preeclampsia (pE) are the leading obstetric complications of pregnancy. Both are associated with a substantial increase in the risk of long-term cardiovascular disease. However, pregnant women are underrepresented in clinical research and the mechanisms of long-term cardiovascular complications in women with obstetric complications remain to be elucidated.

**Objectives** This longitudinal cohort study was designed to assess maternal cardiac alterations during the third trimester of pregnancy and their recovery twelve-months post-partum in women with GDM (n=30) or preeclampsia (n=22) compared to women with healthy pregnancies (HP)(n=38).

**Methods:** $^{31}$P-MRS and CMR were used to define myocardial phosphocreatine to ATP ratio (PCr/ATP), tissue characteristics, left ventricular (LV) volumes, mass, ejection fraction (EF), global longitudinal shortening (GLS), and diastolic function (mitral in-flow E/A ratio). Investigations were repeated 12-months postpartum. With obesity as a major and common risk factor for both GDM and pE, 10 overweight and 10 normal-weight nulliparous women served as non-pregnant controls.

**Results:** Participants were matched for age and ethnicity and the pregnancy groups were matched for gestational age. Both the GDM and pE groups had higher BMI compared to the HP.

Compared to the HP group, women with GDM had higher LV mass (90[85,94] vs 103[96,112] g; p=0.001) and lower myocardial PCr/ATP (2.2[2.1,2.4] vs 1.9[1.7,2]; p<0.0001), LV end-diastolic volumes (EDV) (76[72,80] vs 67[63,71]ml, p=0.03) and GLS (20[18,21] vs 18[17,19] %; p=0.008).

Compared to the HP group, at similar magnitudes to women with GDM, the women with pE exhibited higher LV mass (90[85,94] vs 118[111,125] g; p<0.0001) and lower myocardial PCr/ATP (2.2[2.1,2.4] vs 1.9[1.8,2.1]; p=0.0004) and GLS (20[18,21] vs 16[14,17] %; p=0.01). There were no significant differences in PCr/ATP, LV EDV, mass or GLS between the GDM and pE groups.

Twelve-months postpartum there were no significant changes in any of the cardiac assessments in women in the HP, GDM or pE groups compared to their respective third-trimester pregnancy assessments.

Compared to nulliparous normal-weight controls, HP was associated with no significant differences in myocardial PCR/ATP, LV volumes, mass, EF, diastolic function, or GLS. The overweight nulliparous controls showed significantly higher LV mass and lower myocardial PCr/ATP and GLS than normal-weight controls. There were no significant differences in LV mass, PCr/ATP or GLS between the overweight nulliparous controls and GDM or pE groups during or after pregnancy.

**Conclusions:** Despite distinct aetiologies women with GDM and pE exhibit a similar myocardial phenotype during and after pregnancy with persistent subtle abnormalities in myocardial PCr/ATP ratio, LV mass and GLS compared to women with HP during pregnancy and twelve months' postpartum assessments. Women with GDM and pE show similar myocardial alterations to nulliparous women with obesity, suggesting that the myocardial changes are predominantly driven by obesity-associated metabolic dysfunction.

## 6.2 Introduction

The work described in Chapter 4 and chapter 5 demonstrated that women with overweight/obesity and gestational diabetes mellitus (GDM) and women with preeclampsia exhibit significant reductions in myocardial energetics, smaller hearts with lower left ventricular (LV) end-diastolic volumes, subtle reductions in myocardial contractile function and higher LV mass in the third trimester of pregnancy compared to women with healthy pregnancy (HP). (192). In order to track these imaging-derived subclinical myocardial maternal alterations I have monitored the participants of this study 12 months' post-partum and repeated multi parametric CMR and $^{31}$P-MRS imaging in this longitudinal cohort study. Given the established excess risk of ischemic heart disease in women with GDM and pE, in addition to the non-contrast CMR research cardiac scan protocol performed during the pregnancy, I have assessed rest and adenosine stress myocardial CMR perfusion imaging and non-invasive evaluation of proximal coronary artery disease and anomalous coronary artery origins using three-dimensional coronary magnetic resonance angiography (MRA). Non-invasive coronary MRA imaging was elected despite its limited sensitivity over more conventional approaches for anatomical assessment of epicardial coronary arteries such as X-ray coronary angiography or computed tomography coronary angiography to prevent ionising radiation exposure in this young and asymptomatic group.

Because women in childbearing age are not screened for diabetes the current definition of GDM makes it difficult to distinguish between undiagnosed diabetes and hyperglycemia induced by pregnancy. As a result, GDM often represents a group previously undiagnosed women with prediabetes, type 2 diabetes (T2D) as well as hyperglycemia induced by pregnancy(193). Moreover, due to endothelial cell damage and irreversible metabolic

derangements, pE is recognised as a major risk factor for the development of future cardiovascular disease. I have therefore repeated plasma biochemical assessments and imaging to rule out continued evidence of plasma metabolic and structural abnormalities.

In addition in this study, I have recruited two additional cohorts of age matched nulliparous controls including normal body-weight and overweight/obese non-pregnant women with an aim to better understand: i) the impact of pre-existing overweight or obesity on the myocardial structural, functional and metabolic abnormalities in the GDM and pE cohort in third trimester and ii) the physiological effects of pregnancy in women in the third trimester of a healthy singleton pregnancy on myocardial energetics, function, tissue characteristics. Nulliparous control groups have undergone an identical non-contrast pregnancy CMR and $^{31}$P-MRS cardiac scan protocol; but no coronary imaging or adenosine perfusion CMR.

## 6.3 Methods

### Study design and Oversight

This single-center longitudinal prospective cohort study complied with the Declaration of Helsinki and was approved by the National Research Ethics Committee (REC20/NE/0117 for pregnancy scans and REC18/YH/0168 for non-pregnancy studies), and informed written consent was obtained from each participant.

### Participants

A total of 110 participants including 38 pregnant women with an uncomplicated pregnancy, 30 pregnant women with a diagnosis of gestational diabetes and 22 pregnant women with a diagnosis of preeclampsia were recruited in the study. Twenty healthy volunteers (HV) were recruited (10 lean with BMI<30 and 10 obese with BMI>30) to serve as a control group. The HV volunteers in this study include the 15 mentioned in chapter 3 with the addition of 5 further controls to allow for BMI matching. The pregnant participants were recruited via the Leeds Teaching Hospitals NHS Trust antenatal clinics attendance register and GDM clinics. 30 healthy pregnant women, 26 women with gestational diabetes and 16 women with preeclampsia returned for the 2$^{nd}$ study visit. Figure-6.1, Consort Diagram).

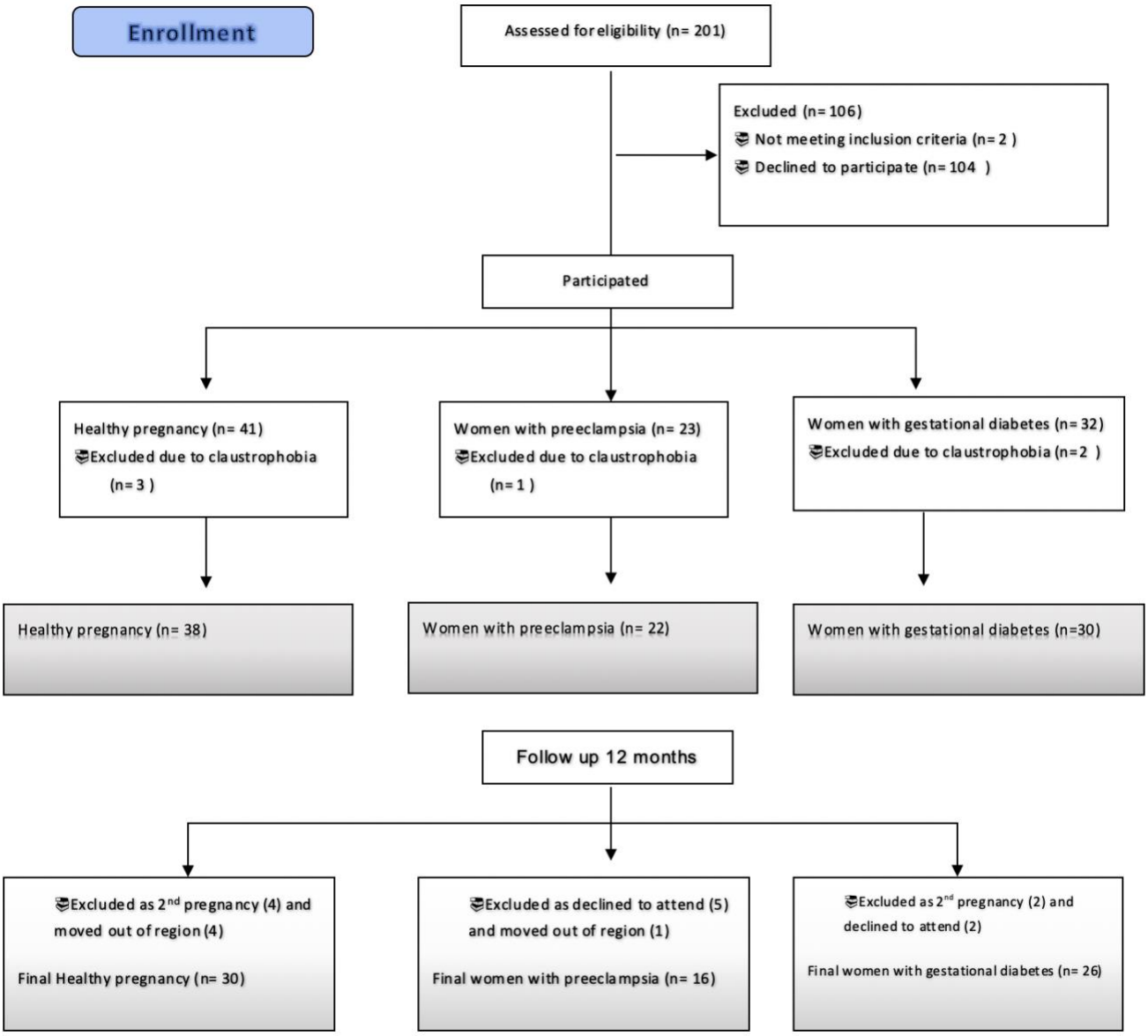


Figure 6.1: Consort diagram

### Inclusion and exclusion criteria

As previously reported, participants with on-going pregnancy, >18 years of age, 26-38 weeks' gestation were recruited(192). Recruitment for both groups was restricted to singleton first pregnancies. Women with antenatally small for gestational age babies on week 33 transabdominal ultrasound (<10$^{th}$ percentile for estimated fetal weight) or any other adverse pregnancy outcomes, known cardiovascular problems (congenital or acquired heart disease), contra-indications to CMR (pacemaker, cranial aneurysm clips, metallic ocular foreign bodies, severe claustrophobia), subjects with medical conditions that could affect cardiac function including women with severe anemia, maternal diabetes (type I or type II), chronic renal disease, chronic hypertension, liver disease, former or current smokers were excluded. Ethnicity group was self-reported by participants.

The presence of pre-existing diabetes or hypertension was checked on electronic health care records at pre-screening stage. The absence of pre-existing diabetes or hypertension was then confirmed with the participants during the research visit.

Nulliparous controls were matched for age, ethnicity and were recruited from among the University of Leeds researchers among those responding to email invitations sent to all university staff.

Neonatal events were defined as any of the following: premature birth (<37 weeks' gestation, small for gestational age birthweight (<10$^{th}$ percentile), respiratory distress syndrome, intraventricular haemorrhage, fetal death (>20 weeks' gestation) or neonatal death (within 28 days after birth).

Obstetric events included non-cardiac death, post-partum haemorrhage (PPH) which was defined as blood loss >500mL (vaginal delivery) or >1000mL (Caesarean section), which required transfusion or was accompanied by a reduction in haemoglobin >20g/L.

Follow up data was obtained during the one year follow up visit.

### Oral glucose tolerance test

Diagnosis of GDM was confirmed on a 75g oral glucose tolerance test (OGTT) in all participants in the GDM group at the antenatal clinics using the U.K. National Institute for Health and Care Excellence (NICE) guideline criteria for GDM of fasting glucose ≥5.6 mmol/L (≥100.8 mg/dL) and/or 2-hour glucose ≥7.8 mmol/L (≥140.4 mg/dL) after 75g oral glucose at ~26 weeks' gestation(90).

### Diagnosis of preeclampsia

The diagnosis of pE was confirmed with a blood pressure of > 140/90mmHg measured on 2 occasions at least 4 hours apart and protein: creatinine ratio > 0.3mg/dL on urinalysis. The cases of pE were identified from the attendance register in the antenatal day units. Cases of pE were also identified directly by members of the clinical team during their clinic appointments. The antenatal medication lists are tabulated below; 2 patients were on 100mg BD labetalol, 1 patient on 100mg TDS labetalol, 2 patients on 200 mg BD labetalol, 4 patients on 200mg TDS labetalol, 3 patients on 200mg QDS labetalol, 1 patient on 400mg TDS labetalol, 3 patients on 400mg QDS labetalol and 6 patients were on 150mg OD aspirin.

### Anthropometric measurements

All women had height and weight recorded, and body-mass index (BMI) calculated at the booking visit performed at approximately the 8$^{th}$ gestational week in antenatal clinics. Brachial artery blood pressure (BP) was recorded as an average of 3 sitting measures taken over 10 min (DINAMAP-1846-SX, Critikon Corp) after an initial 5-minute rest using the

appropriate cuff size based on the mid arm circumference. These assessments were then repeated during the research CMR scan visit performed at third trimester and at the 12-month post-partum follow up. A standard 12-lead ECG was performed in all participants on the same day as the CMR. A venous blood sample was taken for assessments of full blood count, estimated glomerular filtration rate (eGFR), liver function, glycated hemoglobin (HbA1c), lipid profile (triglycerides and high-density lipoprotein (HDL), low-density lipoprotein (LDL) and total cholesterol concentrations) and N-terminal pro hormone B-type natriuretic peptide (NT-proBNP) also on the same day as both the CMR scans. When the patients were pregnant, a flexible approach to blood tests were used and participants were requested to fast for 4 hours prior to research visits as per the recommendations of the local patient and public involvement group at the stage of study design.

### Placental samples

A sample of placental tissue and umbilical cord was obtained from the placenta following delivery. Local procedures were followed for collection, embedding and fixation of placental tissue. Tissue sections were produced as per local protocols and prepared for histological examination. Weight of the placental disc was measured in grams after removal of the cord and membranes. The micro morphological changes in the placenta was examined for both groups.

### $^{31}$Phosphorus magnetic resonance spectroscopy

$^{31}$P-MRS was performed to obtain the PCr/ATP ratio from a voxel placed in the mid-ventricular septum, with the participants lying supine and a $^{31}$P transmitter/receiver cardiac coil (Rapid Biomedical GmbH, Rimpar, Germany) placed over the heart, in the iso-center of the magnet

on a 3.0 Tesla MR system (Prisma, Siemens, Erlangen, Germany). $^{31}$P-MRS data were acquired with a non-gated 3-D acquisition-weighted chemical shift imaging (CSI) sequence as previously described(152).

### Cardiovascular magnetic resonance imaging

All scans were performed on a 3.0 Tesla MR system (Prisma, Siemens, Erlangen, Germany) and all participants underwent cardiac magnetic resonance imaging (MRI) scans lying supine. The CMR protocol for the first visit (Figure-6.2A) consisted of cine imaging, velocity-encoded mitral in-flow imaging, native T1 mapping and T2 mapping. The details for the first visit CMR protocol was described in the methods section in Chapter 3.

In the second visit, the same protocol was repeated with the addition of perfusion imaging, post contrast T1 mapping and three-dimensional whole heart imaging. Post-contrast T1 mapping acquisition was performed 15 minutes after last contrast injection.

Perfusion imaging used free-breathing, motion-corrected automated in-line perfusion mapping. Adenosine was infused at a rate of 140µg/kg/min, for a minimum of 3 minutes according to hemodynamic and symptomatic response (a significant hemodynamic response was defined as >10 beats/min increase in heart rate, or BP drop >10mmHg and >1 adenosine-related symptom e.g., chest tightness, breathlessness). For perfusion imaging, an intravenous bolus of 0.05mmol/kg gadobutrol (Gadovist, Leverkusen, Germany) was administered at 5ml/s followed by a 20ml saline flush using an injection pump (Medrad MRXperion Injection System, Bayer). Two trained cardiologists with an up-to-date advanced life support certification monitored the patients during adenosine stress imaging.

Late gadolinium enhancement imaging was performed using a phase-sensitive inversion recovery sequence in left ventricular short- and long-axis planes >8 minutes after contrast administration.

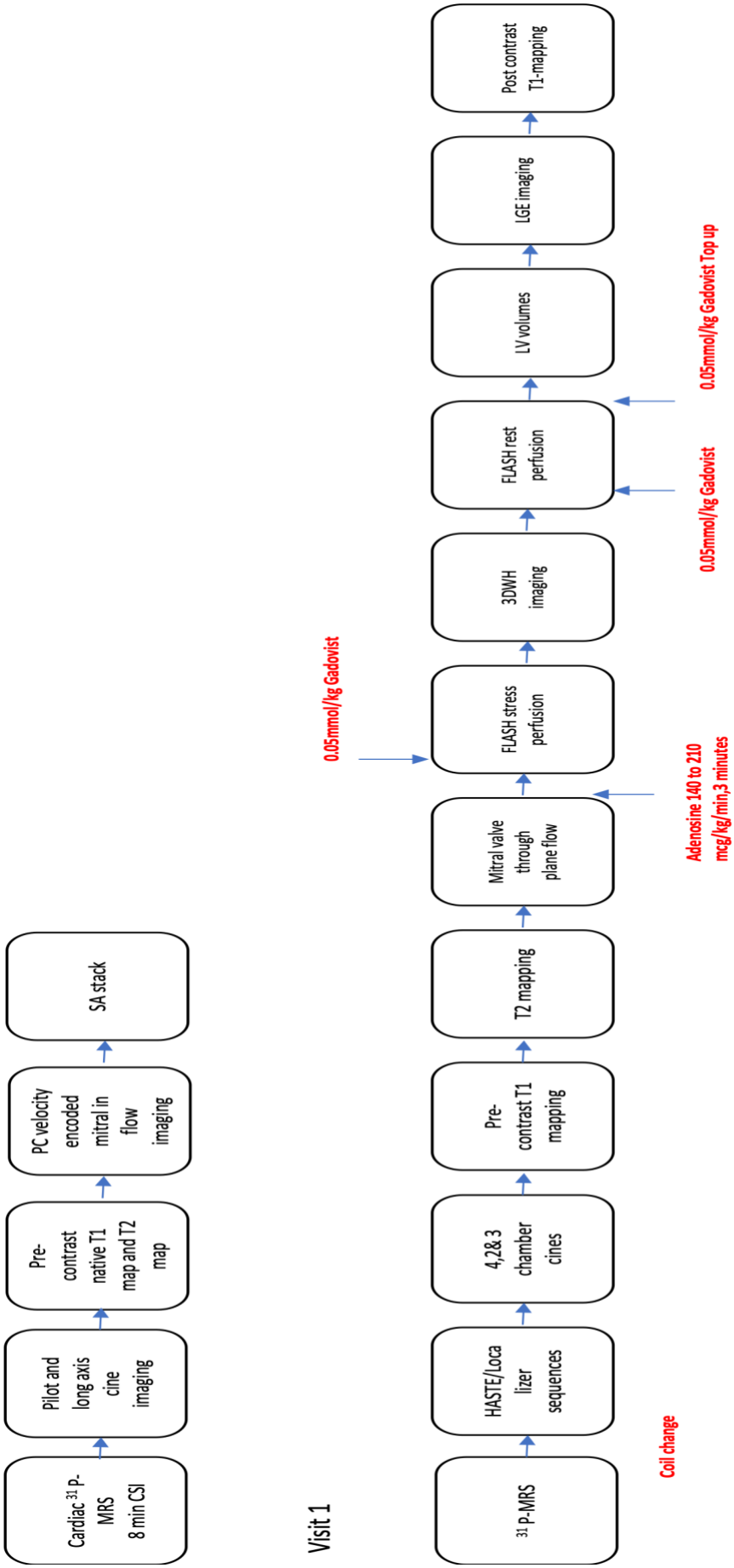
Visit 1
Cardiac 31 P-MRS 8 min CSI
Pilot and long axis cine imaging
Pre-contrast native T1 map and T2 map
PC velocity encoded mitral in flow imaging
SA stack
Visit 2
31 P-MRS
Coil change
HASTE/Localizer sequences
4,2& 3 chamber cines
Pre-contrast T1 mapping
T2 mapping
Mitral valve through plane flow
0.05mmol/kg Gadovist
FLASH stress perfusion
Adenosine 140 to 210 mcg/kg/min,3 minutes
3DWH imaging
0.05mmol/kg Gadovist
FLASH rest perfusion
0.05mmol/kg Gadovist Top up
LV volumes
LGE imaging
Post contrast T1-mapping

Figure 6.2A and 6.2B: The first visit cardiac magnetic resonance (CMR) protocol consisted of cine imaging, velocity-encoded mitral in-flow imaging, native T1 mapping and T2 mapping (6.2A)

The second visit cardiac magnetic resonance (CMR) protocol included additional adenosine stress perfusion, late gadolinium enhancement and 3-dimensional whole heart (3DWH) imaging (6.2B)

### Three-dimensional whole heart coronary magnetic resonance angiography

This protocol was conducted by performing 4 chamber cine free breathing using 40-50 phases to generate more trigger times for assessment. Following this the 3D navigator whole heart was performed using position acquisition volumes to cover the heart and liver dome navigators positioned accordingly. The data window duration was set to less than 150ms using the number of segments. The data window start which should be the same time as the lowest value trigger time is controlled by the trigger delay value. Once scout mode is applied, scanning takes place for about 8 minutes.(109) (Figure 2.8)

### Quantitative imaging data analysis

All $^{31}$P-MRS analysis was performed off-line blinded to participant details by ST using software within Matlab version R2012a (Mathworks, Natick, Massachusetts) as previously

described.(102) The anonymization codes were only unlocked once all data analysis was completed.

CMR post processing analysis using cvi42 software (Circle Cardiovascular Imaging, Calgary, Canada) was performed by me off-line blinded to all participant details after completion of the study and scan contours were subsequently reviewed by EL who was also blinded to participant details.

Global longitudinal shortening (GLS) data were derived from horizontal long-axis and vertical long-axis images, and image reconstruction and processing were implemented using the Gadgetron software framework with the previously developed convolutional neural network for labelling landmarks on CMR images.(124)

Diastolic function was measured from mitral in-flow velocity-encoded images.(125) Regions of interest were manually drawn on one frame to encircle the entire cross section of MV leaflets and propagated using a semi-automated contouring mode on Circle cvi42 software (Circle Cardiovascular Imaging Inc., Calgary, Alberta, Canada), yielding velocity versus time graphs characterizing diastolic E and A waves. The mean of maximum velocity obtained for MV was recorded. The deceleration time (DT) was calculated as previously described from the same images.(125)

Native T1 and T2 maps were analyzed using cvi42 software (Circle Cardiovascular Imaging, Calgary, Canada) which were measured for each of the 16 segments using the AHA classification.

Left atrial (LA) volume and ejection fraction (EF) were calculated using the biplane area-length method in the horizontal and vertical long axes as previously described.(194) Strain measurements were performed using cvi42 Tissue Tracking from the short axis images, and the long axis views. Peak early diastolic strain rate was measured.(195)

Myocardial perfusion image reconstruction and processing was implemented using the Gadgetron software framework.(196) Rest/stress MBF were measured for each of the 16 segments using the AHA classification. T1 maps and ECV were analysed using cvi42 software as previously described.(126)

The LV short axis stack of late gadolinium hyper-enhancement imaging images was first assessed visually for presence of late gadolinium hyper-enhancement, followed by quantification when late gadolinium hyper-enhancement was present as previously described(20). Late gadolinium hyper-enhancement was defined as areas of signal intensity ≥5 standard deviations from normal myocardium and was expressed as the percentage of LV mass, quantified in a blinded fashion.

Three-dimensional whole heart coronary magnetic resonance angiography was analyzed by visualization of the vessel sharpness (proximal vessel and subsequently full vessel length) and maximum visible vessel length of all three coronary arteries.

Sharpness and quality of the image was divided either in those with excellent image quality with sharply defined coronary borders or uninterpretable images with blurred edges, noise and residual artefact.

Artificial intelligence (AI) based analysis has been performed on all our cohorts of patients.

### Statistical analysis

Statistical analysis was performed using GraphPad Prism software (version 9.0.0). Categorical data were compared with Pearson's chi-square test. Continuous variables are presented as mean [LL of 95% confidence interval – UL of 95% confidence interval or median (interquartile range) and were checked for normality using the Shapiro-Wilk tests. Categorical data are presented as numbers and percentages. Comparisons of all CMR and biochemistry data were

performed with two-tailed paired t-test or Mann Whitney U test as appropriate. Comparisons between the 3 groups were performed by 1-way ANOVA with post hoc Bonferroni corrections. Differences in non-parametric variables were assessed using a Kruskal-Wallis test. Bivariate correlations were performed using the Pearson or Spearman method as appropriate. Comparison between baseline and post-partum measurements in patients were performed with 2-tailed paired t-test. P≤0.05 was considered statistically significant.

## 6.4 Results

Between February 2021 and August 2022, 110 participants (38 healthy pregnancy, 30 gestational diabetes, 22 pre-eclampsia) and 20 healthy nulliparous volunteers(HV) with similar age were recruited (10 lean with BMI<30 and 10 obese with BMI>30) to serve as a control group. Maternal age, gestational age and ethnicity distribution were similar between the groups. Ethnicity distribution (33/38 participants in the HP arm were Caucasian, 3 Pakistani, 1 Chinese and 1 Black-African; in the GDM group, (26/30 participants Caucasian, 1 Indian, 2 Chinese and 1 Black-African); in the pE group, (20/22 participants Caucasian, 1 Chinese and 1 Black-African) in the HV group (14 participants Caucasian, 3 Indian, 1 Chinese, 2 Malay) and this was broadly in line with the local population demographics. Both pregnant groups included similar numbers of participants classified as advanced maternal age (>35 years of age) (HP: 6 versus GDM: 4 versus PE: 3, p=0.8). None of the participants in either groups had a family history of T2D or hypertension.

Demographics, clinical, and biochemical data at baseline for all 3 cohorts have been described in chapter 3-5.

**Third-trimester pregnancy and twelve months' post-partum comparison**

**Participant demographics and clinical characteristics:**

Participants were matched for age and ethnicity and the pregnancy cohorts were matched for gestational age. Both the GDM and pE cohorts had higher body-mass index during pregnancy compared to the HP cohort. Despite significant weight reduction post-partum, the average post-partum BMI remained higher the GDM and pE groups compared to the post-partum HP group (HP: 26(27,30) versus GDM 30(29,35) versus pE: 30(24,35) kg/$m^2$, p=0.03). Twelve months' post-partum, all three pregnancy groups showed significant reduction in resting heart rate and systolic blood pressure (Table 6.1). However, average systolic blood pressure (pE 124(117,132) versus HP 103(97,110) mmHg, p=0.004) as well as average diastolic blood pressure (pE 80(75,85) versus HP 70(67,71) mmHg, p<0.001) remained significantly higher in the pE group compared to the HP group 12 months' post-partum.

Amongst the metabolic parameters, plasma HDL and triglyceride concentrations reduced significantly at 12 months postpartum compared to the third trimester of pregnancy scan in all 3 cohorts. Pregnancy is known to be associated with lower circulating HbA1c levels due to haemodilution. In keeping with this the HbA1c levels were higher at 12 months' post-partum in all three groups, but the glucose levels were significantly lower in the HP arm compared to pE and GDM groups even at post-partum assessments.

| | Normal weight controls (n=10) | Controls with overweight/obesity (n=10) | Healthy pregnancy baseline (n=38) | Healthy pregnancy follow up (n=30) | Gestational diabetes mellitus baseline (n=30) | Gestational diabetes mellitus follow up (n=26) | Pre-eclampsia baseline (n=22) | Pre-eclampsia follow up (n=16) | ANOVA |
|---|---|---|---|---|---|---|---|---|---|
| **Age, y** | 31(30,32) | 32(27,37) | 31(30,33) | 32(31,34) | 31(30-33) | 32(30,34) | 31(29,33) | 32(29,35) | 0.4 |
| **Ethnicity, white, %** | 67 | 100 | 87 | 87 | 87 | 83 | 87 | 75 | 0.3 |
| **Gestational date at CMR, wks** | - | - | 30(29,31) * | - | 31(30,32) $ | - | 34(32,36) *$ | - | **0.007** |
| **Booking BMI, kg/m²** | - | - | 25(23,26) @* | - | 31(29,33) @ | - | 30(25,35) *$ | - | **0.0002** |
| **BMI at scan visit, kg/m²** | 23(20,24)! | 30(28,32)A, | 27(26,29)@*! | 26(27,30)!+ | 33(31,35) @! | 30(29,35)! | 33(30,36)! | 30(24,35)! | **<0.0001** |
| **Heart rate, bpm** | 61(56,66)! | 74(66,82), | 88(76,89) !@* | 70(66,75)+ | 91(86,96) !@ | 68(61,74) | 88(82,95) !$ | 75(64,85)! | **<0.0001** |
| **Booking systolic BP, mmHg** | - | - | 113(110,115) @* | - | 120(116,123) @ | - | 125(114,136) * | - | **0.004** |
| **Systolic BP, mmHg** | 112 (105,119) | 114(104,120) | 115(111,119) * | 103(97,110) | 121(116,126) $ | 107(102,112) | 136(131,140) * $ | 124(117,132) | **<0.0001** |
| **Booking diastolic BP, mmHg** | - | - | 69(65-74) @* | | 74(71,77) @ | - | 80(75-85) * | | **0.01** |
| **Diastolic BP, mmHg** | 73(69,77) | 72(68,80) | 72(70,74) @* | 70(67,71) | 76(73,79) @$ | 69(66,72) | 88(84,91) *$ | 80(75,85) | **<0.0001** |
| **Biochemistry** | | | | | | | | | |
| **Hemoglobin, g/L** | 134(127,139) | 131(112,150) | 121(118,124) @ | 134(131,138) % | 122(119,125) ^ | 135(131,138) | 123(117,128) *$ | 134(131,138) & | **<0.0001** |
| **HDL, mmol/L** | 1.9(1.6,2.3) | 2.1(1.9,2.3), | 2.2(2.0-2.3) @ | 1.6(1.4,1.8) | 1.9(1.7,2.1) @ | 1.4(1.2,1.5) | 1.9(1.8,2.1) * | 1.5(1.4,1.7) | **<0.0001** |
| **TG, mmol/L** | 0.9(0.6,1.2)! | 1.2(1,1.4), | 2.5(2.1,2.8) @ | 1.0(0.7,1.3)+ | 3.1(2.8,3.4) @ ^ | 1.3(1.0,1.6) | 3.0(2.5,3.5) & | 1.4(1.0,1.7) | **<0.0001** |

| | | | | | | | | | |
|---|---|---|---|---|---|---|---|---|---|
| **Creatinine, umol/L** | 58(54,62) | 65(55,73) | 47(44,48) % | 59(55,63) | 46(42,50) ^ | 58(52,65) | 50(43,57) & | 65(59,71) | **<0.0001** |
| **eGFR, ml/min/1.73m²** | 90(90,90) | 86(80,92) | 90(89,90) | 88(87,90) | 89(88,91) | 88(86,90) | 89(89-90) | 85(81,90) | 0.3 |
| **Urine Alb/creatinine ratio** | 1.4(0.4,2.4) | 1.4(0.4,2.4) | 1.3(0.8-1.5) * | 1.1(0.8,1.5) % | 1.9(0.5,3.2) $^ | 2.6(0.4,5) | 5.6(1.4-9.7) *$& | 3(0.3,5.6) | **0.03** |
| **HbA1c, mmol/mol** | 32(29,35)! | 32(28,36) | 31(30,32) @* | 34(34,36) | 33(32,35) @^ | 37(36,39) | 34(33,36) * | 36(34,36) | **<0.0001** |
| **Glucose, mmol/L** | 5.1(4.5,5.4) | 4.5(4,5) | 5.2(4.8,5.5) | 4.6(2.5,5.0) | 6.6(3.9,9.2) | 5(4.9,5.6) | 4.7(4.3,5.1) | 4.6(4.4,4.9) | 0.4 |
| **NT-proBNP, ng/L** | 55(36,60) | 36(34,38) | 55(42,66) | 74(53,94) | 46(39,52) | 67(42,93) | 50(36-64) | 71(40,102) | 0.07 |

Values are mean [LL of 95% confidence interval – UL of 95% confidence interval]. * indicates p<0.05 between healthy pregnancy and preeclampsia; $indicates p<0.05 between gestational diabetes and preeclampsia; @ indicates p<0.05 between healthy pregnancy and gestational diabetes;! Indicates p<0.05 between normal weight controls and the pregnant cohort; % indicates p<0.05 between healthy pregnancy and healthy pregnancy follow up; ^ indicated p<0.05 between gestational diabetes and gestational diabetes follow up; & indicates p<0.05 between pre-eclampsia and pre-eclampsia follow up. > indicates p value between lean healthy volunteers and pre-eclampsia; < indicates p value < 0.05 between gestational diabetes and healthy pregnancy follow up; + indicates p value < 0.05 between healthy pregnancy follow up and preeclampsia, = indicates p value< 0.05 between healthy pregnancy and gestational diabetes; - indicates p value< 0.05 between healthy pregnancy and preeclampsia follow up; ~ indicates p<0.05 between lean healthy volunteers and healthy pregnancy and healthy pregnancy follow up; A indicates p value < 0.05 between normal weight controls and controls with overweight/obesity; , indicated p<0.05 between controls with overweight/obesity and healthy pregnancy and healthy pregnancy follow up

BMI indicates body mass index; kg, kilograms; n, number; bpm, beats per minute; mmHg, millimeters of mercury; g/l, gram per Liter; HDL, high density lipoprotein; mmol/L, millimoles per litre; LDL, low density lipoprotein; TG, triglyceride; eGFR, estimated glomerular filtration rate; ml/min/1.73m2, millilitre per minute per (1.73 square meters); pmol/L, picomoles per litre; NT-pro BNP, N-terminal pro hormone B-type natriuretic peptide; HBA1c, glycated haemoglobin; FFA, free fatty acids.

Table 6.1: Pregnancy and post-partum comparisons of clinical characteristics and chemistry

**Myocardial energetics, structure and function comparisons:**

Table 6.2 demonstrates longitudinal CMR/$^{31}$P-MRS changes for women with GDM, pE, HP during and 12-months post-partum pregnancy.

During the pregnancy, compared to the HP group, women with GDM had higher LV mass (90[85,94] vs 103[96,112] g; p=0.001) and lower myocardial PCr/ATP (2.2[2.1,2.4] vs 1.9[1.7,2]; p<0.0001), LV end-diastolic volumes (EDV) (76[72,80] vs 67[63,71]ml, p=0.03) and GLS (20[18,21] vs 18[17,19] %; p=0.008).

At very similar magnitudes to women with GDM, during pregnancy, compared to the HP group, the women with pE exhibited higher LV mass (90[85,94] vs 118[111,125] g; p<0.0001) and lower myocardial PCr/ATP (2.2[2.1,2.4] vs 1.9[1.8,2.1]; p=0.0004) and GLS (20[18,21] vs 16[14,17] %; p=0.01).

There were no significant differences in PCr/ATP, LVEDV, mass or GLS between the GDM and pE groups either during or after the pregnancy.

Twelve months' post-partum, an improvement in myocardial energetics (PCr/ATP ratio), GLS or LV mass was not observed in women with GDM or in women with pE compared to the third trimester of pregnancy scan (Table 6.2).

In the GDM cohort, there was a significant change in the LV mass/LVEDV p=0.02 and LVEDVi p=0.02. The LV ejection fraction was within normal range during the pregnancy scans and did not change at 12 months' post-partum scans.

There was a significant increment in the LVEDVi from baseline to 12 months' post-partum in the GDM (67(63,71) mL/m$^2$ to 73(69,77) mL/m$^2$, p=0.02); but no significant change in LVEDVi was observed in the HP or pE groups.

Myocardial energetics (HP:2.3(2.2,2.4) versus GDM:1.9(1.7,2.1), pE:1.9(1.8,2.1), p=0.003) and GLS (HP:21(20,22) versus GDM:18(17,19), pE -17(16,19) %, p=0.0001) remained significantly

lower and LV mass (HP:88(82,93) versus GDM:104(96,112) PE:118(109,120) g, p=0.0005) higher in women with recent GDM and pE pregnancy compared to women with HP respectively. (figure 6.4 and 6.5) LV mass correlated with BMI both in the GDM (r=0.30, p=0.03) and pE group (r=0.70, p=0.004).

Compared to nulliparous normal-weight controls, HP was associated with no significant differences in myocardial PCr/ATP, LV volumes, mass, EF, diastolic function, or GLS. The overweight nulliparous controls showed significantly higher LV mass and lower myocardial PCr/ATP and GLS than normal-weight nulliparous controls. There were no significant differences in LV mass, PCr/ATP or GLS between the overweight nulliparous controls and GDM or pE groups during or after pregnancy.

| | **Normal weight controls** (n=10) | **Controls with overweight/obesity** (n=10) | **Healthy pregnancy baseline** (n=38) | **Healthy pregnancy follow up** (n=30) | **Gestational diabetes mellitus baseline** (n=30) | **Gestational diabetes mellitus follow up** (n=26) | **Pre-eclampsia baseline** (n=22) | **Pre-eclampsia follow up** (n=16) | **ANOVA** |
|---|---|---|---|---|---|---|---|---|---|
| **Left ventricular structural parameters** | | | | | | | | | |
| **LV end diastolic volume index (ml/m²)** | 79(73,86)>A | 72(66,78), | 76(72,80) @* | 81(78,84) <+ | 67(63,71) @ | 73(70,77) | 64(57,71) *+ | 71(64,76) | **0.0006** |
| **LV end systolic volume index (ml/m²)** | 30(27,34) | 27(23,31) | 31(29,33) | 32(30,35) | 29(27,32) | 29(27,32) | 29(25,32) | 28(24,31) | 0.2 |
| **LV stroke volume (ml)** | 82(75,89) | 91(77,105) | 84(78,88) | 85(81,89) | 77(72,82) | 86(80,92) | 77(69,85) | 82(72,93) | 0.2 |
| **LV ejection fraction (%)** | 62(59,64) | 62(59,65) | 59(57,60) | 61(59,62) | 57(55,59) = | 60(58,62)^ | 58(56,60) | 59(57,62) | **0.05** |
| **LV mass (g)** | 82(75,89)>A | 103(84,122), | 90(85,94) @* | 88(82,93) <+ | 103(96,112) @= | 104(96,112) | 118(111,125) * | 109(98,120)- | **<0.0001** |
| **LV mass index (g/m²)** | 45(43,47)!A | 53(43,63), | 46(45,50) * | 51(48,54)+ | 50(48,53) | 51(52,53) | 57(54,59) *+ | 57(53,60) | **<0.0001** |
| **LV mass/LV EDV (g/ml)** | 0.61(0.56,0.65)!A | 0.70(0.64,0.76), | 0.62(0.58,0.65) @* | 0.62(0.59,0.65) | 0.78(0.70,0.83) = | 0.73(0.68,0.78) | 0.9(0.8,1) *$ | 0.8(0.72,0.87) | **<0.0001** |
| **Cardiac output (l/min)** | 5.6(4.9,6.2)!A | 6.4(5.2,7.6) | 6.6(6.3-7) @* | 5.8(5.5,6.2) < | 6.2(5.9,6.5) = | 5.7(5.3,6.1) | 6.1(5.4-6.9) + | 6(5,7)- | **<0.0001** |
| **Cardiac index (l/min/m²)** | 3.3(3,3.6)! | 3(2.6,3.4) | 3.5(3.3-3.7) @* | 3.3(3.2,3.6) | 3.1(2.9,3.2) @ | 2.9(2.8,3.1) | 3.0(2.6-3.4) * | 3.1(2.6,3.6)- | **<0.0001** |
| **Wall thickness (mm)** | 6(5,6)!A | 7(6.1,7.9), | 7.6(7.2,8.0) @* | 6.6(6.2,7.0) < | 10(9,12) = | 9.7(8.8,10.5) | 9.5(8.6,10.2) * | 8.5(7.5,9.6)- | **<0.0001** |
| **Right ventricular structural parameters** | | | | | | | | | |
| **RV end diastolic volume index (ml/m2)** | 87(80,95)A | 82(74,90), | 83(79,88) @* | 90(85,94) | 72(67,78) @ | 88(78,91) | 65(57,73) *$ | 78(69,88)- | **<0.0001** |
| **RV end systolic volume index (ml/m²)** | 40(35,44)A | 35(30,40), | 38(35,40) * | 40(36,43) | 34(30,38) | 37(32,43) | 28(24,32) *- | 35(31,39) | **<0.0001** |
| **RV stroke volume (ml)** | 79(72,86)A | 97(80,114), | 86(80,91) | 87(83,91) | 77(72,84) | 91(85,98) | 76(67,86) | 84(70,98) | **0.02** |
| **Myocardial energetics** | | | | | | | | | |

| | | | | | | | | | |
|---|---|---|---|---|---|---|---|---|---|
| **PCr/ATP** | 2.4(2.2,2.6)!A | 2.0(1.8,2.2), | 2.2(2.1,2.4) @* | 2.3(2.2,2.4) | 1.9(1.7,2) @^ | 1.9(1.7,2.1) | 1.9(1.8,.2.1) * | 1.9(1.8,2.1) | **<0.0001** |
| **Tissue characteristics** | | | | | | | | | |
| **Native T1 relaxation time (ms)** | 1298(1163,1255)~ | 1284(1231,1337) | 1326 (1314,1337) | 1326(1306,1347) | 1308 (1292,1323) | 1320(1298,1343) | 1296 (1281,1311) | 1320(1296,1344) | **0.02** |
| **Extra Cellular Volume, (%)** | - | - | - | 29(28,30) | - | 29(26,32) | - | 31(25,37) | 0.5 |
| **Functional parameters** | | | | | | | | | |
| **RV ejection fraction (%)** | 55(52,58) | 58(53,63) | 55(53,57) | 56(54,59) | 54(51,56) | 56(53,59) | 57(54,60) | 55(52,58) | 0.07 |
| **Global longitudinal shortening (%)** | -21(19,22)-A | -19(17,21), | -20(18,21) @* | -21(20,22) | -18(17,19) @ | -18(17,19) | -16(14,17) *+ | -17(16,19) | **<0.0001** |
| **MAPSE, (mm)** | 16(14,17) | 15(13,16), | 14(14,15)@* | 16(14,18)% | 14(13,14)@ | 17(16,18)^ | 12(11,14)* | 14(11,14)& | **<0.0001** |
| **Perfusion** | | | | | | | | | |
| **Stress MBF, ml/min/g** | - | - | - | 2.5(2.3,2.8) | - | 2.4[2.1-2.7] | - | 2.4(2.1,2.7) | 0.6 |
| **Rest MBF, ml/min/g** | - | - | - | 0.7(0.6,0.8) | - | 0.8[0.6-0.9] | - | 0.8(0.6,0.9) | 0.2 |
| **MPR** | - | - | - | 3.6(3.1,4.1) | - | 3.5[2.9-4] | - | 3.5(2.9,4) | 0.3 |

Values are mean [LL of 95% confidence interval – UL of 95% confidence interval]. * indicates p<0.05 between healthy pregnancy and preeclampsia; $indicates p<0.05 between gestational diabetes and preeclampsia; @ indicates p<0.05 between healthy pregnancy and gestational diabetes; ! Indicates p<0.05 between normal weight controls and the pregnant cohort; % indicates p<0.05 between healthy pregnancy and healthy pregnancy follow up; ^ indicated p<0.05 between gestational diabetes and gestational diabetes follow up; & indicates p<0.05 between pre-eclampsia and pre-eclampsia follow up. > indicates p value between normal weight controls and pre-eclampsia; < indicates

p value < 0.05 between gestational diabetes and healthy pregnancy follow up; + indicates p value < 0.05 between healthy pregnancy follow up and preeclampsia, = indicates p value< 0.05 between healthy pregnancy and gestational diabetes; - indicates p value< 0.05 between healthy pregnancy and preeclampsia follow up; ~ indicates p<0.05 between normal weight controls and healthy pregnancy and healthy pregnancy follow up; A indicates p value < 0.05 between normal weight controls and controls with overweight/obesity; , indicated p<0.05 between controls with overweight/obesity and healthy pregnancy and healthy pregnancy follow up. LV indicates left ventricular; ml, milliliter; ml/$m^2$, milliliters per square meter of body surface area; g, gram; g/$m^2$, gram per square meter of body surface area; LV, left ventricular; RV, right ventricular; LA, left atrium; MAPSE, mitral annular plane systolic excursion; DT, deceleration time; PCr/ATP phosphocreatine to adenosine triphosphate ratio; MBF myocardial blood flow; MPR myocardial perfusion reserve

Table 6.2: demonstrates longitudinal CMR/$^{31}$P-MRS changes for women with GDM, pE, HP during and 12-months post-partum pregnancy.

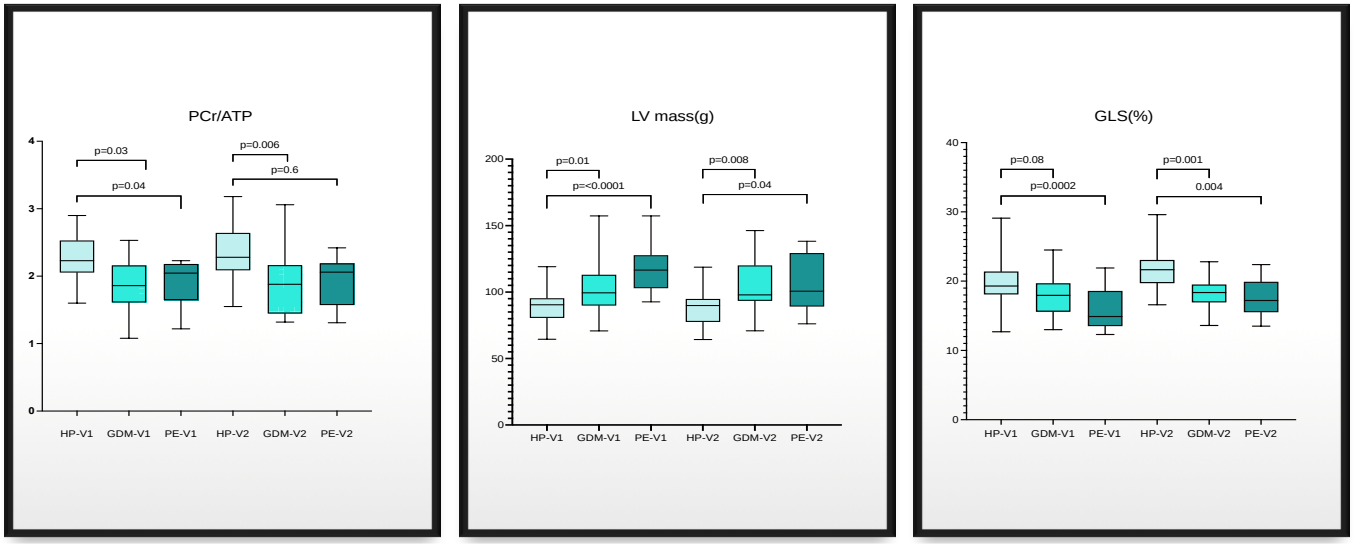


Figure 6.3:Box and whisker plots demonstrating the baseline and post-partum changes between all 3 cohorts (HP, GDM and preeclampsia) in myocardial PCr/ATP ratio, LV mass and global longitudinal shortening (GLS). HP indicates healthy pregnancy; GDM, gestational diabetes mellitus; pE, preeclampsia; V1, visit 1 during trimester scan; V2, visit 2 during 12-month post-partum scan.

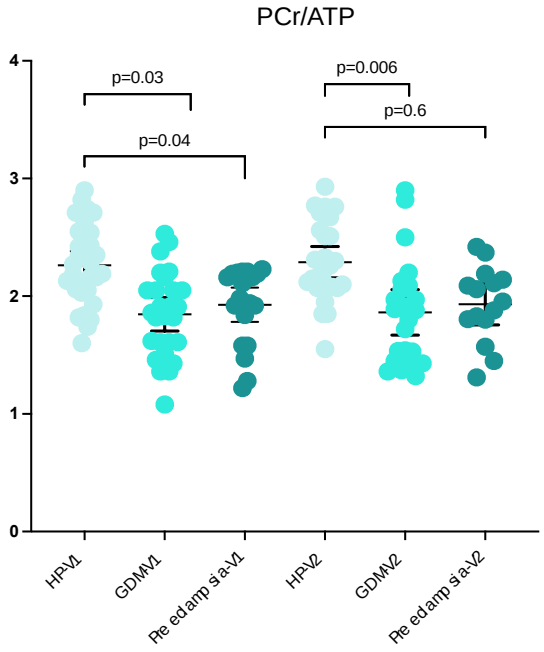
PCr/ATP
p=0.03
p=0.04
p=0.006
p=0.6
4
3
2
1
0
HPVI1
GDMVI1
Pre eclamptic-VI1
HPVI2
GDMVI2
Pre eclamptic-VI2

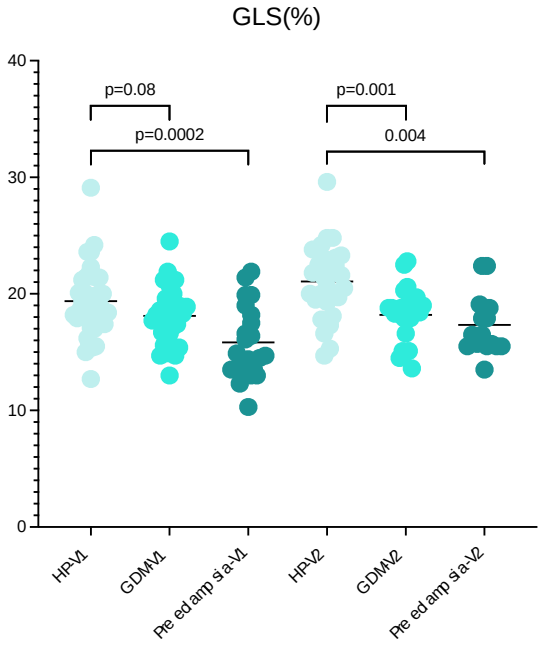
GLS(%)
p=0.08
p=0.0002
p=0.001
0.004
40
30
20
10
0
HPVI1
GDMVI1
Pre eclamptic-VI1
HPVI2
GDMVI2
Pre eclamptic-VI2

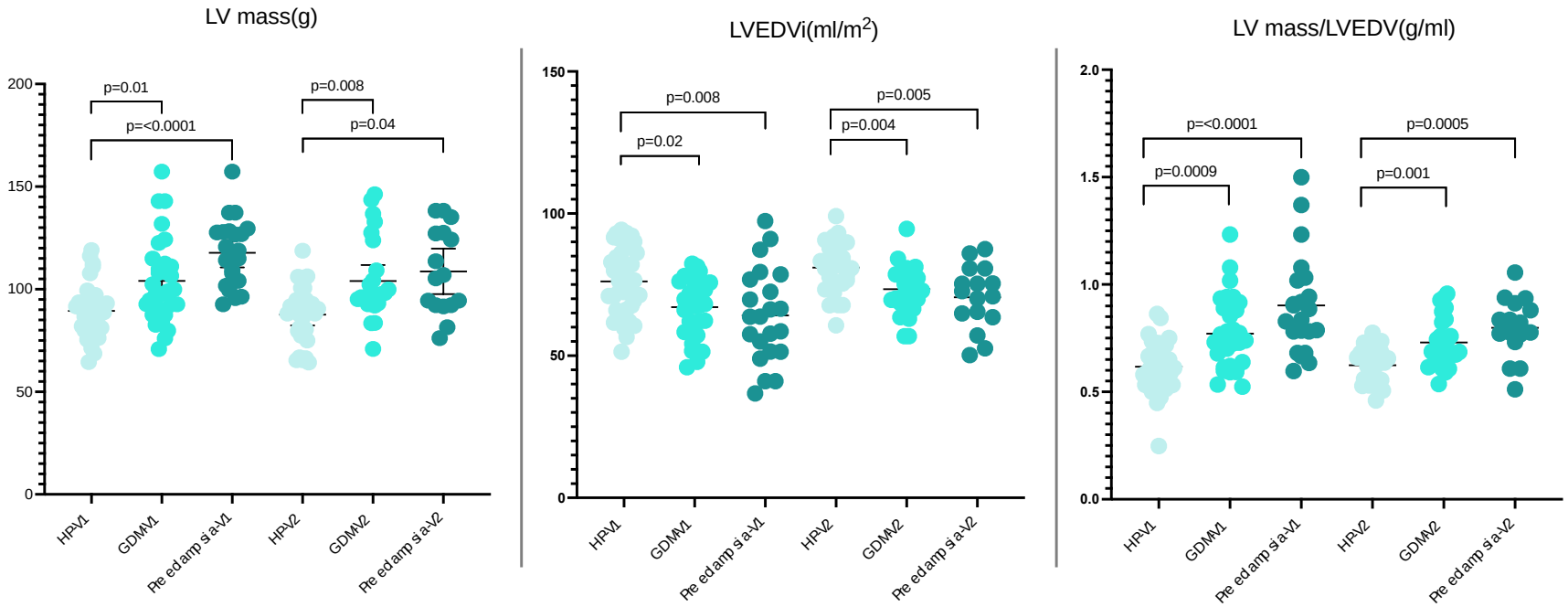
LV mass(g)
p=0.01
p=<0.0001
p=0.008
p=0.04
200
150
100
50
0
HPVI1
GDMVI1
Pre eclamptic-VI1
HPVI2
GDMVI2
Pre eclamptic-VI2
LVEDVi(ml/m2)
p=0.008
p=0.02
p=0.005
p=0.004
150
100
50
0
HPVI1
GDMVI1
Pre eclamptic-VI1
HPVI2
GDMVI2
Pre eclamptic-VI2
LV mass/LVEDV(g/ml)
p=<0.0001
p=0.0009
p=0.0005
p=0.001
2.0
1.5
1.0
0.5
0.0
HPVI1
GDMVI1
Pre eclamptic-VI1
HPVI2
GDMVI2
Pre eclamptic-VI2

Figure 6.4: Scatter plots demonstrating the baseline and post-partum changes between all 3 cohorts (HP, GDM and preeclampsia) in myocardial PCr/ATP ratio, global longitudinal shortening (GLS), LV mass, left ventricular end-diastolic volumes indexed for the body surface area, and left ventricular mass over left ventricular end diastolic volume ratio as a measure of concentricity index. HP indicates healthy pregnancy; GDM, gestational diabetes mellitus; pE, preeclampsia; V1, visit 1 during trimester scan; V2, visit 2 during 12-month post-partum scan.

### Myocardial tissue characteristics:

While numerically the HP group had higher myocardial native T1 measurements this difference was not statistically significant during (HP: 1326(1314,1337), GDM:1308(1294,1323, pE: 1296 (1281,1311) ms; p=0.05) or after pregnancy when comparing the measurements across the three groups (HP: 1326(1306,1347) versus GDM:1320(1298,1343) ms and pE:1320(1298,1344); p=0.2). However, the myocardial native T1 values were significantly higher in HP and GDM groups during pregnancy scans when compared to the normal-weight (1298(1163,1255)) and overweight nulliparous controls (1284(1163,1255), p=0.02).

### Myocardial perfusion

Changes in the rate pressure product (RPP) from rest to stress, rest and stress myocardial blood flow (MBF) and myocardial perfusion reserve (MPR) measurements are summarized in Table-6.2. Participants from all three groups demonstrated a similar increase in RPP during adenosine stress.

There was no significant difference in rest or stress global myocardial blood flow, or myocardial perfusion reserve amongst the women with recent HP, GDM and pE on the 12-month post-partum scan.

### 3D Whole Heart Imaging

We also performed 3D-gadolinium enhanced MR angiography for coronary visualisation.

There were no anomalous coronary artery origins or a visible plaque on visual assessment of the proximal coronaries in any of the participants.

### Neonatal and maternal complications

Infants exposed to labetalol in utero were reviewed for hypoglycaemia (blood glucose < 2.7mmol/l) in first 48 hours of life. Five term babies and 2 preterm babies out of 16 babies exposed to labetalol developed hypoglycaemia (43% vs 12% p=0.02). Mothers of the hypoglycaemic babies received significantly higher doses of labetalol (mg/day) compared to the mothers of non-hypoglycaemic babies (1066±468 vs 433±33 p=0.03).

There was no peri-partum cardiac event in any of the groups.

The average blood loss at delivery in GDM and pE were significantly higher when compared to HP (717±492ml vs 566±405ml vs 337 ±300ml p<0.0001).

### Birth weight, birthweight for gestational age, and sex comparisons:

A subtle difference in birthweight was detected between the HP, GDM and pE group babies, with a higher birthweight in the HP group. Neonatal birthweight adjusted for gestational age recorded in grams was slightly lower in the GDM and pE group (HP: 3390±492g vs GDM: 3196±667g vs pE 2736±997 g, p=0.01). There were no differences in sex distribution of the babies. The average gestational week of pE diagnosis was 32±18. HELLP syndrome developed in 2(9%) of PE's. The rate of preterm delivery was higher in pE when compared to HP and GDM; 4 vs 2 vs 2 (18% vs 5% vs 7%). 100 % rate of live birth was noticed in both groups. The rate of placental abruption needing urgent delivery was higher in pE 3 (13%) vs 0% in HP arm. The Caesarean section rate was high in pE when compared to HP and GDM; 9 vs 6 vs 5 (60% vs 15% vs 19% p=0.002). First and 5$^{th}$ minute Apgar scores were slightly lower in the pE (8.3±1.6 vs 7.2±2.1 p=0.03). Admission to the NNU/SCBU was observed as higher in pE 7 as compared to HP 1 (31% vs 2.6% p=0.01). Respiratory distress syndrome was observed in 4 babies from pE mothers out of which 2 developed HELLP syndrome and 1 (18 % vs 2.6%

p=0.03) from healthy pregnancy. Table 6.3 details the differences in obstetric and neonatal data between the 3 cohorts.

### Placenta

There were significant differences in the weight of the placenta between the three groups; HP vs GDM vs pE (487±62 vs 334±196 vs 379±70 p<0.001). Placentas from pE participants had the highest prevalence of maternal vascular mal-perfusion and infarcts (18% vs 31% vs 15% p=0.02) compared to the HP and GDM groups. 3 (15%) of the placentas from women with pE had retro placental clots compared to 1(2%) in the HP and 2(7%) in the GDM cohort.

| **VARIABLES** | **HP** ***(N=38)*** | **GDM** ***(N=30)*** | **PE** ***(N=22)*** | **ANOVA** |
|---|---|---|---|---|
| **GESTATION AT DELIVERY (WEEKS)** | 39±1.7 | 37±7.2 | 34±11 | 0.001 |
| **DELIVERY BY LSCS** | 6(15%) | 5(19.4%) | 9(60%) | 0.01 |
| **PRE-TERM DELIVERIES** | 2(5%) | 2(6.7%) | 4(18%) | 0.01 |
| **NEONATAL BIRTH WEIGHT(GRAMS)** | 3390±492 | 3196±667 | 2736±997 | 0.01 |
| **APGAR SCORE 1MIN** | 8.3±1.6 | 8.5±1.7 | 7.2±2.1 | 0.02 |
| **APGAR SCORE 5MIN** | 9.7±0.4 | 9.6±1 | 8.8±1.7 | 0.02 |
| **CORD GAS PH** | 7.12±0.4 | 7.2±0.006 | 7.25±0.8 | 0.4 |

| | | | | |
|---|---|---|---|---|
| **NEONATAL UNIT ADMISSION** | 1(2.6%) | 0 | 6(31%) | 0.02 |
| **INTRAPARTUM BLOOD LOSS(ML)** | 337±300 | 717±492 | 566+404 | <0.001 |
| **PLACENTAL WEIGHT(GRAMS)** | 487.29±62 | 334±196 | 279.71±70 | <0.001 |
| **PLACENTAL INFARCTS** | 1(2.6%) | 2(7%) | 4(18%) | 0.02 |
| **PLACENTAL VASCULAR MAL-PERFUSION** | 2(5%) | 2(7%) | 4(18%) | 0.02 |

Values are means (SD) or median (IQR) for continuous variables and number (%) for categorical variables

Table 6.3: details the differences in obstetric and neonatal data between the 3 cohorts.

## 6.5 Discussion

In this longitudinal cohort study, I have shown that despite distinct aetiologies women with GDM and pE exhibit a similar myocardial phenotype during and after pregnancy with persistent subtle abnormalities in myocardial PCr/ATP ratio, LV mass and GLS compared to women with HP during pregnancy and twelve months' postpartum assessments. Women with GDM and pE show similar myocardial alterations to nulliparous women with obesity, suggesting that the maternal myocardial changes are predominantly driven by obesity-associated metabolic dysfunction.

### Healthy pregnancy

During pregnancy, the maternal cardiovascular system is modified to meet the increasing demands of the developing fetus(127). Despite the increased cardiac workload in the pregnant group, with a 40% higher mean resting heart rate, worsened plasma metabolic profile and physiological reductions in hemoglobin levels, myocardial energetics were maintained at normal levels in healthy pregnancy. However, a non-significant increase in myocardial energetics was detected 12 months' post-partum with the improved metabolic profile post-pregnancy. There have been no prior studies to date evaluating longitudinal myocardial energetics in pregnancy.

Contrary to the common assertion that pregnancy leads to an eccentric cardiac remodeling, our findings suggest that healthy pregnancy is associated with no significant changes in cardiac function or mass over a 12-month period but paradoxically a non-significant increase in LVEDV 12 months' post-partum. This could be explained by the variability in diastolic filling pressures, preload and positional changes related to altered intrathoracic and intraabdominal pressures(197) affecting cardiac performance. As our results contradicted the traditional thinking, 2 independent operators analysed these results (ST and EL), as well as a third method of confirmation of the findings by an AI algorithm at a different centre (Barts, London). The mean LVEDV during visit 1 (third trimester pregnancy scans) from our analysis versus AI in the HP was 142±26 vs 144±25 mL, p=0.8 and the mean LVEDV during visit 2 (12-months post-partum scans) from our analysis versus AI in the HP was 142±18 vs 143±19 mL, p=0.8. The mean LVEDV during visit 1 from our analysis versus AI in the GDM cohort was 134±24 vs 138±22 mL, p=0.6 and the mean LVEDV during visit 2 from our analysis versus AI in the GDM cohort was 144±26 vs 149±22 mL, p=0.5.

The discrepancy between our findings in LV volumes during pregnancy and the previous literature was addressed in Chapter 3 discussion section in detail.

### Gestational diabetes mellitus

GDM is characterized by insufficient insulin secretion during pregnancy to overcome the insulin resistance and pancreatic beta cell dysfunction.(198) In our study, there appears to be no significant improvement in GLS or myocardial energetics at 12 months' post-partum.

The left ventricular mass remained higher in the gestational diabetes group 12 months' post-partum. The remaining hypertrophy may continue to influence the worsened CV outcomes in this group of patients.

Left atrial function and volumes increased post pregnancy in the GDM group and the HP group which implies that LA plays an important role in compensating for the hemodynamic alterations (such as increased heart rate) of the pregnancy. (199) The LA likely remodels to maintain adequate LV filling and satisfy increasing cardiac output because LA function is influenced by cardiac output. (200)

Women with GDM showed similar alterations in myocardial energetics, LV mass and GLS to nulliparous women with obesity, suggesting that the maternal myocardial changes are predominantly driven by obesity-associated metabolic dysfunction. While the changes in PCr/ATP ratio were within normal range in both groups these were significantly lower compared to HP and normal body weight nulliparous controls.(201)

LV mass correlation with BMI is also suggestive that the overweight status may have also contributed to the hypertrophic remodelling in patients with gestational diabetes.

Abnormal body weight is associated with slightly increased third trimester HbA1c values compared to HP and may alter long-term glycemic control as defined by an increase in HbA1c

levels in the GDM group 12-months' post-partum. Because pregnancy is a state of altered red blood cell kinetics and haemodilution, it is unsurprising that the HbA1c is increased 12-months' post-partum in both groups but still within acceptable normal range. Most studies suggest that HbA1c is underestimated in pregnant women and is an unreliable marker.(202) Obesity and diabetes are independent risk factors for adverse perinatal outcome and good glycaemic control may modify some of the risks.(203)

Coupled with the biochemistry and CMR findings from the nulliparous controls with overweight/obesity, these results provide further insight that pre-existing obesity does also contribute to the maternal myocardial alterations in women with GDM.

Finally, the changes seen in the GDM highlight the importance in strict risk factor modification to also prevent adverse pregnancy outcomes.

### Preeclampsia

pE is a state of systemic inflammation, endothelial dysfunction and oxidative stress. These changes may lead to permanent vascular and metabolic damage from factors released into the maternal circulation.(11)

In our study, we have found that 12-months' post-partum, the structural changes such as PCr/ATP ratio and GLS remained impaired compared to women with HP and LV mass remained higher. In terms of clinical assessments and biochemistry, there was a reduction in the blood pressure and triglyceride levels at 12 months. The BMI reduced at 12 months albeit it remained within the overweight range.

Higher pre-pregnancy blood pressure, total cholesterol and LDL levels are known to be associated with the development of GDM and hypertensive disorders of pregnancy.

In two prospective studies, women with a history of pE or gestational hypertension had a higher BMI, blood pressure and cholesterol levels when followed up over a mean of 2.5 years and a higher prevalence of metabolic syndrome. These women also had higher biochemical markers such as glucose, HbA1c, cholesterol, triglycerides and C-reactive protein at 2.5 years follow up.(204) (205)

Prior echocardiography studies have reported prevalence of persistent diastolic dysfunction as high as 52% at one-year post-partum in women with a history of preterm pE.(64) In our study, we have also demonstrated similar findings with no improvement in the mitral inflow E/A ratio and mitral annular plane systolic excursion.

Studies have demonstrated a relationship between placental insufficiency and impairment of LV function prior to presentation with pre-eclampsia. Women who present with placental insufficiency and LV impairment are more likely to develop preterm pE as compared with women with placental insufficiency and a normal cardiac profile, suggesting that preterm pre-eclampsia reflects the inability of the maternal cardiac system to respond to placental dysfunction. (206) In our study, reassuringly despite a significant increase in placental infarcts and placental mal-perfusion when compared to those with HP, the left ventricular systolic function remained within normal levels both during pregnancy and at the 12 month follow up visit.

A randomized double blinded placebo controlled trial using postnatal enalapril to improve cardiovascular function following preterm preeclampsia (PICk-UP) demonstrated an improvement in diastolic function, left ventricular remodelling and left ventricular mass index compared to placebo.(207) These positive findings by Ormersher et al were a promising step forward in improving cardiovascular outcomes in this cohort of patients.

Current literature does not demonstrate a causal relationship between maternal placental disorders in pregnancy and the risk of developing cardiovascular disease in the future. A more likely explanation relates to the chronic state of a woman's abnormal metabolic environment which then creates an unfavourable environment during pregnancy which can also lead to impairment in fetal health.

Finally, there were significant differences in the birthweight, placental maternal vascular mal-perfusion and infarcts, pre-term delivery and placental abruption in the pE group which is in line with current literature secondary to the thrombotic risks, decidual arteriopathy and a decreased uterine response to pregnancy. (208)

## 6.6 Conclusions

In this longitudinal cohort study, women with recent GDM and pE have demonstrated non-reversible reductions in energetics, global longitudinal shortening and higher LV mass 12 months' post-partum with persistent significant differences compared to women with recent healthy pregnancy during and after pregnancy. In parallel, the healthy pregnancy cohort did not exhibit any significant changes in any of the cardiac parameters including cardiac volumes, mass, function, global longitudinal shortening or myocardial energetics 12 months' post-partum compared to third trimester pregnancy scans. With post-partum scans considered to serve as a surrogate for the pre-pregnancy baseline values, our findings suggest that the women with GDM and pE show persistent subtle cardiac abnormalities related to intrinsic metabolic alterations likely associated with pre-pregnancy overweight/obesity status as opposed to pregnancy related haemodynamic stresses. Future prospective studies should explore the implications of overweight/obesity in women who intend to get pregnant. These findings suggest that to understand the complexities imposed by cardio-metabolic

comorbidities in patients with GDM and preeclampsia a holistic and patient-centered approach should be undertaken. GDM and preeclampsia patients may require a tailored lifestyle strategy approach prior to pregnancy to prevent deleterious effects on the myocardium from the adverse effects of obesity.

## 6.7 Limitations

This study has a few limitations. A single centre design may increase the risk of bias. Pregnant women who need serial studies by CMR should be imaged in a consistent position either the left lateral or supine position because of the effects on venous return, SV and CO.

We have been unable to identify healthy pregnancy women matching in BMI to the cohort with GDM and pE as by nature obese individuals would not serve as healthy controls.

Six patients were unable to attend for the repeat follow up due to being pregnant again and perhaps this should be factored in for future studies.

A larger study with a longer follow-up duration will be required to confirm the significance of the observed cardiac morphological differences in GDM and preeclampsia.

# *Chapter 7: General Conclusions*

This work was carried out to explore cardiac energy metabolism, maternal myocardial alterations in the third trimester of normal pregnancy, gestational diabetes, preeclampsia and their recovery 12 months' post-partum. Pregnant women are underrepresented in clinical research and the mechanisms of long-term cardiovascular complications in women with obstetric complications remain to be explained. This thesis is the first to report on longitudinal cardiac assessments in pregnancies complicated by gestational diabetes and preeclampsia. Despite distinct etiologies women with GDM and pE exhibit a similar myocardial phenotype during and after pregnancy with persistent subtle abnormalities in myocardial PCr/ATP ratio, LV mass and GLS compared to women with HP during pregnancy and twelve months' postpartum assessments. Women with GDM and pE show similar myocardial alterations to nulliparous women with obesity, suggesting that the myocardial changes are predominantly driven by obesity-associated metabolic dysfunction. It is also plausible that the decrease in energy supply may coexist with intrinsic metabolic dysfunction, such as metabolic inefficiency and mitochondrial dysfunction in patients with gestational diabetes and pE.

Although much is known about GDM and pE pathophysiology, molecular understanding of GDM and pE has not yet been translated into efficacious therapies(148). The current treatment of GDM focuses on optimising glycaemic control. When this is not achieved despite lifestyle and dietary advice, treatment with anti-hyperglycaemic medication is indicated.

However, as the cardiovascular risk associated with GDM does not diminish by attaining normoglycemia there is a clear and pressing need for novel strategies specifically aiming to improve cardiovascular outcomes for women with GDM. The cardiovascular risks for pE also persists after delivery of the baby and strategies are also needed to improve cardiovascular outcomes in these patients. If larger longitudinal studies confirm a consistent association between the cardiac alterations revealed in this study in women with GDM and pE and higher

rates of adverse maternal and fetal outcomes, the early detection of these adverse subclinical myocardial alterations might offer the opportunity of better stratifying women at risk of perinatal complications, as well as future CVD.(113)

While excessive gestational weight gain was shown to increase adverse pregnancy outcomes, pre-pregnancy maternal obesity might be a more important factor in driving these adverse outcomes.(209) Supporting this notion, in this study we have not detected significant differences in gestational weight gain between the two cohorts while the booking BMI was significantly higher in the GDM and pE group. Raising awareness with adequate pre-pregnancy counselling through public health initiatives to achieve ideal body weight in women who plan pregnancy might lead to improved maternal outcomes and their offspring.

The answers provided in this body of work stimulates further questions. Larger longitudinal studies are needed to better understand the mechanisms to then predict risk stratification models and better treatment options in these group of patients.

## References


1. Statistics OoN. Births in England and Wales. England and Wales, 2021.
2. Ducas RA, Elliott JE, Melnyk SF et al. Cardiovascular magnetic resonance in pregnancy: Insights from the cardiac hemodynamic imaging and remodeling in pregnancy (CHIRP) study. Journal of Cardiovascular Magnetic Resonance 2014;16:1.
3. Kotit S, Yacoub M. Cardiovascular adverse events in pregnancy: A global perspective. Glob Cardiol Sci Pract 2021;2021:e202105.
4. Morton A. Physiological Changes and Cardiovascular Investigations in Pregnancy. Heart, Lung and Circulation 2021;30:e6-e15.
5. Litmanovich DE, Tack D, Lee KS, Shahrzad M, Bankier AA. Cardiothoracic imaging in the pregnant patient. J Thorac Imaging 2014;29:38-49.
6. ACOG Committee Opinion No. 762: Prepregnancy Counseling. Obstet Gynecol 2019;133:e78-e89.
7. Liu LX, Arany Z. Maternal cardiac metabolism in pregnancy. Cardiovascular Research 2014;101:545-553.
8. Hauspurg A, Ying W, Hubel CA, Michos ED, Ouyang P. Adverse pregnancy outcomes and future maternal cardiovascular disease. Clinical Cardiology 2018;41:239-246.
9. Sanghavi M, Rutherford JD. Cardiovascular Physiology of Pregnancy. Circulation 2014;130:1003-1008.
10. Poppas A, Shroff SG, Korcarz CE et al. Serial assessment of the cardiovascular system in normal pregnancy. Role of arterial compliance and pulsatile arterial load. Circulation 1997;95:2407-15.
11. Gongora MC, Wenger NK. Cardiovascular Complications of Pregnancy. Int J Mol Sci 2015;16:23905-28.
12. Chaiworapongsa T, Chaemsaithong P, Yeo L, Romero R. Pre-eclampsia part 1: current understanding of its pathophysiology. Nat Rev Nephrol 2014;10:466-80.
13. Ghio A, Bertolotto A, Resi V, Volpe L, Di Cianni G. Triglyceride metabolism in pregnancy. Adv Clin Chem 2011;55:133-53.
14. Morton A, Teasdale S. Review article: Investigations and the pregnant woman in the emergency department - part 1: Laboratory investigations. Emerg Med Australas 2018;30:600-609.
15. Salerno M, Sharif B, Arheden H et al. Recent Advances in Cardiovascular Magnetic Resonance: Techniques and Applications. Circ Cardiovasc Imaging 2017;10.
16. Romagano M, Louis-Jacques A, Quinones J et al. Is there a role for cardiac magnetic resonance imaging during pregnancy? The Journal of Maternal-Fetal & Neonatal Medicine 2020;33:558-563.
17. Stewart RD, Nelson DB, Matulevicius SA et al. Cardiac magnetic resonance imaging to assess the impact of maternal habitus on cardiac remodeling during pregnancy. Am J Obstet Gynecol 2016;214:640.e1-6.
18. Diagnostic criteria and classification of hyperglycaemia first detected in pregnancy: a World Health Organization Guideline.
19. Hadden DR, Hillebrand B. The first recorded case of diabetic pregnancy (Bennewitz HG, 1824, University of Berlin). Diabetologia 1989;32:625.
20. Lever J. Guy's Hospital Report. London, 1847.

21. Plows J, Stanley J, Baker P, Reynolds C, Vickers M. The Pathophysiology of Gestational Diabetes Mellitus. International Journal of Molecular Sciences 2018;19:3342.
22. Jia G, Hill MA, Sowers JR. Diabetic Cardiomyopathy. Circulation Research 2018;122:624-638.
23. Fu Z, Gilbert ER, Liu D. Regulation of insulin synthesis and secretion and pancreatic Beta-cell dysfunction in diabetes. Curr Diabetes Rev 2013;9:25-53.
24. Kishida K, Funahashi T, Shimomura I. Molecular mechanisms of diabetes and atherosclerosis: role of adiponectin. Endocr Metab Immune Disord Drug Targets 2012;12:118-31.
25. Patti ME, Corvera S. The role of mitochondria in the pathogenesis of type 2 diabetes. Endocr Rev 2010;31:364-95.
26. Okoth K, Chandan JS, Marshall T et al. Association between the reproductive health of young women and cardiovascular disease in later life: umbrella review. BMJ 2020;371:m3502.
27. Kramer CK, Campbell S, Retnakaran R. Gestational diabetes and the risk of cardiovascular disease in women: a systematic review and meta-analysis. Diabetologia 2019;62:905-914.
28. Wu P, Gulati M, Kwok CS et al. Preterm Delivery and Future Risk of Maternal Cardiovascular Disease: A Systematic Review and Meta-Analysis. Journal of the American Heart Association;7:e007809.
29. Li J, Song C, Li C, Liu P, Sun Z, Yang X. Increased risk of cardiovascular disease in women with prior gestational diabetes: A systematic review and meta-analysis. Diabetes Research and Clinical Practice 2018;140:324-338.
30. Park K, Quesada O, Cook-Wiens G et al. Adverse Pregnancy Outcomes Are Associated with Reduced Coronary Flow Reserve in Women With Signs and Symptoms of Ischemia Without Obstructive Coronary Artery Disease: A Report from the Women's Ischemia Syndrome Evaluation-Coronary Vascular Dysfunction Study. Journal of women's health (2002) 2020;29:487-492.
31. Association AD. 14. Management of Diabetes in Pregnancy: Standards of Medical Care in Diabetes—2021. Diabetes Care 2020;44:S200-S210.
32. Lauenborg J, Mathiesen E, Hansen T et al. The prevalence of the metabolic syndrome in a danish population of women with previous gestational diabetes mellitus is three-fold higher than in the general population. J Clin Endocrinol Metab 2005;90:4004-10.
33. Gestational diabetes mellitus. Diabetes Care 2000;23 Suppl 1:S77-9.
34. Hebert MF, Ma X, Naraharisetti SB et al. Are we optimizing gestational diabetes treatment with glyburide? The pharmacologic basis for better clinical practice. Clin Pharmacol Ther 2009;85:607-14.
35. Malek R, Davis SN. Pharmacokinetics, efficacy and safety of glyburide for treatment of gestational diabetes mellitus. Expert Opin Drug Metab Toxicol 2016;12:691-9.
36. Feig DS, Donovan LE, Zinman B et al. Metformin in women with type 2 diabetes in pregnancy (MiTy): a multicentre, international, randomised, placebo-controlled trial. Lancet Diabetes Endocrinol 2020;8:834-844.
37. Berry DC, Thomas SD, Dorman KF et al. Rationale, design, and methods for the Medical Optimization and Management of Pregnancies with Overt Type 2 Diabetes (MOMPOD) study. BMC Pregnancy Childbirth 2018;18:488.

38. Tranquilli AL, Brown MA, Zeeman GG, Dekker G, Sibai BM. The definition of severe and early-onset preeclampsia. Statements from the International Society for the Study of Hypertension in Pregnancy (ISSHP). Pregnancy Hypertension: An International Journal of Women's Cardiovascular Health 2013;3:44-47.
39. Robillard PY, Dekker G, Chaouat G, Scioscia M, Iacobelli S, Hulsey TC. Historical evolution of ideas on eclampsia/preeclampsia: A proposed optimistic view of preeclampsia. J Reprod Immunol 2017;123:72-77.
40. Ambrozic J, Brzan Simenc G, Prokselj K, Tul N, Cvijic M, Lucovnik M. Lung and cardiac ultrasound for hemodynamic monitoring of patients with severe pre-eclampsia. Ultrasound in Obstetrics & Gynecology 2017;49:104-109.
41. Rana S, Lemoine E, Granger JP, Karumanchi SA. Preeclampsia. Circulation Research 2019;124:1094-1112.
42. Wu P, Haththotuwa R, Kwok CS et al. Preeclampsia and Future Cardiovascular Health. Circulation: Cardiovascular Quality and Outcomes 2017;10:e003497.
43. Brandt Y, Ghossein-Doha C, Gerretsen SC, Spaanderman MEA, Kooi ME. Noninvasive Cardiac Imaging in Formerly Preeclamptic Women for Early Detection of Subclinical Myocardial Abnormalities: A 2022 Update. Biomolecules 2022;12:415.
44. Dennis AT, Castro J, Carr C, Simmons S, Permezel M, Royse C. Haemodynamics in women with untreated pre-eclampsia*. Anaesthesia 2012;67:1105-1118.
45. Sircar M, Thadhani R, Karumanchi SA. Pathogenesis of preeclampsia. Curr Opin Nephrol Hypertens 2015;24:131-8.
46. Ives CW, Sinkey R, Rajapreyar I, Tita ATN, Oparil S. Preeclampsia—Pathophysiology and Clinical Presentations: JACC State-of-the-Art Review. Journal of the American College of Cardiology 2020;76:1690-1702.
47. Kendall RL, Thomas KA. Inhibition of vascular endothelial cell growth factor activity by an endogenously encoded soluble receptor. Proc Natl Acad Sci U S A 1993;90:10705-9.
48. Levine RJ, Maynard SE, Qian C et al. Circulating angiogenic factors and the risk of preeclampsia. N Engl J Med 2004;350:672-83.
49. Baird RC, Li S, Wang H et al. Pregnancy-Associated Cardiac Hypertrophy in Corin-Deficient Mice: Observations in a Transgenic Model of Preeclampsia. Can J Cardiol 2019;35:68-76.
50. Hecht JL, Zsengeller ZK, Spiel M, Karumanchi SA, Rosen S. Revisiting decidual vasculopathy. Placenta 2016;42:37-43.
51. Soleymanlou N, Jurisica I, Nevo O et al. Molecular evidence of placental hypoxia in preeclampsia. J Clin Endocrinol Metab 2005;90:4299-308.
52. O'Brien TE, Ray JG, Chan WS. Maternal body mass index and the risk of preeclampsia: a systematic overview. Epidemiology 2003;14:368-74.
53. O'Brien TE, Ray JG, Chan W-S. Maternal Body Mass Index and the Risk of Preeclampsia: A Systematic Overview. Epidemiology 2003;14:368-374.
54. Hermes W, Ket JCF, van Pampus MG et al. Biochemical Cardiovascular Risk Factors After Hypertensive Pregnancy Disorders: A Systematic Review and Meta-analysis. Obstetrical & Gynecological Survey 2012;67.
55. De Haas S, Ghossein-Doha C, Geerts L, van Kuijk SMJ, van Drongelen J, Spaanderman MEA. Cardiac remodeling in normotensive pregnancy and in pregnancy complicated by hypertension: systematic review and meta-analysis. Ultrasound Obstet Gynecol 2017;50:683-696.

56. Barr LC, Liblik K, Johri AM, Smith GN. Maternal Cardiovascular Function following a Pregnancy Complicated by Preeclampsia. Am J Perinatol 2020.
57. Chen SSM, Leeton L, Castro JM, Dennis AT. Myocardial tissue characterisation and detection of myocardial oedema by cardiovascular magnetic resonance in women with pre-eclampsia: a pilot study. Int J Obstet Anesth 2018;36:56-65.
58. Birukov A, Wiesemann S, Golic M et al. Myocardial Evaluation of Post-Preeclamptic Women by CMR: Is Early Risk Stratification Possible? JACC Cardiovasc Imaging 2020;13:1291-1293.
59. Ersbøll AS, Bojer AS, Hauge MG et al. Long-Term Cardiac Function After Peripartum Cardiomyopathy and Preeclampsia: A Danish Nationwide, Clinical Follow-Up Study Using Maximal Exercise Testing and Cardiac Magnetic Resonance Imaging. Journal of the American Heart Association 2018;7.
60. Askie LM, Duley L, Henderson-Smart DJ, Stewart LA. Antiplatelet agents for prevention of pre-eclampsia: a meta-analysis of individual patient data. Lancet 2007;369:1791-1798.
61. Ersbøll AS, Goetze JP, Johansen M et al. Biomarkers and Their Relation to Cardiac Function Late After Peripartum Cardiomyopathy. J Card Fail 2021;27:168-175.
62. Kalapotharakos G, Salehi D, Steding-Ehrenborg K et al. Cardiovascular effects of severe late-onset preeclampsia are reversed within six months postpartum. Pregnancy Hypertens 2020;19:18-24.
63. Levine LD, Lewey J, Koelper N et al. Persistent cardiac dysfunction on echocardiography in African American women with severe preeclampsia. Pregnancy Hypertens 2019;17:127-132.
64. Melchiorre K, Sutherland GR, Liberati M, Thilaganathan B. Preeclampsia is associated with persistent postpartum cardiovascular impairment. Hypertension 2011;58:709-15.
65. Ahmed S, Shellock FG. Magnetic resonance imaging safety: implications for cardiovascular patients. J Cardiovasc Magn Reson 2001;3:171-82.
66. Ntusi NA, Samuels P, Moosa S, Mocumbi AO. Diagnosing cardiac disease during pregnancy: imaging modalities. Cardiovasc J Afr 2016;27:95-103.
67. Jellis CL, Kwon DH. Myocardial T1 mapping: modalities and clinical applications. Cardiovascular diagnosis and therapy 2014;4:126-137.
68. Salerno M, Sharif B, Arheden H et al. Recent Advances in Cardiovascular Magnetic Resonance: Techniques and Applications. Circulation Cardiovascular imaging 2017;10:e003951.
69. Ferreira VM, Piechnik SK. CMR Parametric Mapping as a Tool for Myocardial Tissue Characterization. Korean circulation journal 2020;50:658-676.
70. Strizek B, Jani JC, Mucyo E et al. Safety of MR Imaging at 1.5 T in Fetuses: A Retrospective Case-Control Study of Birth Weights and the Effects of Acoustic Noise. Radiology 2015;275:530-537.
71. Herrey AS, Francis JM, Hughes M, Ntusi NAB. Cardiovascular magnetic resonance can be undertaken in pregnancy and guide clinical decision-making in this patient population. European Heart Journal - Cardiovascular Imaging 2019;20:291-297.
72. Ray JG, Vermeulen MJ, Bharatha A, Montanera WJ, Park AL. Association Between MRI Exposure During Pregnancy and Fetal and Childhood Outcomes. JAMA 2016;316:952-961.

73. Kok RD, de Vries MM, Heerschap A, van den Berg PP. Absence of harmful effects of magnetic resonance exposure at 1.5 T in utero during the third trimester of pregnancy: a follow-up study. Magnetic Resonance Imaging 2004;22:851-854.
74. Kodzwa R. Updates to the ACR Manual on Contrast Media. Radiol Technol 2017;89:186-189.
75. King JC. Physiology of pregnancy and nutrient metabolism. Am J Clin Nutr 2000;71:1218s-25s.
76. Murashige D, Jang C, Neinast M et al. Comprehensive quantification of fuel use by the failing and nonfailing human heart. Science 2020;370:364-368.
77. Neubauer S. The Failing Heart — An Engine Out of Fuel. New England Journal of Medicine 2007;356:1140-1151.
78. Hudsmith LE, Neubauer S. Detection of myocardial disorders by magnetic resonance spectroscopy. Nat Clin Pract Cardiovasc Med 2008;5 Suppl 2:S49-56.
79. Neubauer S, Krahe T, Schindler R et al. 31P magnetic resonance spectroscopy in dilated cardiomyopathy and coronary artery disease. Altered cardiac high-energy phosphate metabolism in heart failure. Circulation 1992;86:1810-8.
80. Neubauer S, Horn M, Pabst T et al. Contributions of 31P-magnetic resonance spectroscopy to the understanding of dilated heart muscle disease. Eur Heart J 1995;16 Suppl O:115-8.
81. Neubauer S, Horn M, Cramer M et al. Myocardial phosphocreatine-to-ATP ratio is a predictor of mortality in patients with dilated cardiomyopathy. Circulation 1997;96:2190-6.
82. Okada M, K. M, Inubushi T, Kinoshita M. Influence of aging or left ventricular hypertrophy on the human heart: Contents of phosphorus metabolites measured by 31P MRS. MRM 1998;39:772-782.
83. Beer M, Sandstede J, Landschütz W et al. Absolute concentrations of myocardial high-energy phosphate metabolites in normal, hypertrophied and failing human myocardium, measured non-invasively with 31P-SLOOP-magnetic resonance spectroscopy. J Am Coll Cardiol 2002;40:1267-74.
84. Levelt E, Rodgers CT, Clarke WT et al. Cardiac energetics, oxygenation, and perfusion during increased workload in patients with type 2 diabetes mellitus. Eur Heart J 2016;37:3461-3469.
85. Tran DH, Wang ZV. Glucose Metabolism in Cardiac Hypertrophy and Heart Failure. Journal of the American Heart Association 2019;8:e012673.
86. Wikström M, Springett R. Thermodynamic efficiency, reversibility, and degree of coupling in energy conservation by the mitochondrial respiratory chain. Communications Biology 2020;3:451.
87. Balestrino M. Role of Creatine in the Heart: Health and Disease. Nutrients 2021;13.
88. Neubauer S, Horn M, Cramer M et al. Myocardial Phosphocreatine-to-ATP Ratio Is a Predictor of Mortality in Patients With Dilated Cardiomyopathy. Circulation 1997;96:2190-2196.
89. Ingwall JS. Energy metabolism in heart failure and remodelling. Cardiovascular research 2009;81:412-419.
90. Excellence NIfHaC. Diabetes in pregnancy: management from preconception to the postnatal period. 2020.
91. Mayhew TM, Ohadike C Fau - Baker PN, Baker Pn Fau - Crocker IP, Crocker Ip Fau - Mitchell C, Mitchell C Fau - Ong SS, Ong SS. Stereological investigation of placental

morphology in pregnancies complicated by pre-eclampsia with and without intrauterine growth restriction.
92. Su EJ, Xin H Fau - Yin P, Yin P Fau - Dyson M et al. Impaired fetoplacental angiogenesis in growth-restricted fetuses with abnormal umbilical artery doppler velocimetry is mediated by aryl hydrocarbon receptor nuclear translocator (ARNT).
93. Pennell DJ, Sechtem UP, Higgins CB et al. Clinical indications for cardiovascular magnetic resonance (CMR): Consensus Panel report. J Cardiovasc Magn Reson 2004;6:727-65.
94. Tyler DJ, Emmanuel Y, Cochlin LE et al. Reproducibility of 31P cardiac magnetic resonance spectroscopy at 3 T. NMR in biomedicine 2009;22:405-13.
95. Sairia Dass, Lowri E Cochlin, Cameron J Holloway et al. Development and validation of a short 31P cardiac magnetic resonance spectroscopy protocol. Journal of Cardiovascular Magnetic Resonance 2010:123.
96. Vanhamme L, van den Boogaart A, S. VH. Improved method for accurate and efficient quantification of MRS data with use of prior knowledge. J Magn Reson 1997;129:35-43.
97. Zhang X, Heberlein K, Sarkar S, X. H. A multiscale approach for analyzing in vivo spectroscopic imaging data. Magn Reson Med 2000;43:331-334.
98. Lucian A. B. Purvis, William T. Clarke, Luca Biasiolli, Matthew D. Robson, Rodgers CT. Linewidth constraints in Matlab AMARES using per-metabolite T2 and per-voxel ΔB0". ISMRM 2014.
99. Bottomley PA, R. O. Optimum flip-angles for exciting NMR with uncertain T1 values. Magn Reson Med 1994;July:137-141.
100. Neubauer S, Krahe T, Schindler R et al. 31P magnetic resonance spectroscopy in dilated cardiomyopathy and coronary artery disease. Altered cardiac high-energy phosphate metabolism in heart failure. Circulation 1992;86:1820-1818.
101. Rodgers CT, Clarke WT, Snyder C, Vaughan JT, Neubauer S, Robson MD. Human cardiac (31)P magnetic resonance spectroscopy at 7 tesla. Magnetic Resonance in Medicine 2014;72:304-315.
102. Lucian AB Purvis, William T. Clarke, Luca Biasiolli, Robson MD, CT R. Linewidth constraints in Matlab AMARES using per-metabolite T2 and per-voxel ΔB0. *ISMRM* 2014.
103. Xue H, Artico J, Fontana M, Moon JC, Davies RH, Kellman P. Landmark Detection in Cardiac MRI by Using a Convolutional Neural Network. Radiol Artif Intell 2021;3:e200197.
104. Kellman P, Arai AE, Xue H. T1 and extracellular volume mapping in the heart: estimation of error maps and the influence of noise on precision. J Cardiovasc Magn Reson 2013;15:56.
105. Messroghli DR, Bainbridge GJ, Alfakih K et al. Assessment of regional left ventricular function: accuracy and reproducibility of positioning standard short-axis sections in cardiac MR imaging. Radiology 2005;235:229-36.
106. Giri S, Chung Y-C, Merchant A et al. T2 quantification for improved detection of myocardial edema. Journal of Cardiovascular Magnetic Resonance 2009;11:56.
107. Layland J, Rauhalammi S, Lee MMY et al. Diagnostic Accuracy of 3.0-T Magnetic Resonance T1 and T2 Mapping and T2-Weighted Dark-Blood Imaging for the Infarct-Related Coronary Artery in Non-ST-Segment Elevation Myocardial Infarction. Journal of the American Heart Association 2017;6:e004759.

108. Kellman P, Hansen MS, Nielles-Vallespin S et al. Myocardial perfusion cardiovascular magnetic resonance: optimized dual sequence and reconstruction for quantification. J Cardiovasc Magn Reson 2017;19:43.
109. Amano Y, Yanagisawa F, Tachi M et al. Three-dimensional Cardiac MR Imaging: Related Techniques and Clinical Applications. Magn Reson Med Sci 2017;16:183-189.
110. Virani SS, Alonso A, Aparicio HJ et al. Heart Disease and Stroke Statistics—2021 Update. Circulation 2021;143:e254-e743.
111. Arora S, Stouffer George A, Kucharska-Newton Anna M et al. Twenty Year Trends and Sex Differences in Young Adults Hospitalized With Acute Myocardial Infarction. Circulation 2019;139:1047-1056.
112. Bhatnagar P, Wickramasinghe K, Wilkins E, Townsend N. Trends in the epidemiology of cardiovascular disease in the UK. Heart 2016;102:1945.
113. Parikh NI, Gonzalez JM, Anderson CAM et al. Adverse Pregnancy Outcomes and Cardiovascular Disease Risk: Unique Opportunities for Cardiovascular Disease Prevention in Women: A Scientific Statement From the American Heart Association. Circulation 2021;143:e902-e916.
114. Kramer CM, Barkhausen J, Bucciarelli-Ducci C, Flamm SD, Kim RJ, Nagel E. Standardized cardiovascular magnetic resonance imaging (CMR) protocols: 2020 update. Journal of Cardiovascular Magnetic Resonance 2020;22:17.
115. Nii M, Ishida M, Dohi K et al. Myocardial tissue characterization and strain analysis in healthy pregnant women using cardiovascular magnetic resonance native T1 mapping and feature tracking technique. Journal of Cardiovascular Magnetic Resonance 2018;20:52.
116. Germain Alfredo M, Romanik Mary C, Guerra I et al. Endothelial Dysfunction. Hypertension 2007;49:90-95.
117. de Resende Guimarães MFB, Brandão AHF, de Lima Rezende CA et al. Assessment of endothelial function in pregnant women with preeclampsia and gestational diabetes mellitus by flow-mediated dilation of brachial artery. Archives of Gynecology and Obstetrics 2014;290:441-447.
118. Axtell AL, Gomari FA, Cooke JP. Assessing Endothelial Vasodilator Function with the Endo-PAT 2000. Journal of Visualized Experiments : JoVE 2010:2167.
119. Hamburg NM, Keyes MJ, Larson MG et al. Cross-sectional relations of digital vascular function to cardiovascular risk factors in the Framingham Heart Study. Circulation 2008;117:2467-2474.
120. Tyler DJ, Emmanuel Y, Cochlin LE et al. Reproducibility of 31 P cardiac magnetic resonance spectroscopy at 3 T. NMR in Biomedicine 2009;22:405-413.
121. Dass S, Cochlin LE, Holloway CJ et al. Development and validation of a short 31P cardiac magnetic resonance spectroscopy protocol. Journal of Cardiovascular Magnetic Resonance 2010;12:P123.
122. Captur G, Gatehouse P, Keenan KE et al. A medical device-grade T1 and ECV phantom for global T1 mapping quality assurance—the T1 Mapping and ECV Standardization in cardiovascular magnetic resonance (T1MES) program. Journal of Cardiovascular Magnetic Resonance 2016;18:58.
123. Purvis LAB, Clarke WT, Biasiolli L, Valkovič L, Robson MD, Rodgers CT. OXSA: An open-source magnetic resonance spectroscopy analysis toolbox in MATLAB. PLOS ONE 2017;12:e0185356.

124. Xue H, Artico J, Fontana M, Moon JC, Davies RH, Kellman P. Landmark Detection in Cardiac MRI Using a Convolutional Neural Network. Radiology: Artificial Intelligence 2021:e200197.
125. Rathi VK, Doyle M, Yamrozik J et al. Routine evaluation of left ventricular diastolic function by cardiovascular magnetic resonance: A practical approach. Journal of Cardiovascular Magnetic Resonance 2008;10:36.
126. Swoboda PP, McDiarmid AK, Erhayiem B et al. Diabetes Mellitus, Microalbuminuria, and Subclinical Cardiac Disease: Identification and Monitoring of Individuals at Risk of Heart Failure. Journal of the American Heart Association: Cardiovascular and Cerebrovascular Disease 2017;6:e005539.
127. Hall ME, George EM, Granger JP. El corazón durante el embarazo. Revista Española de Cardiología 2011;64:1045-1050.
128. van der Zande ISE, van der Graaf R, Oudijk MA, van Delden JJM. Vulnerability of pregnant women in clinical research.
129. Abalos E, Cuesta C, Grosso AL, Chou D, Say L. Global and regional estimates of preeclampsia and eclampsia: a systematic review. European Journal of Obstetrics & Gynecology and Reproductive Biology 2013;170:1-7.
130. Meah VA-O, Cockcroft JR, Backx K, Shave R, Stöhr EJ. Cardiac output and related haemodynamics during pregnancy: a series of meta-analyses.
131. Greenwood JP, Scott EM, Stoker JB, Walker JJ, Mary DASG. Sympathetic Neural Mechanisms in Normal and Hypertensive Pregnancy in Humans. Circulation 2001;104:2200-2204.
132. Loerup L, Pullon RM, Birks J et al. Trends of blood pressure and heart rate in normal pregnancies: a systematic review and meta-analysis. BMC Medicine 2019;17:167.
133. Katz R, Karliner JS, Resnik R. Effects of a natural volume overload state (pregnancy) on left ventricular performance in normal human subjects. Circulation 1978;58:434-441.
134. Piechnik SK, Ferreira VM, Dall'Armellina E et al. Shortened Modified Look-Locker Inversion recovery (ShMOLLI) for clinical myocardial T1-mapping at 1.5 and 3 T within a 9 heartbeat breathhold. Journal of Cardiovascular Magnetic Resonance 2010;12:69-69.
135. Moon JC, Messroghli DR, Kellman P, Piechnik SK, Robson MD, Ugander M. Myocardial T1 mapping and extracellular volume quantification: a Society for Cardiovascular Magnetic Resonance (SCMR) and CMR Working Group of the European Society of Cardiology consensus statement. J Cardiovasc Magn Reson 2013;15.
136. Ervasti M, Kotisaari S, Heinonen S, Punnonen K. Elevated serum erythropoietin concentration is associated with coordinated changes in red blood cell and reticulocyte indices of pregnant women at term. Scandinavian Journal of Clinical and Laboratory Investigation 2008;68:160-165.
137. Nickander J, Themudo R, Sigfridsson A, Xue H, Kellman P, Ugander M. Females have higher myocardial perfusion, blood volume and extracellular volume compared to males – an adenosine stress cardiovascular magnetic resonance study. Scientific Reports 2020;10:10380.
138. Rosmini S, Bulluck H, Captur G et al. Myocardial native T1 and extracellular volume with healthy ageing and gender. European Heart Journal - Cardiovascular Imaging 2018;19:615-621.

139. Vikse BE, Irgens LM, Leivestad T, Skjaerven R, Iversen BM. Preeclampsia and the risk of end-stage renal disease. N Engl J Med 2008;359:800-9.
140. McDonald SD, Malinowski A, Zhou Q, Yusuf S, Devereaux PJ. Cardiovascular sequelae of preeclampsia/eclampsia: a systematic review and meta-analyses. Am Heart J 2008;156:918-30.
141. Cho L, Davis M, Elgendy I et al. Summary of Updated Recommendations for Primary Prevention of Cardiovascular Disease in Women: JACC State-of-the-Art Review. Journal of the American College of Cardiology 2020;75:2602-2618.
142. Bellenger NG, Burgess MI, Ray SG et al. Comparison of left ventricular ejection fraction and volumes in heart failure by echocardiography, radionuclide ventriculography and cardiovascular magnetic resonance. Are they interchangeable? European Heart Journal 2000;21:1387-1396.
143. Hyperglycemia and Adverse Pregnancy Outcomes. New England Journal of Medicine 2008;358:1991-2002.
144. McDonald SD, Malinowski A, Zhou Q, Yusuf S, Devereaux PJ. Cardiovascular sequelae of preeclampsia/eclampsia: A systematic review and meta-analyses. American Heart Journal 2008;156:918-930.
145. Zhang C, Ning Y. Effect of dietary and lifestyle factors on the risk of gestational diabetes: review of epidemiologic evidence. The American journal of clinical nutrition 2011;94:1975S-1979S.
146. Yu Y, Soohoo M, Sørensen HT, Li J, Arah OA. Gestational Diabetes Mellitus and the Risks of Overall and Type-Specific Cardiovascular Diseases: A Population- and Sibling-Matched Cohort Study. Diabetes Care 2021;45:151-159.
147. Bellamy L, Casas J-P, Hingorani AD, Williams D. Type 2 diabetes mellitus after gestational diabetes: a systematic review and meta-analysis. The Lancet 2009;373:1773-1779.
148. McIntyre HD. Discovery, Knowledge, and Action—Diabetes in Pregnancy Across the Translational Spectrum: The 2016 Norbert Freinkel Award Lecture. Diabetes Care 2018;41:227-232.
149. Mecacci F, Ottanelli S, Vannuccini S et al. Maternal hemodynamic changes in gestational diabetes: a prospective case–control study. Archives of Gynecology and Obstetrics 2021.
150. McIntyre HD, Catalano P, Zhang C, Desoye G, Mathiesen ER, Damm P. Gestational diabetes mellitus. Nature Reviews Disease Primers 2019;5:47.
151. Lopaschuk GD, Karwi QG, Tian R, Wende AR, Abel ED. Cardiac Energy Metabolism in Heart Failure. Circulation Research 2021;128:1487-1513.
152. Thirunavukarasu S, Jex N, Chowdhary A et al. Empagliflozin Treatment Is Associated With Improvements in Cardiac Energetics and Function and Reductions in Myocardial Cellular Volume in Patients With Type 2 Diabetes. Diabetes 2021;70:2810-2822.
153. Thirunavukarasu S, Jex N, Chowdhary A et al. Empagliflozin Treatment is Associated With Improvements in Cardiac Energetics and Function and Reductions in Myocardial Cellular Volume in Patients With Type 2 Diabetes. Diabetes 2021:db210270.
154. American Diabetes A. 13. Management of Diabetes in Pregnancy: Standards of Medical Care in Diabetes—2018. Diabetes Care 2018;41:S137.

155. Lopaschuk GD, Ussher JR, Folmes CDL, Jaswal JS, Stanley WC. Myocardial Fatty Acid Metabolism in Health and Disease. Physiological Reviews 2010;90:207-258.
156. Burrage MK, Hundertmark M, Valkovič L et al. Energetic Basis for Exercise-Induced Pulmonary Congestion in Heart Failure With Preserved Ejection Fraction. Circulation 2021;144:1664-1678.
157. Rayner JJ, Peterzan MA, Clarke WT, Rodgers CT, Neubauer S, Rider OJ. Obesity modifies the energetic phenotype of dilated cardiomyopathy. European Heart Journal 2021:ehab663.
158. Levelt E, Rodgers CT, Clarke WT et al. Cardiac energetics, oxygenation, and perfusion during increased workload in patients with type 2 diabetes mellitus. European Heart Journal 2016;37:3461-3469.
159. Chu SY, Callaghan WM, Kim SY et al. Maternal Obesity and Risk of Gestational Diabetes Mellitus. Diabetes Care 2007;30:2070-2076.
160. Levelt E, Mahmod M, Piechnik SK et al. Relationship between Left Ventricular Structural and Metabolic Remodelling in Type 2 Diabetes Mellitus. Diabetes 2015.
161. Levelt E, Rodgers CT, Clarke WT et al. Cardiac energetics, oxygenation, and perfusion during increased workload in patients with type 2 diabetes mellitus. European heart journal 2015.
162. Rawshani A, Rawshani A, Franzén S et al. Risk Factors, Mortality, and Cardiovascular Outcomes in Patients with Type 2 Diabetes. New England Journal of Medicine 2018;379:633-644.
163. Rider OJ, Francis JM, Ali MK et al. Effects of Catecholamine Stress on Diastolic Function and Myocardial Energetics in Obesity. Circulation 2012;125:1511-1519.
164. Rider OJ, Francis JM, Tyler D, Byrne J, Clarke K, Neubauer S. Effects of weight loss on myocardial energetics and diastolic function in obesity. The International Journal of Cardiovascular Imaging 2013;29:1043-1050.
165. Rayner JJ, Peterzan MA, Watson WD et al. Myocardial Energetics in Obesity: Enhanced ATP Delivery Through Creatine Kinase With Blunted Stress Response. Circulation 2020;141:1152-1163.
166. Levy D, Garrison RJ, Savage DD, Kannel WB, Castelli WP. Prognostic Implications of Echocardiographically Determined Left Ventricular Mass in the Framingham Heart Study. New England Journal of Medicine 1990;322:1561-1566.
167. Oliveira AP, Calderon IM, Costa RA, Roscani MG, Magalhães CG, Borges VT. Assessment of structural cardiac abnormalities and diastolic function in women with gestational diabetes mellitus. Diabetes and Vascular Disease Research 2015;12:175-180.
168. Buddeberg BS, Sharma R, O'Driscoll JM, Kaelin Agten A, Khalil A, Thilaganathan B. Impact of gestational diabetes mellitus on maternal cardiac adaptation to pregnancy. Ultrasound in Obstetrics & Gynecology 2020;56:240-246.
169. Appiah D, Schreiner PJ, Gunderson EP et al. Association of Gestational Diabetes Mellitus With Left Ventricular Structure and Function: The CARDIA Study. Diabetes Care 2016;39:400-407.
170. Verma N, Srodulski S, Velmurugan S et al. Gestational diabetes triggers postpartum cardiac hypertrophy via activation of calcineurin/NFAT signaling. Scientific Reports 2021;11:20926.

171. Backs J, Song K, Bezprozvannaya S, Chang S, Olson EN. CaM kinase II selectively signals to histone deacetylase 4 during cardiomyocyte hypertrophy. The Journal of clinical investigation 2006;116:1853-1864.
172. Yang Y, Wang Z, Mo M et al. The association of gestational diabetes mellitus with fetal birth weight. Journal of Diabetes and its Complications 2018;32:635-642.
173. Abalos E, Cuesta C, Grosso AL, Chou D, Say L. Global and regional estimates of preeclampsia and eclampsia: a systematic review. Eur J Obstet Gynecol Reprod Biol 2013;170:1-7.
174. Chappell LC, Cluver CA, Kingdom J, Tong S. Pre-eclampsia. Lancet 2021;398:341-354.
175. Smith GCS, Pell JP, Walsh D. Pregnancy complications and maternal risk of ischaemic heart disease: a retrospective cohort study of 129 290 births. The Lancet 2001;357:2002-2006.
176. Irgens HU, Roberts JM, Reisæter L, Irgens LM, Lie RT. Long term mortality of mothers and fathers after pre-eclampsia: population based cohort studyPre-eclampsia and cardiovascular disease later in life: who is at risk?. BMJ 2001;323:1213.
177. Grandi SM, Filion KB, Yoon S et al. Cardiovascular Disease-Related Morbidity and Mortality in Women With a History of Pregnancy Complications. Circulation 2019;139:1069-1079.
178. Matyas M, Hasmasanu M, Silaghi CN et al. Early Preeclampsia Effect on Preterm Newborns Outcome. Journal of Clinical Medicine 2022;11:452.
179. Hudsmith LE, Neubauer S. Magnetic Resonance Spectroscopy in Myocardial Disease. JACC: Cardiovascular Imaging 2009;2:87-96.
180. González A, Ravassa S, López B et al. Myocardial Remodeling in Hypertension. Hypertension 2018;72:549-558.
181. Drazner MH. The Progression of Hypertensive Heart Disease. Circulation 2011;123:327-334.
182. Braunthal S, Brateanu A. Hypertension in pregnancy: Pathophysiology and treatment. SAGE Open Med 2019;7:2050312119843700.
183. Rayner JJ, Peterzan MA, Watson WD et al. Myocardial Energetics in Obesity. Circulation 2020;141:1152-1163.
184. Al-Maawali A, Walfisch A, Koren G. Taking angiotensin-converting enzyme inhibitors during pregnancy: is it safe? Can Fam Physician 2012;58:49-51.
185. Seko Y, Kato T, Morita Y et al. Impact of left ventricular concentricity on long-term mortality in a hospital-based population in Japan. PLoS One 2018;13:e0203227.
186. Melchiorre K, Sutherland G, Sharma R, Nanni M, Thilaganathan B. Mid-gestational maternal cardiovascular profile in preterm and term pre-eclampsia: a prospective study. Bjog 2013;120:496-504.
187. Nagueh SF, Smiseth OA, Appleton CP et al. Recommendations for the Evaluation of Left Ventricular Diastolic Function by Echocardiography: An Update from the American Society of Echocardiography and the European Association of Cardiovascular Imaging. J Am Soc Echocardiogr 2016;29:277-314.
188. Rafik Hamad R, Larsson A, Pernow J, Bremme K, Eriksson MJ. Assessment of left ventricular structure and function in preeclampsia by echocardiography and cardiovascular biomarkers. J Hypertens 2009;27:2257-64.

189. Bamfo JE, Kametas NA, Chambers JB, Nicolaides KH. Maternal cardiac function in normotensive and pre-eclamptic intrauterine growth restriction. Ultrasound Obstet Gynecol 2008;32:682-6.
190. Whittemore R, Hobbins JC, Engle MA. Pregnancy and its outcome in women with and without surgical treatment of congenital heart disease. Am J Cardiol 1982;50:641-51.
191. Joubert LH, Doubell AF, Langenegger EJ et al. Cardiac magnetic resonance imaging in preeclampsia complicated by pulmonary edema shows myocardial edema with normal left ventricular systolic function. Am J Obstet Gynecol 2022;227:292.e1-292.e11.
192. Thirunavukarasu S, Ansari F, Cubbon R et al. Maternal Cardiac Changes in Women With Obesity and Gestational Diabetes Mellitus. Diabetes Care 2022:dc220401.
193. American Diabetes A. 14. Management of Diabetes in Pregnancy: Standards of Medical Care in Diabetes—2021. Diabetes Care 2020;44:S200-S210.
194. Hudsmith LE, Petersen SE, Tyler DJ et al. Determination of cardiac volumes and mass with FLASH and SSFP cine sequences at 1.5 vs. 3 Tesla: a validation study. J Magn Reson Imaging 2006;24:312-8.
195. Gulsin GS, Swarbrick DJ, Hunt WH et al. Relation of Aortic Stiffness to Left Ventricular Remodeling in Younger Adults With Type 2 Diabetes. Diabetes 2018;67:1395.
196. Kellman P, Hansen MS, Nielles-Vallespin S et al. Myocardial perfusion cardiovascular magnetic resonance: optimized dual sequence and reconstruction for quantification. Journal of Cardiovascular Magnetic Resonance 2017;19:43.
197. Rossi A, Cornette J, Springeling T et al. Cardiac Magnetic Resonance in pregnant women: supine or left lateral position? Journal of Cardiovascular Magnetic Resonance 2010;12:P124.
198. Moyce BL, Dolinsky VW. Maternal β-Cell Adaptations in Pregnancy and Placental Signalling: Implications for Gestational Diabetes. Int J Mol Sci 2018;19.
199. Chirinos JA, Sardana M, Satija V et al. Effect of Obesity on Left Atrial Strain in Persons Aged 35–55 Years (The Asklepios Study). The American Journal of Cardiology 2019;123:854-861.
200. Greenberg B, Chatterjee K, Parmley WW, Werner JA, Holly AN. The influence of left ventricular filling pressure on atrial contribution to cardiac output. Am Heart J 1979;98:742-51.
201. Thirunavukarasu S, Ansari F, Cubbon R et al. Maternal Cardiac Changes in Women With Obesity and Gestational Diabetes Mellitus. Diabetes Care 2022;45:3007-3015.
202. Edelson PK, James KE, Leong A et al. Longitudinal Changes in the Relationship Between Hemoglobin A1c and Glucose Tolerance Across Pregnancy and Postpartum. J Clin Endocrinol Metab 2020;105:e1999-2007.
203. Rosenn B. Obesity and diabetes: A recipe for obstetric complications. The Journal of Maternal-Fetal & Neonatal Medicine 2008;21:159-164.
204. Hermes W, Franx A, van Pampus MG et al. Cardiovascular risk factors in women who had hypertensive disorders late in pregnancy: a cohort study. Am J Obstet Gynecol 2013;208:474.e1-8.
205. Al-Nasiry S, Ghossein-Doha C, Polman SE et al. Metabolic syndrome after pregnancies complicated by pre-eclampsia or small-for-gestational-age: a retrospective cohort. Bjog 2015;122:1818-23.
206. Thayaparan AS, Said JM, Lowe SA, McLean A, Yang Y. Pre-eclampsia and long-term cardiac dysfunction: A review of asymptomatic cardiac changes existing well beyond

the post-partum period. Australasian Journal of Ultrasound in Medicine 2019;22:234-244.
207. Ormesher L, Higson S, Luckie M et al. Postnatal Enalapril to Improve Cardiovascular Function Following Preterm Preeclampsia (PICk-UP). Hypertension 2020;76:1828-1837.
208. McBride CA, Bernstein IM, Sybenga AB, McLean KC, Orfeo T, Bravo MC. Placental Maternal Vascular Malperfusion Is Associated with Prepregnancy and Early Pregnancy Maternal Cardiovascular and Thrombotic Profiles. Reproductive Medicine 2022;3:50-61.
209. Catalano PM. Reassessing strategies to improve pregnancy outcomes in overweight and obese women. The Lancet Diabetes & Endocrinology 2019;7:2-3.